Pre-Permian evolution of the Sele High, Central North Sea

Gard Lyngby Eliassen

Master Thesis in Geosciences
Sedimentology, paleontology and stratigraphy
60 Credits

Department of Geosciences
Faculty of Mathematics and Natural Sciences

UNIVERSITY OF OSLO

May 2023

Supervisors: Muhammad Hassaan, Jan Inge Faleide and Alvar Braathen

Pre-Permian evolution of the Sele High, Central North Sea.

This work is published digitally through DUO – “Digitale Utgivelser ved UiO”.

http://www.duo.uio.no

Preface

This master's thesis (ECTS 60) is submitted to the Department of Geosciences, University of Oslo (UiO), in the candidacy of the Master of Science in Geosciences (ECTS 120) following the Structural geology and tectonics program. The main supervisor of this thesis is Dr. Muhammad Hassaan (Vår Energi, UiO), together with the co-supervisors Professor Jan Inge Faleide (UiO, UiT), and Professor Alvar Braathen (UiO).

This thesis serves as a contribution to the Suprabasins project, funded by the Research Council of Norway (grant number 295208) together with 6 academic and 4 industry partners (Equinor, Aker BP, Lundin Energy Norway, and Spirit Energy). Well data is courtesy of the NPD Diskos repository and software is courtesy of SLB (Petrel E&P Software Platform).

Suprabasins project: https://www.mn.uio.no/geo/english/research/projects/suprabasins/

Data availability statement

The seismic and well data that support the findings of this study are available from the Norwegian Petroleum Directorate (NPD), TGS NOPEC, and DISKOS database. Restrictions apply to the availability of these data, which were used under license for this study.

Acknowledgements

First, I want to express my gratitude and appreciation to my main supervisor Dr. Muhammad Hassaan for your devotion and guidance at every stage of this process. I am also grateful to my co-supervisors Prof. Jan Inge Faleide and Prof. Alvar Braathen for your valuable insight and critical assessments. I would also like to give thanks to all participants in the productive discussions at Bifrost.

Secondly, I want to thank my fellow students and friends at the Department of Geoscience at UiO who have made the day-to-day exciting and joyful during all my five years. I am also thankful and admiring for all the wonderful teachers I have had over the years, at UiO and UNIS, for dedicating their time to share their knowledge.

Finally, a personal thank you to my partner, Helene Wang, and my family for your encouragement and support throughout this process.

Abstract

The Pre-Permian history of the North Sea within the Norwegian Continental Shelf (NCS) is poorly understood due to a complex history of rifting, thermal cooling, sedimentation, subsidence and erosion resulting in limited quality and quantity of geological and geophysical data. However, pre-existing structures exert a significant influence on later evolution making this time-period important for understanding of the Post-Permian evolution. Therefore, the basement highs are of great importance, offering better resolution and accessibility to the older stratigraphy with less overprint from younger stratigraphy. The Sele High is a prominent basement culmination in the Central North Sea of the NCS with sedimentary strata dating back to the Devonian. The area has an excellent 3D seismic data coverage making it optimal for investigating the Pre-Permian history.

The Sele High was evolved in five complex stages from Devonian until Middle Jurassic. 1) Devonian: Deposition of Unit A-C, likely the Old Red Group which conformably superimpose the basement. The deposition probably occurred in a broad basin as Devonian units are also identified outside the Sele High, in areas such as Ling Depression, Åsta Graben, Norwegian-Danish Basin and Egersund Basin (Well 17/12-2). 2) Late Devonian – Late Carboniferous: Rifting creating the thick-skinned master faults (MF1, MF2, MF3, MF3C, MF5 and MF6) and syn-rift deposition of Unit D and possibly other units. 3) Late Carboniferous: Compression caused by far-field effects of the Variscan Orogeny causing inversion on MF3C and creation of the PPF in a transpression regime. The compression also induced uplift and erosion of Unit A-D and possibly other units deposited in stage 2. Erosion of these units are seen in the Sele High and neighboring areas. Creating a hiatus from Upper Devonian/Lower Carboniferous to the Lower Permian – Saliaan Unconformity. 4) Early Permian – Early Jurassic: this stage can be subdivided in three parts; i) Early Permian extension and subsequent thermal subsidence in Mid Permian with deposition of Rotliegend and Zechstein Groups; ii) Late Permian – Early Triassic (RP1) continuous deposition of Zechstein Supergroup, Smith Bank and Skagerrak fms; iii) Mid Triassic – Mid Jurassic thermal subsidence following RP1 and continuous deposition of sediments. 5) Mid Jurassic doming: Thermal doming centered bellow the triple junction in the North Sea caused widespread uplift and erosion of the North Sea, resulting in a hiatus from Middle Triassic to Middle/Late Jurassic in the Sele High area – Mid Jurassic Unconformity.

Table of content

1. Introduction

This study provides an assessment of the structural architecture, stratigraphic infill and evolution of the Sele High in the Central North Sea. It discusses the possible structural inheritance since the late Devonian Caledonides collapse and its impact on the high and surrounding basin development. This chapter introduces the study area, motivation, primary research objectives and previous research work of this region.

1.1 Study area

The current study focuses on the Sele High along with adjacent regions concerning the structural and stratigraphic development of the pre-Zechstein Supergroup strata (Fig. 1). The Sele High is a local high in the Central North Sea approximately 150 km southwest of the Stavanger and 100 km east of the junction of trilete rift system (Davies et al., 2001). The high has an excellent 3D seismic coverage and much of the Pre-Zechstein strata is visible. The Sele High and Ling Depression marks the Northeastern limit of Zechstein evaporites (Fig. 2.9) (Fazlikhani et al., 2017). The Zechstein Supergroup is the uppermost unit in the Permian stratigraphy.

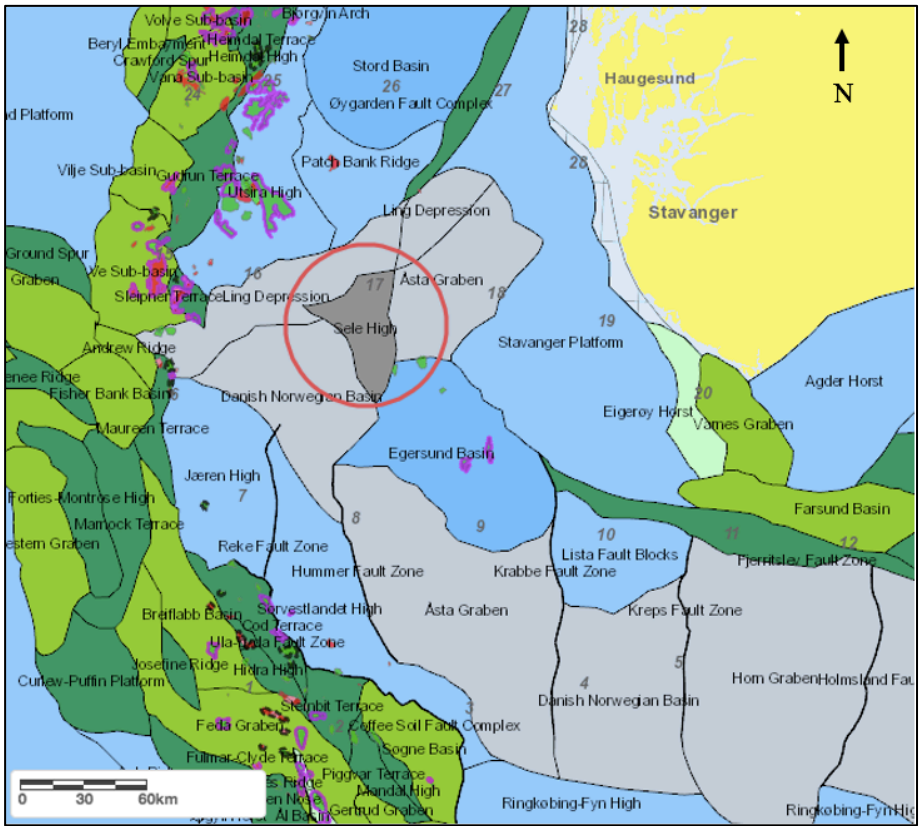

Figure 1. Regional map showing the location of the study area encircled in red. The Sele High is located 150 km southwest of Stavanger. (modified from npd.no/factmaps).

1.2 Motivation

The regions of extension typically occur in crust that has earlier been part of orogenic events. The rifts and extensional tectonics usually occur in a heterogeneous lithosphere which may exert considerable stress influence over the geometry, distribution of faults, and the overall deformation that may lead to a complex interplay and fracture network (e.g., Fazlikhani et al., 2017; Phillips et al., 2019). The Sele High is developed in a structurally complex area that has been a part of two orogenic events and at least three phases of extensional tectonics, creating several interesting questions which will be studied during the current research work, such as:

- Were Devonian sediments within the Sele High deposited in basins resulting from collapse tectonics at the end of the Caledonian Orogeny?
- Can the Ling Depression be linked to the Hardangerfjord Shear Zone mapped onshore?
- To what degree did the structural template inherited from the Devonian control later rifting events in the Permian-Triassic and Jurassic-Cretaceous?
- What controlled the distribution of evaporite deposits in the Permian?
- How did faulting affect mobilization of evaporites, and how did active fault systems evolve in the presence of salt?

The excellent 3D seismic images and the shallowness of these older stratigraphic units make the area perfect for interpreting deeper pre-Zechstein stratigraphy.

1.3 Research objectives

The objectives of this research are:

- Generate a seismic-stratigraphic framework of the Sele High.
- Assess the spatial and temporal evolution of faults.
- Analyze the tectonostratigraphic evolution of Sele High with emphasize on the Pre-Permian evolution.
- Distribution and role of different Zechstein facies.

1.4 Research backgrounds

The local highs in the North Sea are often of substantial interest to oil and gas companies as the generated hydrocarbons from the deep graben system migrate to these shallow highs, making them a perfect target for hydrocarbon exploration. The Sele High is no difference; although the most recent exploration well drilled by Lundin was dry, the area is still of considerable interest

due to its presence in the proximity of the Johan Sverdrup oil field over the Utsira High. The Johan Sverdrup field is the third-largest oilfield ever found on the Norwegian Continental Shelf. It is the main reason for the continued interest in understanding the geological evolution of this region (e.g. Hansen et al., 2020; Jackson and Lewis, 2016; Kalani et al., 2020; Phillips et al., 2016). The Johan Sverdrup is located on the Utsira High, separated from the Sele High by the 20-30 km wide Ling Depression. A detailed understanding of Sele High would help to further understand how Utsira High has developed.

The North Sea is an intracratonic rift basin that developed on an heterogenous crust with structural elements originating from the Caledonian orogeny and the Devonian post-orogenic extension. The heterogeneous crust heavily dictated the deformation and rifting in the later extensional events occurring during the Late Permian-Early Triassic and Late Jurassic-Early Cretaceous, oriented E-W and NW-SE, respectively, in the North Sea (e.g., Bird et al., 2014; Clemson et al., 1997; Daly et al., 1989; Færseth, 1996; Paton and Underhill, 2004; Phillips et al., 2019; Phillips et al., 2016; Scheiber et al., 2015; Whipp et al., 2014).

The long history of hydrocarbon exploration in the North Sea has made it one of the world's most studied and well-documented areas due to the availability of extensive and advanced geological and geophysical datasets. However, the pre-Triassic history and related heterogeneities are poorly understood due to a complex history of rifting, thermal cooling, subsidence and sedimentation. In addition, the Zechstein strata (evaporitic successions) impact the seismic imaging of the deeply buried strata and complex structural geometries in this region (Kalani et al., 2020). Thus, the Permian and older periods' evolution in the North Sea is poorly understood compared to the younger periods (Serck et al., 2022). Therefore, the basement highs are of great importance, offering better resolution and accessibility to the older stratigraphy with less overprint from younger stratigraphy.

2. Geological setting

The following chapter places the study area in geological context. The units of most interest are those preceding the Zechstein Supergroup. So, the chapter will focus on describing the structural and stratigraphical framework and the geological evolution of the central North Sea in general and with extra emphasis on the Sele High.

2.1 Structural framework

The Norwegian Continental Shelf (NCS) is located offshore southern, western, and northern Norway. It comprises three regions; the Western Barents Sea in the north; the Norwegian-Greenland Sea in the northwest; and the North Sea in the south and southwest. The North Sea is an intracratonic rift basin confined by the Norwegian Sea and the Shetland Islands to the north, Great Britain to the west, core Europe to the south, and Scandinavia to the east. The North Sea has a dominant structural feature, the trilete rift system (Davies et al., 2001). It contains the three failed rift arms: Viking Graben stretching North-South, Central Graben going northwest-southeast, and Moray Firth Basin oriented east-west (Fig. 1.1).

The orientation and distribution of faults in the central North Sea are affected by the proximity to the triple junction of the three failed rift arms. In the southern part of the central North Sea, the faults align with the Central Graben, and in the Northern part the faults align with the Viking Graben. However, in the central part, another central feature seems to dominate the orientation, namely the Ling Depression. The Ling Depression has an SW-NE orientation and is believed to originate from the Hardangerfjord Shear Zone (HSZ) (Færseth, 1996). The Ling Depression separates two main features in the central North Sea, the Sele High to the south and the Utsira High to the north. The Åsta Graben, Egersund Basin, and Norwegian-Danish Basin are also prominent structural elements within the central North Sea. The Sele High is a Paleozoic high that is enclosed by the Ling depression to the north, Danish Norwegian Basin and Åsta Graben to the west and east respectively and Egersund Basin to the south (Fig. 1.1).

2.2 Geological evolution

The most important periods for the geological composition of the North Sea starts with the Caledonian Orogeny which occurred during Ordovician to Early Devonian (Ziegler, 1975). Then extension and collapse of the Caledonian Orogen during the Devonian times led to the

formation of some major shear zones (e.g., Andersen and Jamtveit, 1990; Andersen et al., 1999; Fossen, 1992; Norton, 1986). Later the Late Permian-Early Triassic and Late Jurassic-Early Cretaceous extensional events with the E-W and NW-SE orientation respectively, led to the regional rifting, extensional faulting and reactivation of the detachment zones in the North Sea caused formation of the complex structures and geometries (e.g., Bird et al., 2014; Færseth, 1996; Phillips et al., 2019; Phillips et al., 2016).

The most important events in the geological evolution of the North Sea are summarized as:

1. Formation of the Caledonian Orogeny during the Ordovician to Early Devonian (Ziegler, 1975).
2. Extension driven by the collapse of the Caledonian Orogen during the Early Devonian which led to formation of some major shear zones (e.g., Andersen and Jamtveit, 1990; Andersen et al., 1999; Fossen, 1992; Norton, 1986).
3. Rifting phase 1 (RP1): Permian – Early Triassic with an extensional direction of E-W.
4. Rifting phase 2 (RP2): Late Jurassic – Early Cretaceous with an extensional direction of NW-SE.

2.2.1 Ordovician to Early Devonian: Caledonian Orogeny

The Caledonian orogeny was initiated with the collision of Laurentia, Baltica and Avalonia from 490-390 Ma / Late Ordovician-Early Devonian (McKerrow et al., 2000). Before the collision of the three continents, they were separated by ancient seas. The southern and northern Iapetus Ocean separated Laurentia from Avalonia and Laurentia from Baltica, respectively, and the Tornquist Sea separated Avalonia from Baltica (Coward et al., 2003; Trench and Torsvik, 1992). The collision created a massive mountain chain, and two sutures called the Iapetus Suture and the Trans-European Suture Zone, Thor Suture or Tornquist Suture Zone. The Iapetus Suture separating Avalonia and Laurentia lies to the west (Beamish and Smythe, 1986), while the Trans-European Suture Zone separating Baltica and eastern Avalonia is to the east (Pharaoh, 1999) (Fig. 2.1). The northern margin of the Iapetus Ocean is believed to have had an oblique subduction during the Late Ordovician and Silurian, resulting in a transpressive regime responsible for developing an accretionary wedge and major sinistral strike-slip movements along the trend of the Iapetus Ocean creating the terranes in the British Isles (Hutton, 1987; Leggett et al., 1983; McKerrow, 1988; Soper and Hutton, 1984). The southern boundary of the Southern Uplands is presumed to correlate with the Iapetus Suture (Hutton, 1987), which can

be traced into the Central North Sea on deep seismic data (Freeman et al., 1988; Watson, 1985), the continued eastward path is not clear (Fig. 2.1). The Caledonian Deformation Front (CDF) represent the present-day extent of Caledonian rocks (Fig. 2.1), although the name argues it represent the easternmost limit of deformation which is not correct as there is Caledonian deformation in the Oslo region (Morley, 1986). Therefore an more realistic deformation front is proposed by (Kalani et al., 2020).

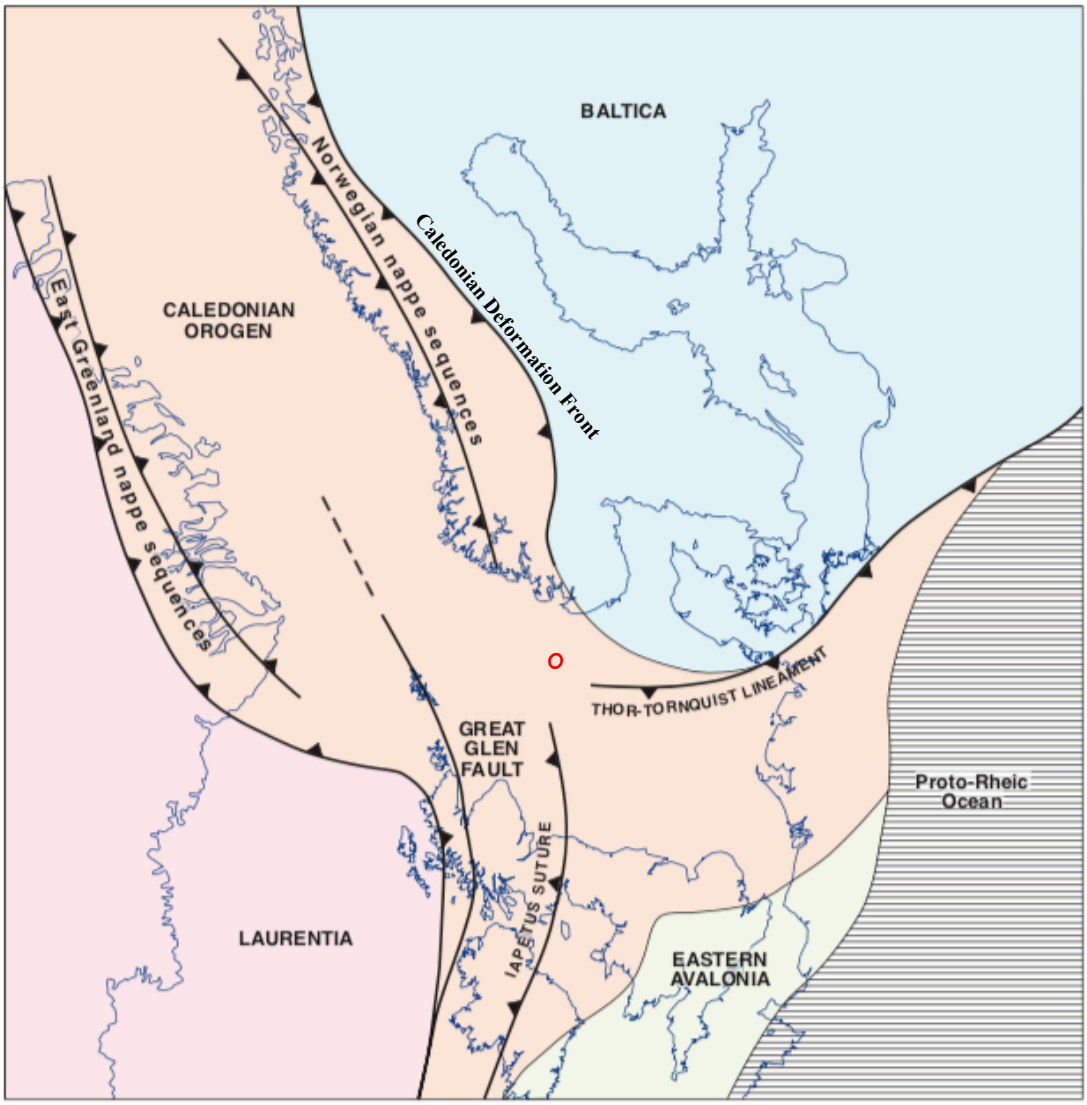

Figure 2.1. Shows the geographical extent of the three different plates, the Iapetus suture, the Tornquist suture, and the Caledonian Deformation Front. The study area is encircled in red. Modified from (Evans et al., 2003).

2.2.2 Devonian: Caledonian collapse

In the Devonian, the build-up of the Caledonian Orogeny entered its terminal phase and the weight of the over-thickened crust resulted in gravitational collapse, changing the stress regime from compressive to extensional (Andersen and Jamtveit, 1990; Andersen et al., 1991; Braathen

and Erambert, 2014; Braathen et al., 2004; Dewey, 1988; Fossen, 1992; McClay et al., 1986; Osmundsen and Andersen, 2001). In the Mid- to Late Devonian extension was accommodated by left-lateral strike-slip movement in Northwest Europe (NW Europe), giving rise to a pull-apart system (i.e., Mode II reactivation (Fossen, 1992)) bounded by Møre-Trøndelag fault zone in the northeast and the Iapetus Suture in the Southwest (Chauvet and Séranne, 1994; Osmundsen et al., 2006; Roberts et al., 1999; Séguret M et al., 1989; Seranne, 1992). This system is believed to have accommodated more than 200-300 km of extension to achieve at least 60 km vertical uplift of the eclogites in the western Norwegian bedrock (Roberts et al., 1999). Several shear zones seen onshore in western Norway were formed in the extensional setting, which accommodated much of the extension (Fig. 2.2). The shear zones range from 1-5 km in thickness (Andersen and Jamtveit, 1990). Some of the shear zones are believed to continue offshore and influence the later developments in the North Sea, such as the Ling Depression. During the mode II reactivation, several Devonian basins were created, which today are seen both onshore and offshore in southern and western Norway and the northern part of the British Isles. The Devonian basins seen onshore western Norway are located within E-W trending synclines in the syncline-anticline system created by the extension of the orogenic welt (Andersen, 1998; Braathen and Erambert, 2014; Osmundsen and Andersen, 2001). The Devonian basins are considered to be much more widespread and numerous than evident today (Sherlock, 2001). The paleo-magnetic data confirm the lateral movement of the Laurentia and Baltic relative to each other (Torsvik et al., 1996).

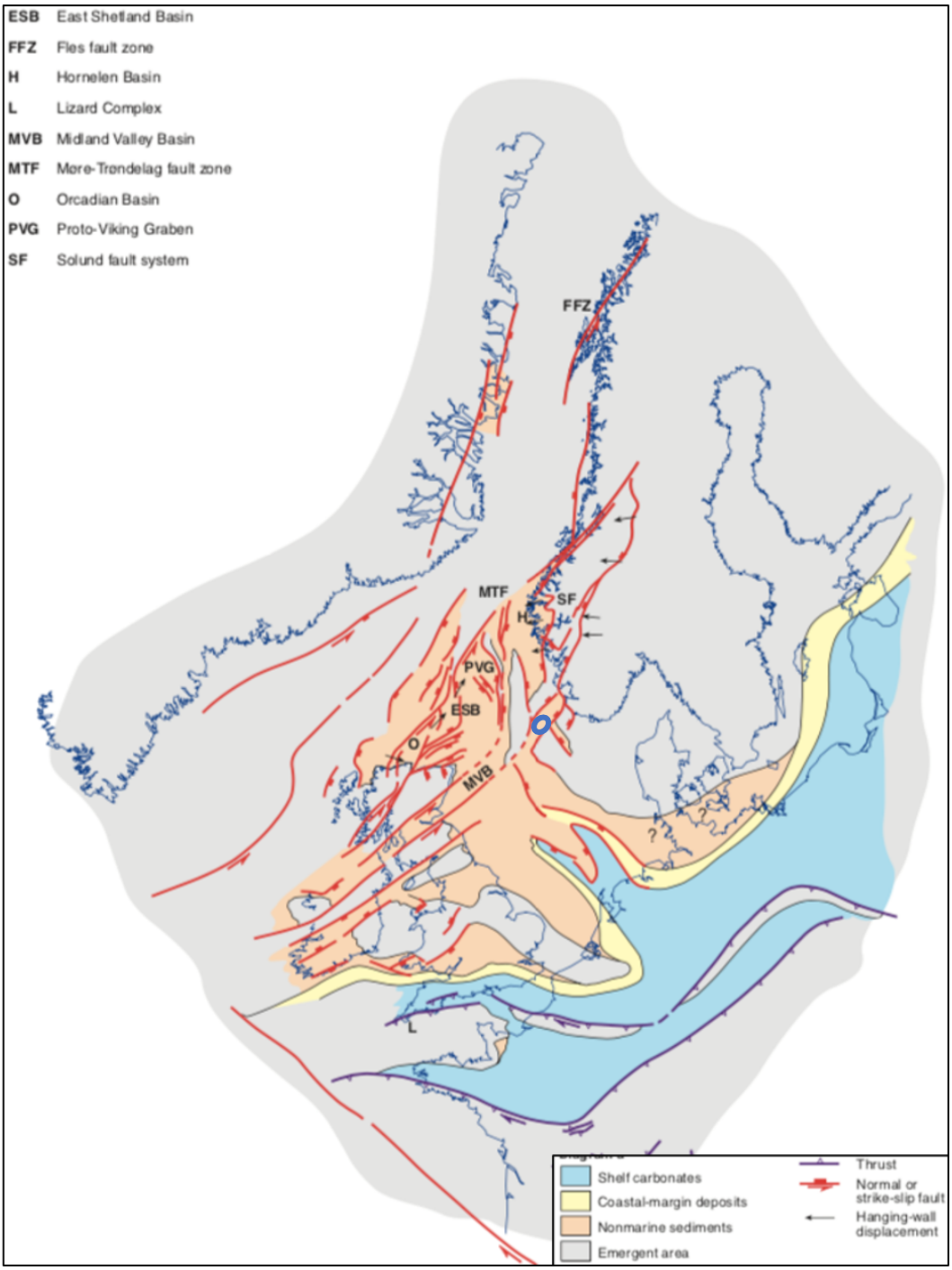

Figure 2.2. Mid-Devonian palinspastic map showing the active structures and sediment facies. The study area is encircled in blue. Modified from (Coward et al., 2003).

2.2.3 Carboniferous to Late Permian

The Carboniferous is the poorest understood period in the North Sea, especially within the NCS, as there are no findings of Carboniferous strata. However, the Devonian basins throughout the western Norway, the North Sea, and the northern British Isles record inversion and east-west oriented compressional folds (Chauvet and Séranne, 1994; Coward et al., 1989; Roberts et al.,

1999; Seranne, 1992). The timing of these folds for the northern North Sea is disputed and there seem to be different origins for the folds in British sector and onshore Western Norway. The post-folding magnetic overprint seen in western Norway are dated to the Late Devonian (Torsvik et al., 1988) and new research from Osmundsen et al. (2023) assert that the folds from western Norway are extension-parallel folds forming during basin infill in an three-stage process during the Devonian. For the British sector Coward et al. (1989) argue it originates from the Devonian and tectonic events during the Variscan and Late Carboniferous, and consensus now seem to be on the Late Carboniferous (Armitage et al., 2021). The southern North Sea also recorded inversion during the Carboniferous, also originated from the Variscan Orogeny in the Late Carboniferous (Coward et al., 2003). Uplift during the Late Carboniferous – Early Permian led to erosion and truncation of the Devonian and Carboniferous strata throughout the North Sea (Ziegler, 1992) as earlier work on the Mid North Sea High Region (Brackenridge et al., 2020), Orcadian Basin (Armitage et al., 2021; Coward et al., 1989; Dichiarante et al., 2020) Kraken High and Fladen Ground Spur (Patruno and Reid, 2017) confirm. This large unconformity represents several kilometers of uplift and is related to thermal instability and the Variscan fault movements (Coward et al., 1989; Glennie and Underhill, 1998; Seranne, 1992).

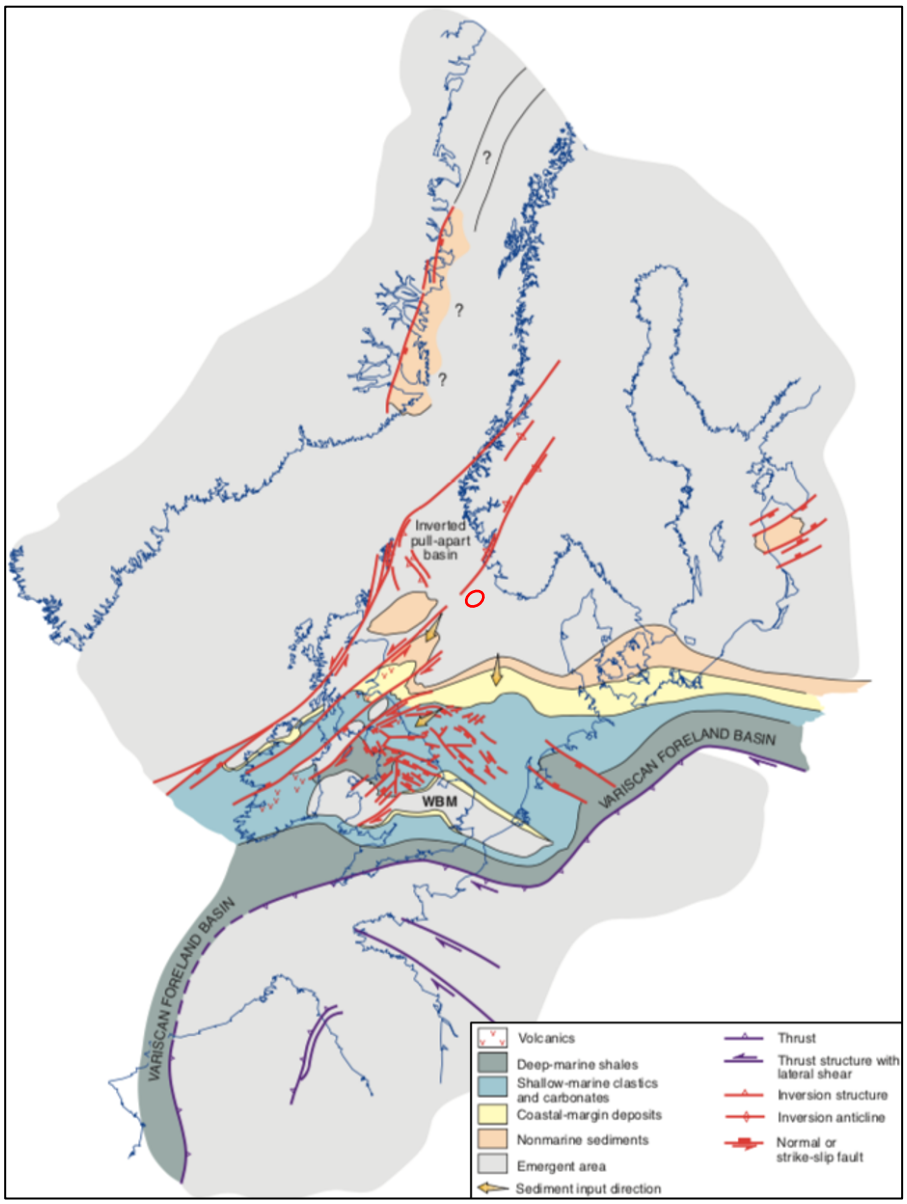

Figure 2.3. Palinspastic map showing the active structures and sediment facies during the Early Carboniferous. The study area is encircled in red. Modified from (Coward et al., 2003).

At the Carboniferous-Permian transition, a complex strike-slip fault system developed over the North Sea with some reactivation of the Devonian strike-slip faults. Early Permian extension led to the formation of several major faults in the Central North Sea, such as the Sele High and Stavanger fault systems (Jackson and Lewis, 2013, 2016; Sørensen et al., 1992). The extension was possibly a response to the collapse of the Variscan orogeny (Phillips et al., 2016; Ziegler, 1992). At the end of the Early Permian, the extension abated, and the subsequent thermal subsidence accompanied by thermal relaxation of the lithosphere resulted in the North and South Permian Basins (Phillips et al., 2016; Ziegler, 1992). Sele High is located within the North Permian Basin.

2.2.4 Late Permian to Early Triassic: Rift Phase 1

In Late Permian, Pangea started to rift apart, creating an extensional setting in NW Europe (Ziegler, 1992). This led to Rift Phase 1 of the North Sea which developed from the Late Permian to the Early Triassic (Færseth et al., 1995; Lervik et al., 1989; Steel and Ryseth, 1990). The E-W rifting created several N-S trending structures in the northern North Sea (Færseth, 1996) and reactivated N-S trending faults in the central North Sea (Jackson and Lewis, 2013, 2016; Sørensen et al., 1992) to create the continuous Åsta Graben and Horda Platform basin (Fig. 2.4) (Færseth, 1996). It also formed the foundation for the Viking Graben (Fig. 2.4) (Badley et al., 1988; Badley et al., 1984; Gabrielsen et al., 1990; Lervik et al., 1989; Yielding et al., 1991). However, some structures with deviating strikes, mainly on the East Shetland Platform, are created during this rifting period. This indicate either a multidirectional extension (Goldsmith et al., 2003; Ziegler, 1988) or reactivation of pre-existing Caledonian or Devonian structures, which is angular discordant to the Permo-Triassic structures (Færseth, 1996). Regardless the structural framework from the Caledonian and the Devonian have influenced the extension of the northern North Sea (Coward, 1993; Fossen et al., 2000; Færseth, 1996; Ziegler, 1992). At the more structurally complex central North Sea several Paleozoic elements have exerted their influence. The Utsira and Sele were intra-basinal highs during this rifting and have no syn-rift deposition. In the central and southern North Sea, the rifting triggered flow of the ductile Zechstein Supergroup (Jackson et al., 2013; Lewis et al., 2013).

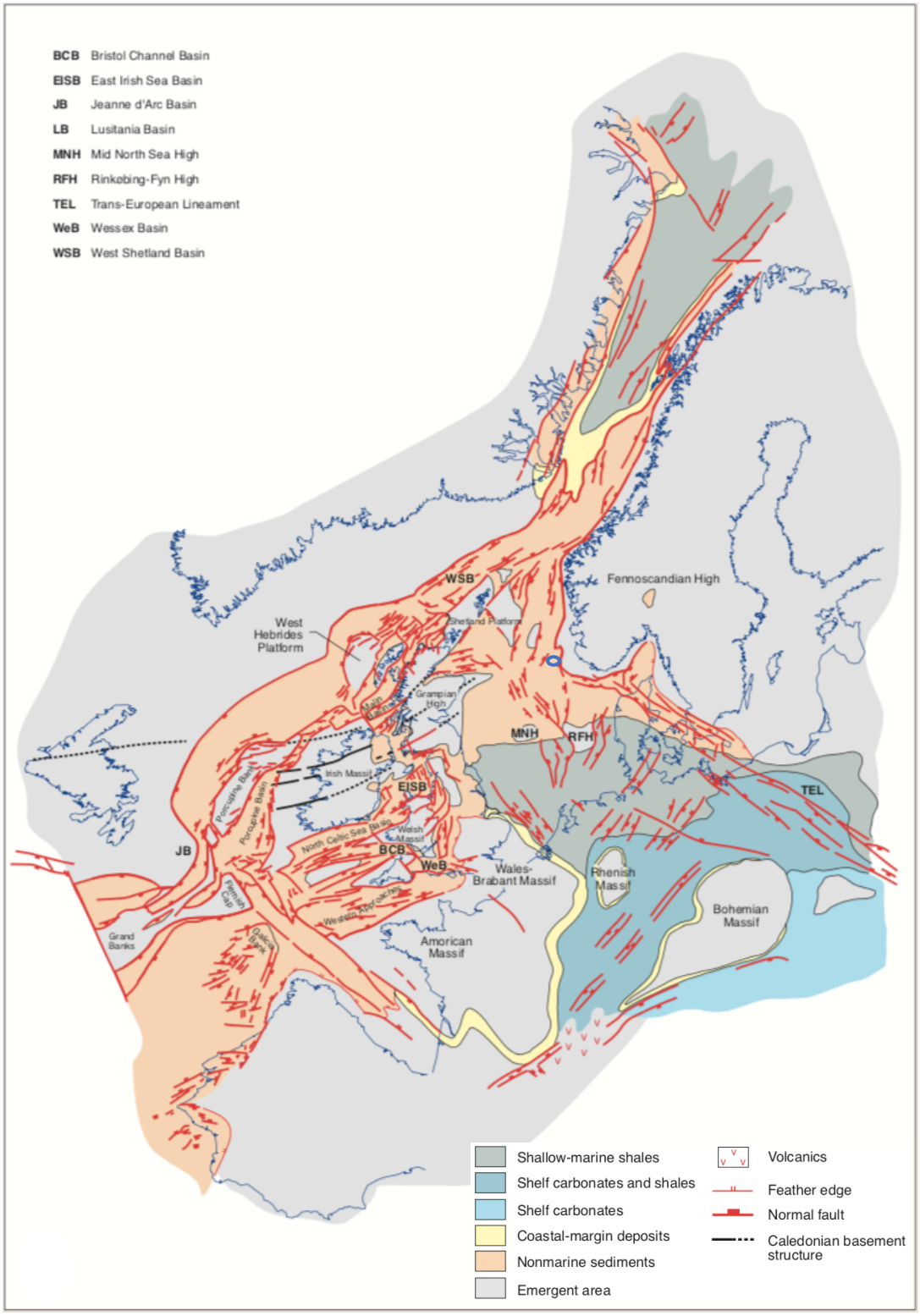

Figure 2.4. Mid-Triassic palinspastic map showing the position of the active structures and sedimentary facies. The study area is encircled in blue. Modified from (Coward et al., 2003).

2.2.5 Middle Triassic to Late Jurassic

At Middle Triassic, the extension abated, initiating a period of approximately 70 million years of tectonic quiescence and thermal subsidence (Færseth, 1996; Roberts et al., 1993). The thermal subsidence and sedimentary loading in this inter-rift period caused a broad basin to be

developed in the North Sea, with deposition on the intra-basinal highs as well (Bartholomew et al., 1993; Færseth, 1996; Ziegler, 1990). The Mid-Cimmerian or intra-Aalenian Unconformity is presumed to originate from a thermal up-doming during the Early–Middle Jurassic transition (Fig. 2.5) (Davies et al., 1999; Underhill and Partington, 1993). It is centered around the North Sea triple junction, 100 km west of the study area, and caused widespread erosion removing large thicknesses of Lower Jurassic and Upper Triassic strata, especially in the Central North Sea but also other areas of the North Sea (Fig. 2.5). Late Jurassic marine sediments are deposited above the unconformity, indicating a fast transgression associated with the dome's collapse. This doming may be interlinked with the 7400 km^2 large province of the Rattray Volcanics, which is of Mid-Jurassic age and centered in the North Sea triple junction (Quirie et al., 2019) as the dome is generally believed to originate from volcanic activity (Davies et al., 2001; Smith and Ritchie, 1993).

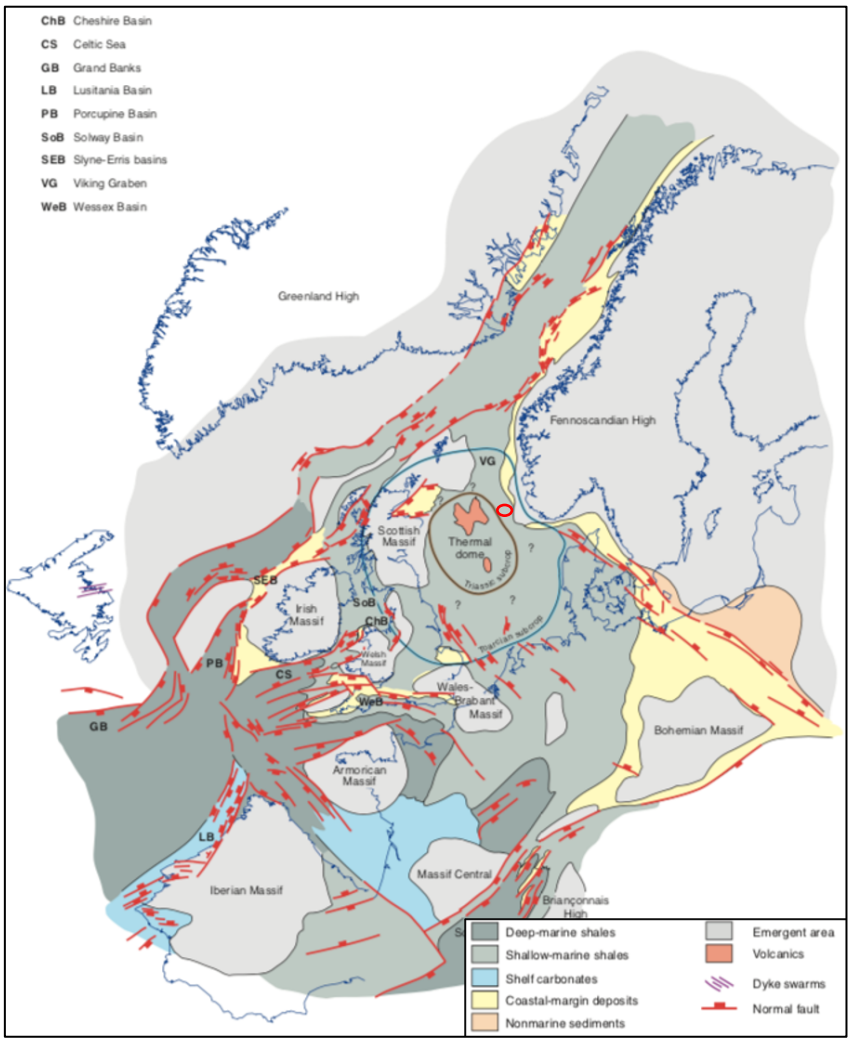

Figure 2.5. Palinspastic map of the Early Jurassic showing active structures and sedimentary facies and especially the location of the thermal doming in the central North Sea. The study area are encircled in red. Modified from (Coward et al., 2003).

2.2.5 Late Jurassic to Early Cretaceous Rift Phase 2 (RP2) and Post-rift Evolution

In the Middle to Late Jurassic collapse of the aforementioned dome initiated a phase of renewed rifting in the North Sea lasting until the Early Cretaceous (i.e., Rift Phase 2; e.g., Badley et al., 1988; Færseth, 1996; Phillips et al., 2019; Underhill and Partington, 1993; Ziegler, 1992). Rift Phase 2 started before thermal equilibrium was reached from Rift Phase 1, causing wider thermal subsidence to be active simultaneously with the more localized stretching (Gabrielsen et al., 1990; Giltner, 1987; Roberts et al., 1993). The extension direction is debated either as E-W (Bartholomew et al., 1993; Bell et al., 2014) or WNW-ESE (Doré et al., 1997; Færseth, 1996). Rift Phase 2 localized in what is identified as the center of Rift Phase 1 (Giltner, 1987; Klemperer, 1988), and reactivating pre-existing structures as well as initiating new faults (Færseth, 1996; Phillips et al., 2016) to create the trilete rift system we see today comprising of the Central Graben, Moray Firth Basin and the Viking Graben (Fig. 2.6) (Davies et al., 2001). The rifting of Viking Graben was not synchronous, initiating in the triple junction in the Central North Sea before migrating northwards (Phillips et al., 2019) until another triple junction connecting with the spreading ridge of the northern Atlantic (Fig. 2.6). The eustatic sea level rose simultaneously as rifting, which induced rapid subsidence and deposition of upward-deepening marine sediments (Jackson and Lewis, 2013; Sørensen et al., 1992). This also led to rapid growth of the salt diapirs in the Sele High area. When rifting abated during Early Cretaceous, the North Sea became a thermal subsiding sag basin because extension localized in the future spreading ridge of Northern Europe and Greenland (Ziegler, 1992). In the South and Central North Sea, the thermal subsidence was interfered by an inversion phase during Late Cretaceous associated with the Alpine orogeny (Biddle and Rudolph, 1988; Jackson et al., 2013; Ziegler, 1992). Around the Sele High area, the inversion caused minor uplift of the hanging wall and compression of salt diapirs and created a longitudinal buttress fold on the Stavanger Fault System (Jackson et al., 2013; Jackson and Lewis, 2016).

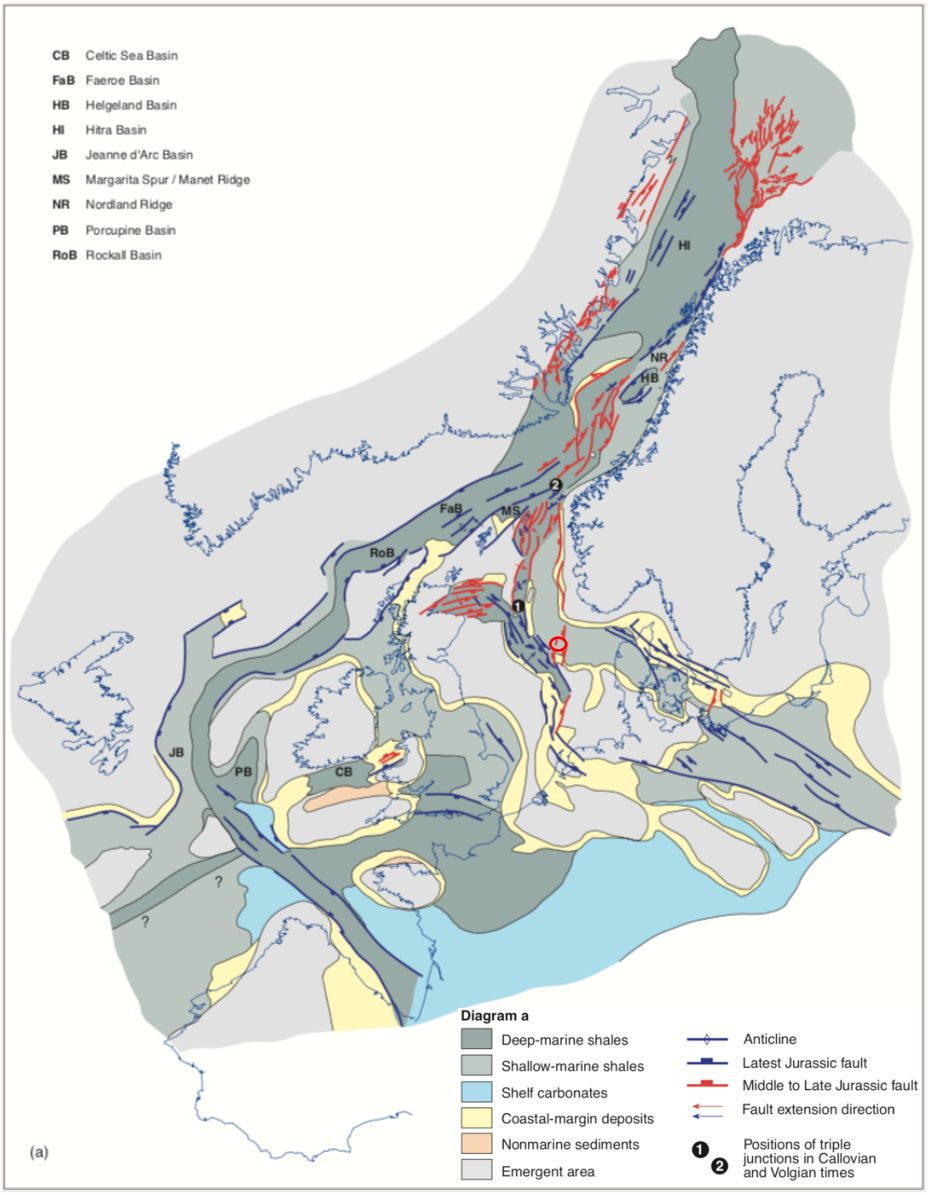

Figure 2.6. Palinspastic map of the Late Jurassic showing the position of active structures and sedimentary facies. Also shows the migration of the active triple junction. Study area are encircled in red. Modified from (Coward et al., 2003).

2.2.6 Cenozoic

During the Cenozoic the North Sea was a wide epicontinental basin centered on the Viking Graben. It experienced two phases of uplift (Faleide et al., 2002). The first caused by the Iceland Plume during Late Paleocene to Early Eocene, which uplifted the entire North Sea but affected the western North Sea to a greater extent causing tilting and erosion of the East Shetland Platform, which was deposited to the east (Faleide et al., 2002). The second is related to the isostatic response to the unloading caused by glacial erosion and melting of the Scandinavian Ice sheet at the Pliocene – Pleistocene transition, also feeding the North Sea basin. At the central North Sea, Cenozoic reaches an approximate thickness of 2.5 km.

2.3. Regional stratigraphic framework

2.3.1. Silurian - Devonian stratigraphy

North Sea position during Late Silurian and Devonian was between 15-30 degrees south, meaning it was a warm and arid to semi-arid climate throughout the North Sea (Tarling, 1985; Torsvik and Cocks, 2016a). At the start of the Devonian, NW Europe was an onshore landscape dominated by mountains with numerous locally restricted basins caused by extension and collapse of the Caledonides (Fig. 2.7) (Marshall and Hewett, 2003). Leading to internal drainage and alluvial and lacustrine depositional environments. During Mid-Devonian, the deposition became widespread and stretched from the shores of Moray Firth to western Norway and eastern Greenland. The depositional environment also became more lacustrine dominated. Several extensive depocenters, such as on the Sele High, Hornelen Basin and Orcadian Basin, also occurred (Fig. 2.7). The rifting activity is argued to stop during Late Devonian (Marshall and Hewett, 2003), however this is very uncertain and some argue it continued during the Carboniferous (Eide et al., 2002), and the drainage system became much larger and more open. The depositional environment was now mainly fluvial (Stuart et al., 2001). The Old Red Group was later eroded, evident by seismic transects and wells that encountered the basement without penetrating the Old Red stratigraphy (Marshall and Hewett, 2003).

2.3.1.1. Lower Old Red Group

The Lower Old Red Group is deposited subsequent to the uplift and erosion of the Caledonian orogeny; hence the base of the group is a basement-cover contact. The group was deposited during Late Silurian and until the end of Early Devonian. It contains sandstones and conglomerates (Marshall and Hewett, 2003).

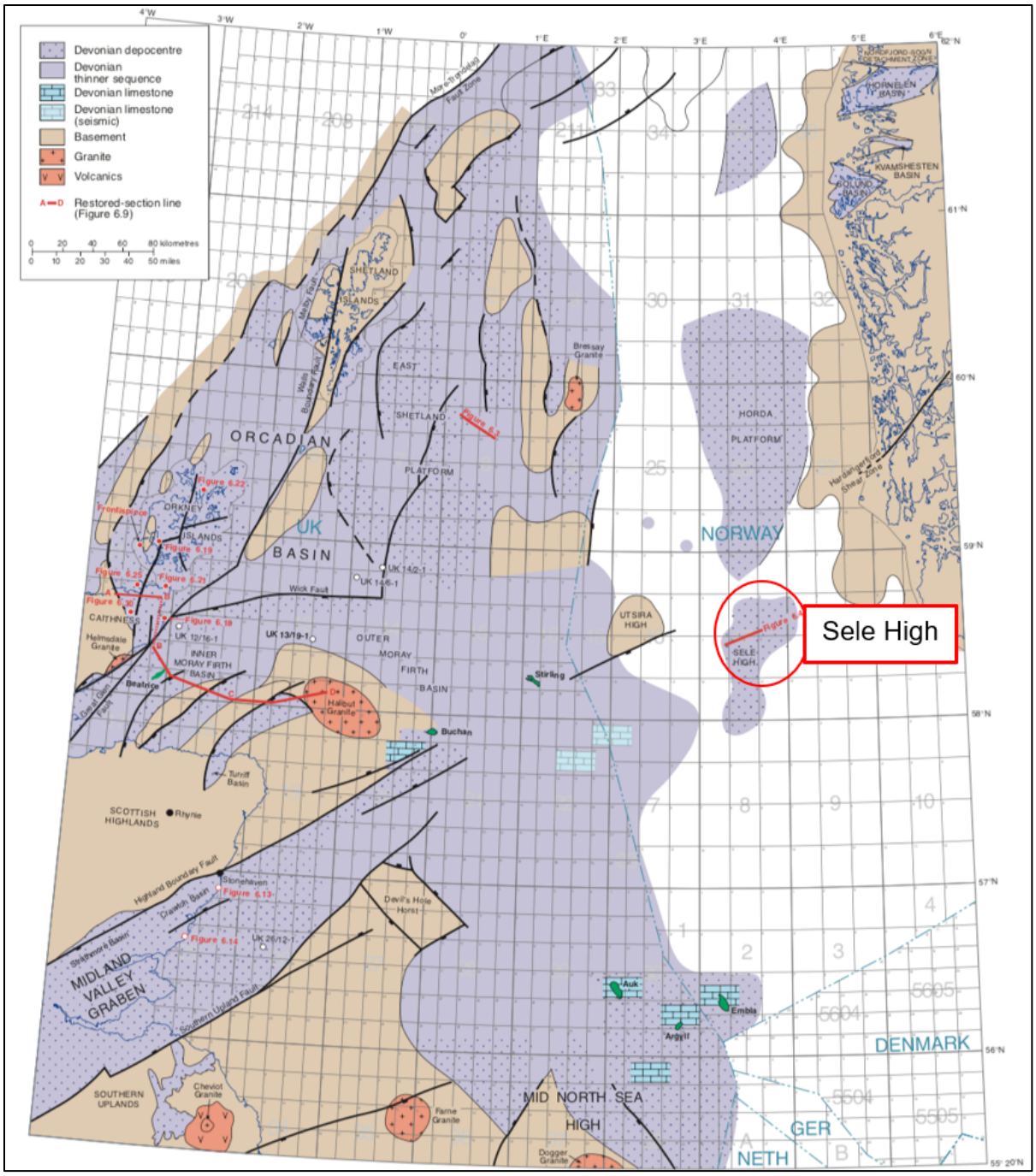

Figure 2.7. Shows the Norwegian and UKs continental shelfs. Black dotted purple indicates Devonian depocenters while purple indicate thinner Devonian sequences. Sele High was a depocenter during Devonian. The study area is encircled in red. (Marshall and Hewett, 2003)

2.3.1.2. Middle Old Red Group

The Middle Old Red group is the dominant stratigraphy in the Orcadian Basin and surrounding area (Marshall and Hewett, 2003). It was deposited during Mid-Devonian times and consists of conglomerates, sandstones, shales and some marl.

2.3.1.3. Upper Old Red Group

Upper Old Red was deposited during Late Devonian until Viséan and are sandstone dominated (Marshall and Hewett, 2003).

2.3.2. Carboniferous stratigraphy

During the Carboniferous, NW Europe was drifting northwards. At the Viséan age, the North Sea had reached latitudes between 20-10 degrees south, making the climate more humid. Entering Moscovian, NW Europe was 0-10 degrees north, meaning the North Sea was at tropical latitude during this period (Torsvik and Cocks, 2016b). A transgression, entering from the south, arises at the beginning of the Carboniferous (Anderton, 1979). Both events changed the depositional environment from the red continental beds of the Devonian to a broader spectrum during the Carboniferous period containing deltaic, marine, continental, and fluvial sedimentation (Bruce and Stemmerik, 2003). The Carboniferous is probably the least understood period in the North Sea, especially within the NCS (Fig. 2.10). Findings of the strata from Mississippian and Early Pennsylvanian in Carboniferous are restricted to the Southern North Sea and British Northern North Sea (Fig. 2.8). The Early to Late Pennsylvanian strata are abundant in the Southern North Sea and onshore UK and exist to a lesser extent in the Oslo Graben area. However, it is absent in the Central and Northern North Sea, indicating nondeposition or later erosion (Fig. 2.8).

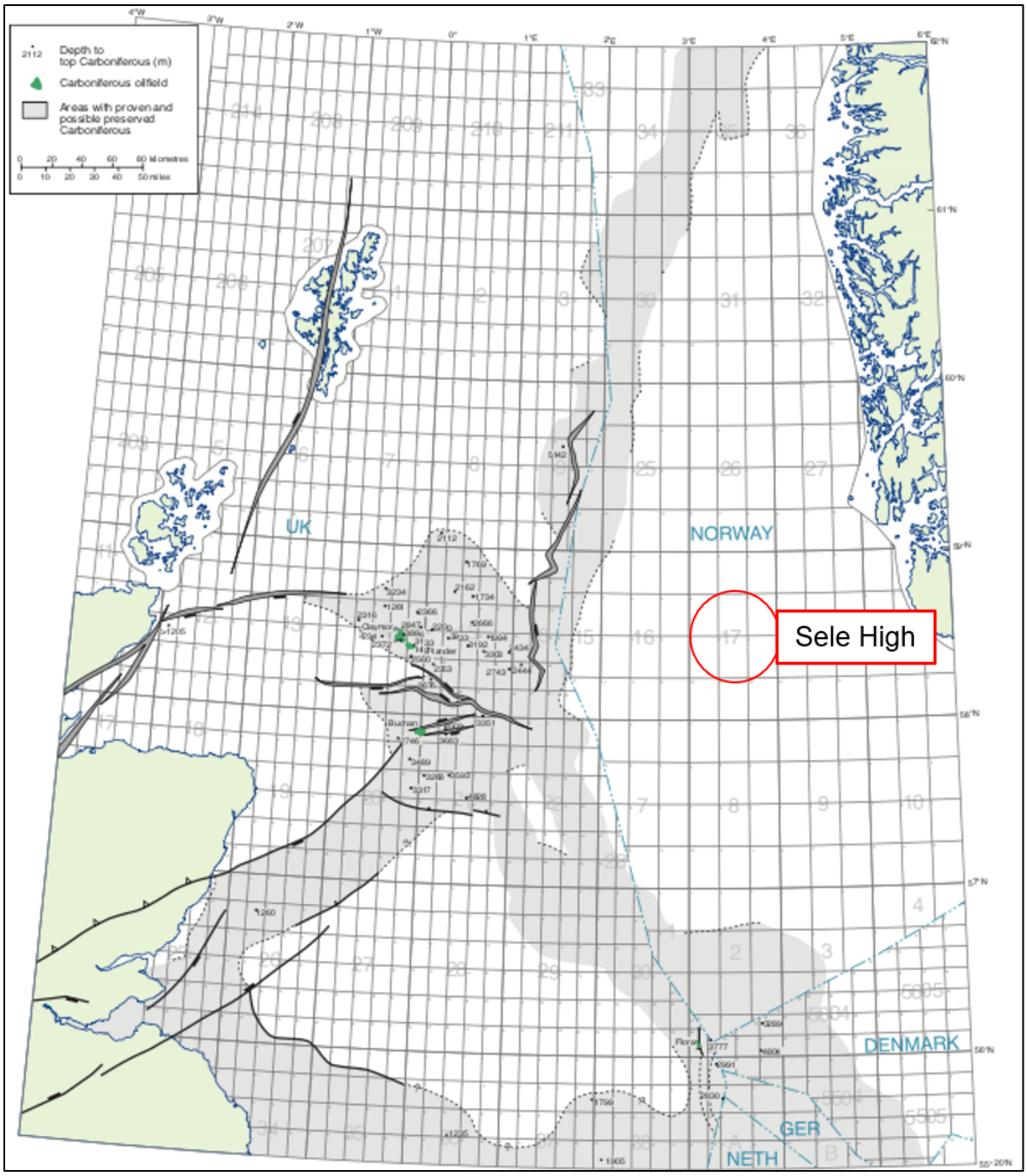

Figure 2.8. Illustrates the proven and possible extent of Carboniferous deposition. red encircles the study area. Modified from (Bruce and Stemmerik, 2003).

2.3.3. Permian stratigraphy

There are two dominant stratigraphic groups during the Permian, the Rotliegend Group and the Zechstein Supergroup (Fig. 2.10). The Rotliegend Group base is often an unconformity and usually superimposes the strata of Devonian, Silurian or Caledonian crust on the NCS caused by the Carboniferous hiatus (Glennie et al., 2003). The Lower Rotliegend is locally dominated by volcanic rocks or continental siliciclastic sediments (Fig. 2.10). In Early Permian, the climate

of the North Sea area was again arid, with desert conditions in the northern hemisphere much like Arabia today (20-30° N) (Glennie, 1997). This led to aeolian sand and sabkhas depositing in low structural areas, while on the Sele High, a structural high at this point, deposition was mainly of continental arkosic sediments (Sørensen et al., 1992). Rotliegend Group is very alike the Old Red Group from the Devonian and is often formed by recycled Old Red deposits making it difficult to differentiate where the Carboniferous strata are missing (Glennie et al., 2003).

The subsidence was greater than the sedimentation resulting in transgression during Permian for south and central North Sea area, causing the continental Rotliegend to be superimposed by the marine Zechstein Supergroup, which is an evaporitic unit composed of mainly halite, anhydrite, carbonates and sulfates, deposited during Late Permian (Heeremans et al., 2004; Jackson and Lewis, 2013) (Fig. 2.10). Zechstein Supergroup is a pan-European unit which documents flooding and desiccation of a restricted marine sea, and its limit is outlined in figure 2.9 (Jackson and Lewis, 2013). The Zechstein Supergroup have significant across-fault changes in thickness and lithology, such as on the eastern boundary fault of the Sele High (halite on hanging wall - carbonate on footwall) (Sørensen et al., 1992). However, it is unclear if the deposition is post-, syn- or pre-faulting (Clark et al., 1998; Dickinson, 1996; Høiland et al., 1993; Penge et al., 1993; Stewart and Clark, 1999). In the same way, the Zechstein Supergroup is overall halite-rich in the basin center, and carbonate- and anhydrite-rich on the basin margin (Stewart and Clark, 1999; Tucker, 1991), which infer that halite is deposited in the structural lower areas while carbonate and anhydrite in the structural higher areas. The sea level fluctuated during the deposition of the Zechstein Supergroup, probably driven by the melting and growth of the Permian ice sheets (Glennie, 1997), which gave rise to 3 to 4 depositional cycles of the Zechstein Supergroup (Glennie et al., 2003). Sediment thickness reached a maximum of 2000 m in the North Permian basin and 3500 m in the southern (Ziegler, 1992).

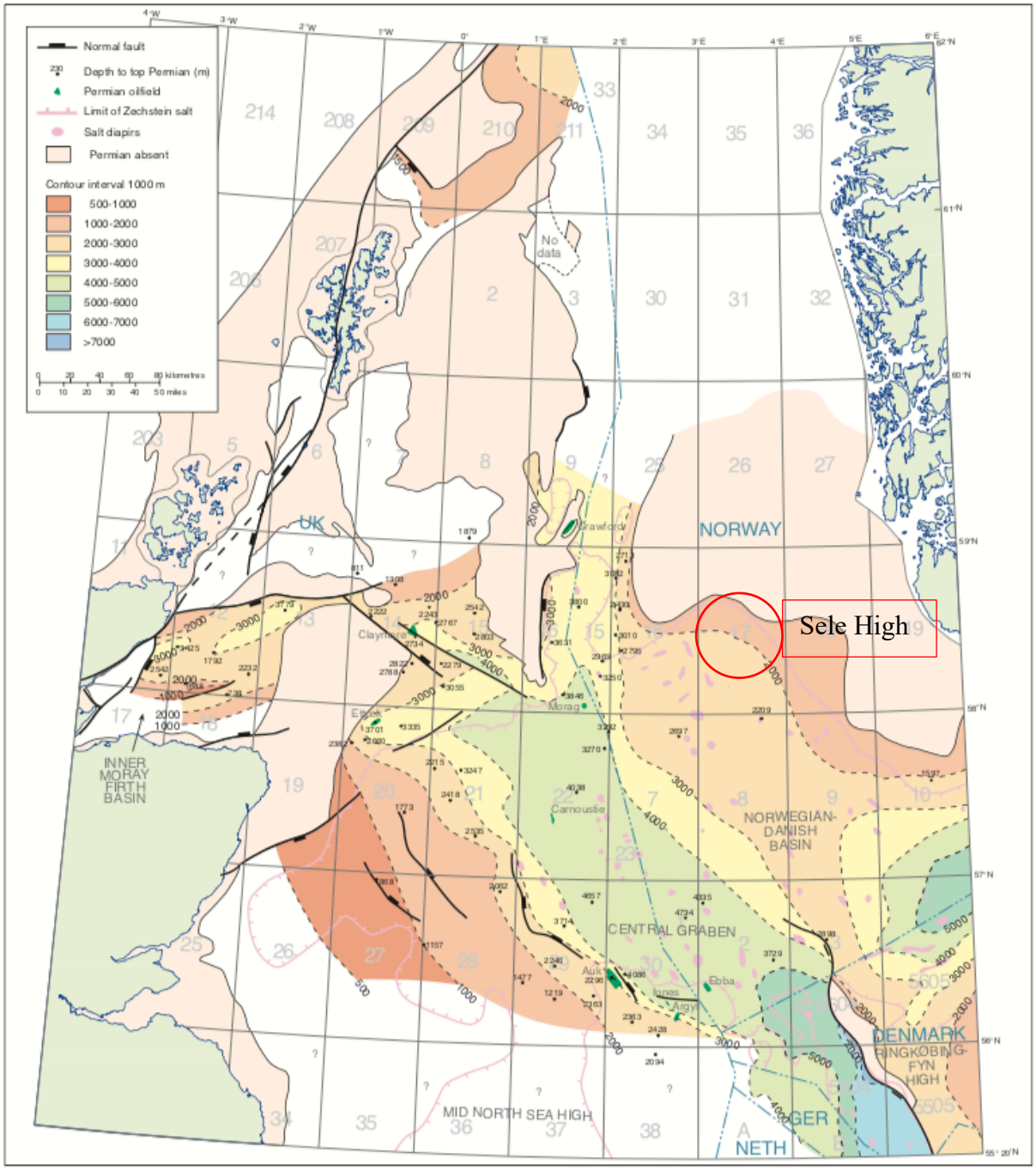

Figure 2.9. Shows the depth to the Permian stratigraphy and where it is absent. white area is where there is no data on the Permian stratigraphy. The study area is encircled in red. Modified from (Goldsmith et al., 2003)

2.3.4. Triassic stratigraphy

The Triassic stratigraphy consists of Smith Bank, Teist, Lomvi, Alke, Skagerrak, and Gassum Fm's in the Sele High area (Deegan and Scull, 1977) (Fig. 2.10). Their deposition was controlled by the regional extension and flow of the Zechstein Supergroup (Jackson and Lewis, 2013). NW Europe was at 20-30°N at the start of the Triassic (Doré, 1992) and drifted 11-12° northwards during this period (Torsvik et al., 2001). Triassic strata are therefore deposited in

arid to semi-arid conditions becoming more cool and humid throughout Triassic (Goldsmith et al., 2003). All formations are continental deposits though some marine influence is identified in the eastern and southern parts of the Central North Sea. Transgression occurred throughout Triassic, culminating in Early Jurassic (Haq et al., 1987). The tectonostratigraphic development of NW Europe was dominated by the discontinuous rifting and overall subsidence during Triassic and Jurassic (Goldsmith et al., 2003). Vast amounts of sediments were deposited in the Early Triassic induced by the accommodation space provided by the dissolution and withdrawal of the underlying Zechstein and the overall rifting and subsidence. Smith Bank formation was deposited in Lower Triassic in a playa-lake environment and consisted mainly of red silty mudstones with a complete absence of palynomorphs (Fig. 2.10). The Teist Formation consists of sandstone, mudstone, claystone, and marl, which are interbedded. The Lomvi Formation is comprised of fine to coarse-grained kaolinitic sandstone. The Skagerrak Formation is sandstone dominated but includes three cycles of mudstone (Fig. 2.10). The earliest Skagerrak Formation, composed of sandstone, was deposited around the Lower to Middle Triassic boundary (Goldsmith et al., 1995). The depositional environment alternates between fluvial, arid and swamp-like conditions (Goldsmith et al., 2003). The Viking Graben contain approximately 3 km of Triassic sediments (Giltner, 1987).

2.3.5. Jurassic stratigraphy

At the end of the Early Jurassic, NW Europe was at 40-50° N. The Jurassic period contains several unconformities making most of the Lower and Middle Jurassic stratigraphy missing in all areas of the North Sea except the Northern (Husmo et al., 2003) (Fig. 2.10). The uplift inducing the erosion was caused by doming in the Mid-Jurassic and rotation of fault blocks during the Late-Jurassic (Bartholomew et al., 1993; Færseth, 1996; Underhill and Partington, 1993). The Lower-Jurassic formations Gassum and Fjerritslev are only sporadically present, and Middle Jurassic rocks usually unconformably overlay Triassic strata (Husmo et al., 2003). Gassum Formation is sand-dominated, and Fjerritslev Formation is shale-dominated. The Middle Jurassic unit comprises the nonmarine Bryne Formation, succeeded by the marine Hugin or Sandnes Formations (Fig. 2.10). The aforementioned formations are usually conformably superimposed by Haugesund, Egersund, Lola or Middle Graben shale formations. The Upper Jurassic succession consists of several diachronous and finite formations belonging to the Viking Group on the NCS (Vollset and Doré, 1984) and the Humber Group on the UK sector (Richards et al., 1993). This epoch's most essential and dominant formations are the

diachronous mudstone-dominated Draupne, Kimmeridge Clay, and Heather formations (Fraser et al., 2003) (Fig. 2.10). The first two mudstones mentioned were deposited in anaerobic bottom-water conditions, creating excellent source rocks (Keym et al., 2006; Miller, 1990). Upper Jurassic also comprises a plethora of finite predominantly sandstone intervals, where the two most significant on NCS are the coastal-shallow marine Sognefjord and Ula formations (Fig. 2.10). The Upper Jurassic stratigraphy reaches a thickness of 3000 m in the three grabens created in this epoch. The Sele High area was a shelf at this interval.

2.3.6. Cretaceous stratigraphy

There are three main groups in the Cretaceous, Cromer Knoll covering the entire Early Cretaceous stratigraphy and Shetland and Chalk covering most of Late Cretaceous (Deegan and Scull, 1977) (Fig. 2.10). Cromer Knoll Group consists of carbonates and claystone deposited under oxic conditions (Copestake et al., 2003), indicating a rapid facies change from the anoxic mudstones of the Late Jurassic (Rawson and Riley, 1982). This makes the base of the Cretaceous, dubbed Base Cretaceous Unconformity, pronounced on seismic data, even though it is largely not an unconformity (Fig. 2.10). Chalk and Shetland Groups are of similar age, but the Shetland Group cower northern North Sea while the Chalk Group cowers over the rest of the North Sea (Ziegler, 1988).

2.3.7. Cenozoic stratigraphy

Cenozoic stratigraphy in the Norwegian-Danish Basin consists mainly of Maureen/Våle, Lista, and Sele Formation, all marine to deep marine mudstone dominated but also local sandstones (Holloway et al., 1992) (Fig. 2.10). The mainly Cretaceous Chalk Group are deposited in the lower part of the Early Paleocene. The stratigraphy is mainly unfaulted throughout the North Sea.

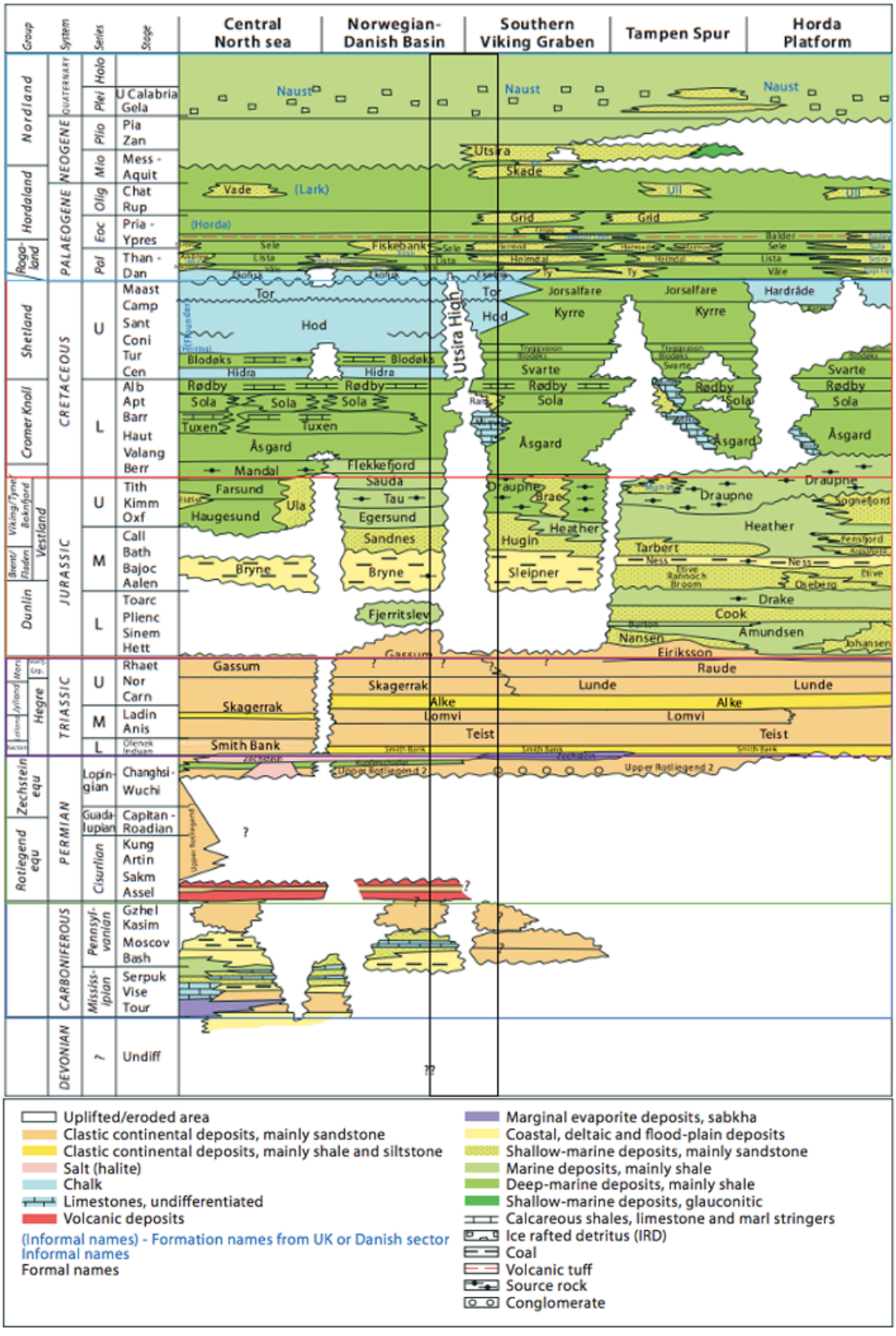

Figure 2.10. Lithostratigraphic chart of the Norwegian North Sea. Black box added between Norwegian-Danish Basin and Southern Viking Graben encompasses the lithostratigraphy of Utsira High, the closest resemblance of the Sele High lithostratigraphy. The chart starts at the Devonian stratigraphy (lowermost, gray) and shows all time periods above until present (uppermost, light blue). The legend shows which lithology is associated with which color, white indicate nondeposition or later erosion, hiatus. Modified from NPD 2014.

3. Theory, Data, and Methods

3.1 Theory

3.1.1 Basement inheritance

Mechanical and rheological heterogeneities in the crystalline basement are long-lived zones of weakness usually inherited from orogenic events (e.g., Tommasi and Vauchez, 2001; Vauchez et al., 1998), collapse tectonics (e.g., Dewey, 1988; Fossen et al., 2000; McClay et al., 1986) and/or previous rifting (e.g., Færseth, 1996). These are abundant in Earth's continental lithosphere resulting from 60-80% of continental lithosphere being established simultaneously as the onset of plate tectonics ~3 Ga ago (Campbell, 2003; Cawood et al., 2013; Dhuime et al., 2017; Hawkesworth et al., 2020; Pujol et al., 2013; Shirey and Richardson, 2011). Most continental lithosphere has therefore been reworked and gone through several Wilson cycles (Shirey and Richardson, 2011; Vauchez et al., 1998; Wilson, 1966). The anisotropic nature of olivine, which constitutes more than 50% of the Earth's mantle (McDonough and Sun, 1995), can create a pervasive fabric inducing a significant mechanical anisotropy of the lithosphere (Vauchez et al., 1998). However, early work to understand continental rifting, often considered rifting to occur on a laterally homogeneous lithosphere (Gawthorpe and Leeder, 2000; Prosser, 1993).

Although these intra-basement structures and fabric heterogeneities, ranging from micro to large crustal-scale, may greatly influence the rift evolution; 1) directly, by being inverted and reactivated; 2) alter, localize and partition the stress regime; and 3) operate as a nucleation site for later fault activity; significantly altering rift architecture (e.g., location, geometry and magnitude) (e.g., Corti, 2009; Daly et al., 1989; Fazlikhani et al., 2017; Fraser and Gawthorpe, 1990; Færseth, 1996; Færseth et al., 1995; Phillips et al., 2016; Whipp et al., 2014). The orientation of heterogenetic lineaments relative to the extension direction are of great importance for its probability of being reused (White et al., 1986), as structures perpendicular to the extension direction would have little effect on the evolution (Phillips et al., 2016; Serck et al., 2022).

Before RP1, the North Sea had experienced both contractional and extensional orogeny, resulting in extensive lithospheric heterogeneities. During the RP2, previous rifting also had occurred, resulting in even further heterogeneities. Caledonian thrusts and collapse shear zones

are interpreted to be reactivated during RP1 accommodating some of the extension. Additionally, several normal faults created seem to root in the mechanically weaker shear zones located beneath (Phillips et al., 2016). It has been documented that faults were reactivated during RP2 and reused lithospheric weaknesses established during RP1 to create the through-going fault zones constituting the Viking Graben (Færseth, 1996).

3.1.2 Evaporites – Key concepts

Evaporites are deposited in restricted basins, where there is a net inflow of seawater, and evaporation exceeds precipitation and runoff, elevating the concentration of naturally occurring ions such as chloride (Cl^-), sodium (Na^-), magnesium (Mg^{2+}), calcium (Ca^{2+}) and sulfate (SO_4^{2-}) (Scruton, 1953). Concentration above solubility prompts the dissolved ions to precipitate as halite, carbonates and sulfates. Since the basins where evaporites develop require hot and arid to semi-arid conditions, these deposits usually occur at latitudes of about 30 degrees, such as the present Persian Gulf. The presence of evaporites, especially halite, greatly affects the basin architecture and deposition. An idealized evaporitic basin has four evaporitic facies zones (Clark et al., 1998), where the most marginal (Zone 1) has a halite concentration of less than 10% and most basinal (Zone 4) has a halite concentration of more than 80% (Fig. 3.1).

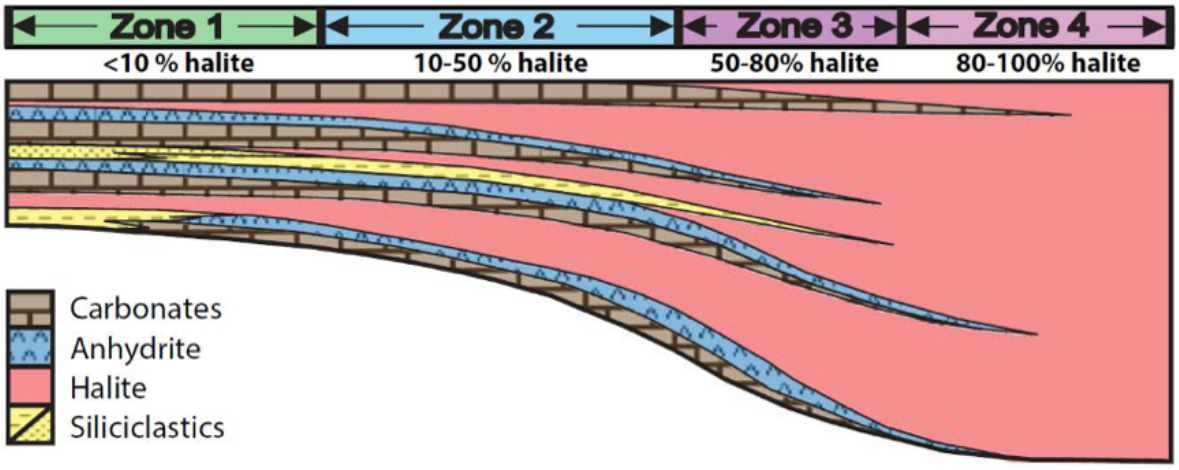

Figure 3.1. Shows the four different evaporitic zones, the concentration of the different evaporitic facies associated with each zone and where they are in the basin, going from most marginal at zone 1 to most basinal at zone 4. The legend shows the different evaporitic facies and their corresponding color. (Clark et al., 1998).

Halokinesis means the movement of salt under the influence of gravity and is caused by its unusual physical (e.g., density, thermal conductivity) and mechanical properties (e.g., strength, ductility) (Jackson and Talbot, 1986). Salt is soluble and mechanically weak making it flow as fluid over geological time and incompressible resulting in a density decrease with depth because of thermal expansion, from 2.2 g/cm^2 at the surface (Fig. 3.2) (Jackson and Talbot, 1986).

This has created the field of salt tectonics, which covers deformation caused by halokinesis and may also involve contraction and extension (Warren, 2016).

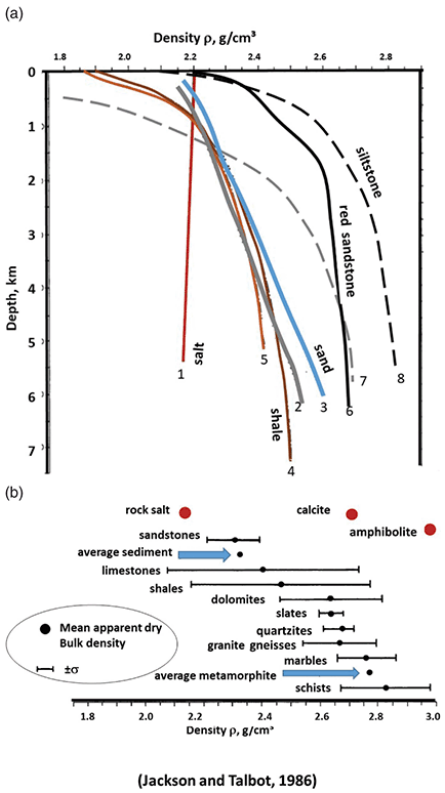

Figure 3.2. a) Shows the different sedimentary units and their corresponding density with depth. b) Shows the dry bulk density interval of the different sedimentary units. Taken from (Jackson and Talbot, 1986).

Salt flow can be both lateral and horizontal and may be triggered by numerous mechanisms (e.g., differential loading, tectonic forces). Several have studied and created physical properties as a function of depth (e.g., Hamilton, 1976; Marcussen et al., 2010; Tenzer and Gladkikh, 2014), but because several variables (e.g. mineralogy (Mondol et al., 2008)) there is not a uniform answer. However, at approximately 1.3-1.5 km, most sediments have a higher density than 2.2 g/cm^3, caused by compaction, dehydration and cementation, creating a zone of density inversion (Jackson and Talbot, 1986; Warren, 2016). Halite may also affect faulting because of its ductile nature. It may cause faults to disconnect or be softly linked sub- and supra-salt (Fig. 3.3) (Lewis et al., 2013). This effect is connected to the halite layer's thickness and the fault's displacement. It may also relate to other ductile layers, such as shale.

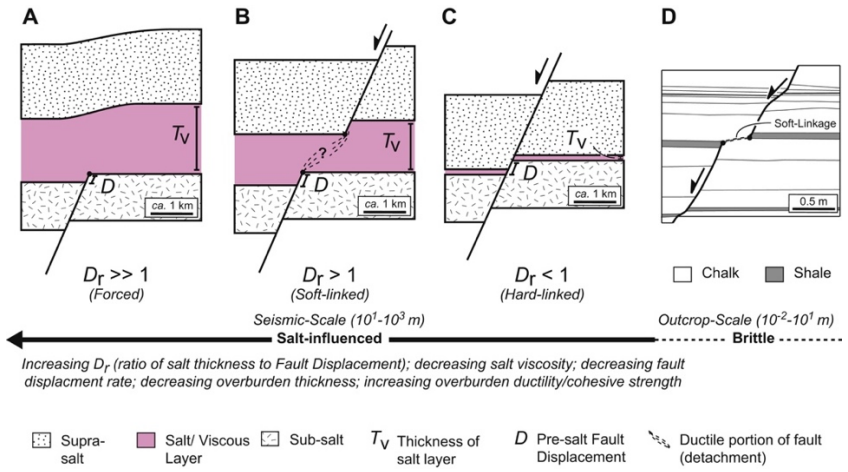

Figure 3.3. Illustrates how faulting is connected sub- and supra-salt dependent on the thickness of the halite layer and the displacement of the fault. Displacement ratio (D_r) is the ratio between halite layer thickness and displacement of sub-salt normal fault. At A) D_r is much lower than 1 resulting in a forced fold supra-salt. At B) the D_r are smaller than 1 leading in a soft-link between sub- and supra-salt. At C) the D_r is above 1 resulting in a hard-link between sub- and supra-salt. D) illustrates that disconnections may also appear in other ductile layers, such as shale. (Lewis et al., 2013)

3.1.3 Fault analysis

Fault geometry is often given in strike, dip, throw and displacement. The strike is given in azimuth and delineates the horizontal direction of a fault. In this study the right-hand rule is applied for strike and dip, meaning if strike is indicated as one direction it will always be to the right when your back is the same direction as the dip. Dip is the highest angle between a horizontal plane and the fault plane in a range between 0-90 degrees. Throw is the amount of vertical separation between two points that were interlinked before rifting, while heave is the horizontal separation, and displacement is the combined separation of the two (Fig. 3.4). Faulting has three endmembers; normal fault; reverse fault; and strike-slip fault. In normal and reverse faulting, one distinguishes between the fault's two sides, the hanging wall and footwall. The hanging wall is the side that overlies the footwall and is downthrown in normal faulting (Fig. 3.4) and upthrown in reverse faulting. Normal faulting is associated with an extensional regime meaning maximum principal stress axis (σ_1) is vertical and minimum principal stress axis (σ_3) is horizontal (Fig. 3.16) (Anderson, 1905). Reverse faulting, on the other hand, is linked with a compressional regime were maximum principal stress axis (σ_1) is horizontal and minimum principal stress axis (σ_3) is vertical. The orientation of the fault plane is described in Anderson's theory of faulting, which says that faulting usually occurs 30 degrees on maximum principal stress. This means normal faults usually have a higher angle than reverse faults, with the textbook example indicated 60 degrees for normal faults and 30 degrees for reverse. Strike-slip faults differ from the two other types as they normally do not have a hanging wall or

footwall. Strike-slip faults are horizontal created by a stress regime where both maximum and minimum principal stresses are horizontal. A fault plane usually has an elliptical shape, where the displacement is maximum in the center of the ellipse and decreases radially. Faults are also distinguished if the basement is involved in the faulting or not, if the basement is involved it is called a thick-skinned fault, if the basement is not involved it is called thin-skinned fault.

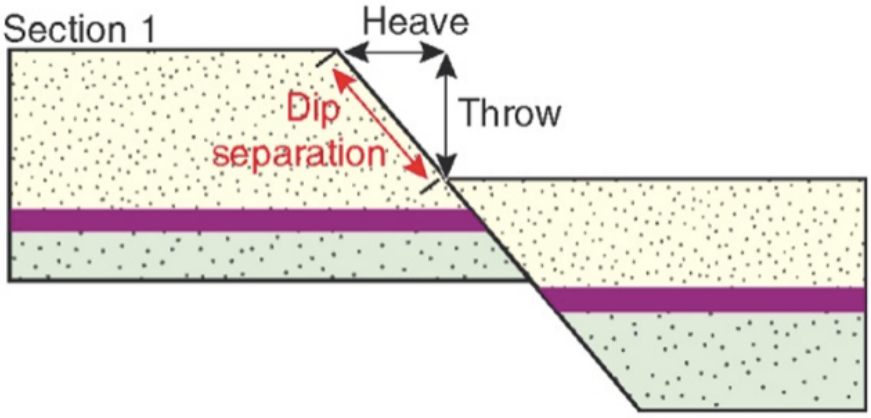

Figure 3.4. Illustrates a fault in the vertical section with footwall to the left and hanging wall to the right. Heave is shown as the horizontal separation, throw the vertical separation and the red arrow shows the displacement. (Fossen, 2016)

When normal faulting occurs, the hanging wall will subside, creating increased accommodation space on the hanging wall. This leads to thicker sedimentary units above the hanging wall than the footwall. More accommodation space is created above the fault center where the displacement and throw are maximum. Because the sedimentary units are thicker above the hanging wall, we can interpret when a normal fault is active. Reactivation is inferred if there are two stratigraphic units with changes in sedimentary thickness across faults interposed by a layer with a homogenous thickness on both sides of the fault (Fig. 3.6). Inversion is when a normal fault is reused as a reverse fault and is ascertained when the hanging wall's base post-rift is above the footwall's base post-rift (Fig. 3.7).

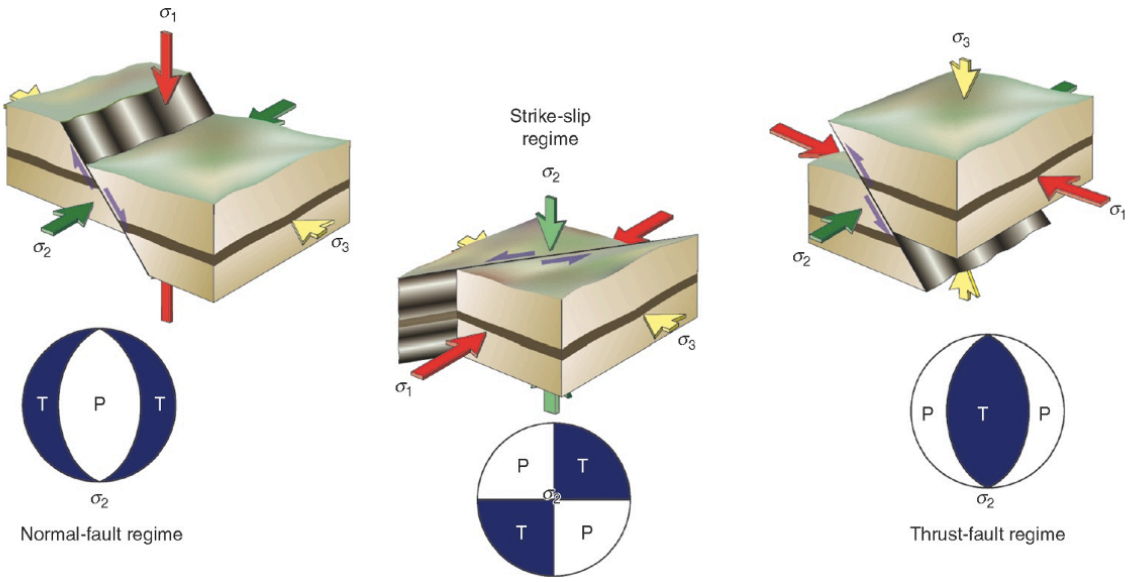

Figure 3.5: Anderson fault theory which illustrates orientation of principal stresses for the different fault regimes. Taken from (Fossen, 2016)

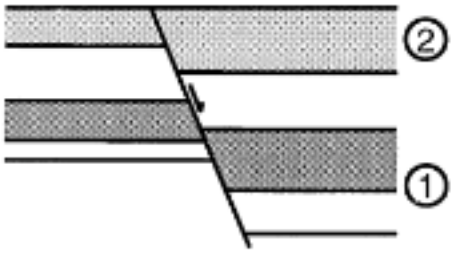

Figure 3.6. Illustrates repeated changes in the thickness of the sediment packages across the normal fault with one intermediate package with homogenous thickness across the fault, which represent reactivation. (1) first package with an increased thickness on hanging wall, indicate fault was active during deposition. A homogenous layer interposed of 1 and 2 indicate a period of tectonic quiesced. (2) another layer with increased thickness indicating reactivation of the fault.

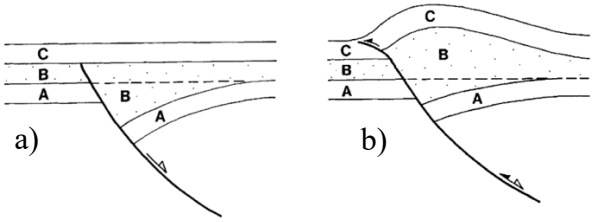

Figure 3.7. a) Illustrates an inactive normal fault with a pre-rift sequence (A), a syn-rift sequence (B) with increased thickness on the hanging wall, and a post-rift sequence (C). b) Illustrates the same stratigraphy where the normal fault has been positively inverted meaning the normal fault has been reused as a reverse fault, which can be interpreted because the base post-rift (null point) of the hanging wall is above the base post-rift in the footwall. Modified from (Williams et al., 1989).

3.2 Data

3.2.1 3D seismic data

Seismic reflection data serve as a subsurface image by measuring the time (ms) it takes for a pressure wave to travel from the source, propagate down to a rock interface and reflect up to a receiver (i.e., two-way-time; TWT). The strength of the reflected signal is governed by the difference in acoustic impedance (AI) at the rock interface. Acoustic impedance is the product of the compressional wave velocity (v_p) and the bulk rock density (ρ). Since both velocity and density varies as a function of depth and petrophysical properties (i.e., porosity, pore fluids and mineralogy), can acoustic impedance be related to lithological variations in the subsurface (Brown, 2011). The seismic reflection data can either be in 2D lines or 3D volume and are extensively used for hydrocarbon exploration, offshore wind and in academia for better geological understanding. For the seismic to resemble a true image of the subsurface several processing steps have to be applied.

The current study utilized the LO1101-KPSTM 3D seismic survey for the bulk of seismic interpretations and the creation of geomodels (Table 3.1). The LO1101 survey uses the coordinate reference system UTM zone 32N and covers the production license PL503 that overlaps the Norwegian quadrants 17/7 and 17/8, encompassing large parts of the Sele High in the North Sea. Bergen Oilfield Services AS acquired it in 2011 for LOTOS Exploration and Production Norge AS. The area it covers is approximately 1200 km^2. The inline and crossline spacing (bin size) is 12.5 m and is rotated 16.7 degrees clockwise from North and East, respectively. LO1101 is displayed in ms TWT and recorded down to 6500 ms TWT.

Understanding the seismic survey polarity is essential in seismic interpretation. The polarity is defined in which direction the seismic wiggle is drawn in the seismic section. There are two polarity conventions according to the Society of Exploration Geophysicists, the normal (American polarity) and reverse (European polarity). In normal polarity, a rock interface with an increase in AI is displayed as a peak, while a decrease is displayed as a trough. Reverse polarity will display the opposite. The polarity for the survey LO1101 is normal and the seabed is displayed as a peak (black) (Fig. 3.8). The signature of the seismic signal resembles the zero-phase wavelet, therefore, the LO1101 seismic cube is interpreted to be zero-phase survey (Fig. 3.8).

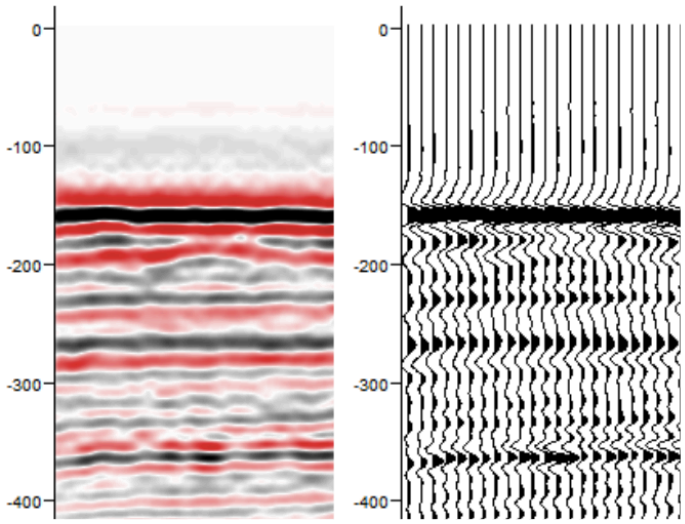

Figure 3.8. Displaying the seabed as a peak at 160 ms TWT, indicating normal polarity.

3.2.2 2D seismic data

2D seismic reflection data, like 3D, provides an image of the subsurface, but rather along a single line instead of a volume. In this study five 2D lines (table 3.1), which extend laterally outside of the 3D cube were used. As the 3D cube does not cover the entire extent of the Sele High the 2D seismic lines make it possible to determine the outline of the Sele High, while also connecting the observations on the Sele High with observations from the neighboring structural elements giving a regional context to the observable structural and stratigraphic trends on the Sele High.

Table 3.1 summary of the 3D and 2D seismic surveys used herein. Information about the survey is from the NPD Diskos repository. Abbreviations: ILN = inline and XLN = crossline.

	3D	2011	Bergen Oilfield Service AS (acquisition). LOTOS Exploration and Production Norge AS (operator)	6500	Approx. 1200 km^2	ILN: NNE-SSW XLN: ESE-WNW	Sele High	Good
	2D	2004	TGS Nopec Geophysical Company ASA	9000	(3) 113 km (2) 138 km	(3) NE-SW (2) ESE-WNW	Sele High	Good

The 2D data sets utilized in this study are five NSR lines. Repeatedly, the seabed reflector is examined to determine the polarity of the 2D seismic survey. The seabed is displayed as a trough meaning the 2D seismic lines have reversed polarity.

3.2.3 Limitations of seismic data

When interpreting seismic data, it is essential to consider the limitations and uncertainties associated with the seismic as these may influence the results. Some limitations may occur at acquisition (e.g., seismic resolution, acquisition geometry) and processing stage (e.g., noise reduction, seismic multiple removal). There are mainly four limitations; seismic resolution; depth limitations; distortion and scattering of seismic signal; and ambiguity.

Vertical and lateral resolution is characterized as the minimum distance between two features that can be individually distinguished (Sheriff, 1977). They are both controlled by the wavelength (λ) of the seismic signal. The wavelength is a function of seismic velocity (v) divided by the dominant frequency (f_d) of the seismic (Sheriff, 1977) and can be found by measuring the distance between two peaks. Seismic velocity increases with depth due to compaction, while the dominant frequency decreases due to attenuation of high frequencies, ensuing an overall increase in wavelength with depth (Sheriff, 1977), leading to poorer resolution, both vertically and laterally.

Vertical resolution is usually between one-eighth and one-quarter of the wavelength, dependent on background noise and the receiver's sensitivity (Sheriff, 1977). A straightforward process of measuring the dominant frequency from seismic is to measure the time difference over an arbitrary number of cycles, at the depth of interest. At the LO1101 survey, ten cycles are measured between 2767-3013 ms TWT (0.246 seconds), giving a dominant frequency of 40.7 Hz. If we assume an average velocity of 2.5 kms^{-1} at this depth, the dominant wavelength will be 60 m (Equation 3.2.1) corresponding to a vertical resolution of 7.5-15 m ($\lambda/8 - \lambda/4$).

$$\lambda_d = \frac{v}{f_d} = \frac{2.5\ kms^{-1}}{40.7\ Hz} = 0.06km = 60m \qquad (3.2.1)$$

Lateral resolution is connected to the concept of the Fresnel zone. The Fresnel zone is that portion of the wavefront, which is reflected from an interface, so it arrives at the receiver within half a wavelength, resulting in constructive interference of the signal (Denham and Sheriff,

1981). The lateral resolution is improved by collapsing the diffraction through migration (Loewenthal et al., 1976). The migration has a much greater effect on 3D seismic data compared to 2D seismic (Cartwright and Huuse, 2005). The lateral resolution of the 3D seismic is thus close to the bin spacing (Here 12.5 x 12.5 m; Sheriff, 1977).

Complex structures and lateral differences in seismic velocity may distort the seismic image. Evaporite and especially halite create complex structures, and have usually higher seismic velocity compared to other sedimentary rocks, causing strong acoustic impedance difference reducing the seismic signal penetrating while also having an undulating top surface, which create substantial lateral variations in seismic velocity (Jones and Davison, 2014). All of these can potentially reduce both the visibility and accuracy of interfaces subsalt. Seismic attenuation is another problem which amplifies with depth. At each rock interface, some of the energy of the seismic signal is reflected to the surface (Reflection coefficient (R0)), dependent on the acoustic impedance, thus reducing the seismic signal, which continues to propagate downwards (Transmission coefficient (T0)). Attenuation of the seismic signal also derive from geometrical spreading, which is when a wavefront radiates from a point in as a spherical surface increasing in size. Ambiguity is another common problem leading to error. It is important to note that seismic data may be ambiguous and therefore open to multiple interpretations. This is especially relevant where the subsurface is poorly understood, has complex structures, and the seismic signal is limited (Bond et al., 2007). All of the aforementioned are relevant to this study.

3.3 Methods

Through this section the workflow and methods applied to achieve the main objectives; i) Generate a seismic-stratigraphic framework of the Sele High; ii) Assess the spatial and temporal evolution of faults; iii) Analyze the tectonostratigraphic evolution of Sele High with emphasize on the Pre-Permian evolution; and iv) distribution and role of different Zechstein facies; will be described. The workflow is illustrated in Table 3.2 and encompasses 3 stages (1 preparation; 2 seismic interpretation; and 3 geomodelling and analysis). The Petrel E&P Software Platform (v.2022.1) with Blueback tools was used for seismic interpretation, modelling and analysis. Figures of time-structure and time-thickness maps are presented with the color template (Hawaii) (Fig. 3.9) created by Crameri et al. (2020) which is uniform and adapted to color blindness to reduce visual errors and distortion effects.

Table 3.2: Shows the three stages of the methodology for this study with associated substages and results.

Main stages	*Substage*	*Results*
Stage 1: Preparation	Examination of data Literature study	
Stage 2: Interpretation	Horizon interpretation Fault interpretation	Time-structure maps Time-thickness maps
Stage 3: Analysis	Analysis of time-structure maps Detailed analysis of selected transects Analysis of time-thickness maps Analysis of timing and style of faulting	

3.3.1 Surface interpretation

Interpretation of seismic data enables identification of the chronological order of geological events and deposition which significantly helps to understand the stratigraphic framework and the overall structural evolution of an area. A detailed interpretation of eight seismic surfaces (table 3.3) was therefore interpreted and are identified as (stated from uppermost to lowermost): Top Skagerrak Fm, Top Zechstein, Base Zechstein, Unit D, Unit C, Unit B, Unit A and Basement.

A three-stage process was used for this study (table 3.2). The first stage (Preparation) was used to get an overall understanding of the study area to better connect observations in the second stage (Interpretation) with regional events identified in other studies. The first target within the second stage was to find and interpret key surfaces within the 3D seismic dataset. The target for this thesis is mainly the periods Devonian to Permian. Since there are no available wells, no well-ties are performed. To compensate for this, the distinctive Zechstein Supergroup is used to acknowledge and correlate where the different surfaces are in the lithostratigraphy and in which period they were deposited.

Different techniques were used for different surfaces. Auto 3D tracker was used for the interpretation of the Upper Unconformity and Top Zechstein as they are strong and easily distinguishable. Nonetheless, some voids were left uninterpreted which were filled with widely spaced inlines, crosslines and/or arbitrary lines. Remaining surfaces were however created through other methods not utilizing the 3D auto tracker. The Base Zechstein and Unit D were

created through a grid of inlines and crosslines with 50 increment spacing. As for the three Units A-C and the Basement, which are highly abrupted by faults and mainly only interpretable on the northern and western part of the Sele High, arbitrary lines were used for the interpretation of these surfaces as they can be oriented orthogonal to the structural elements. After the creation of the grid, areas identified with higher complexity needed more detailed interpretation (Fig. 3.9). The complexity usually increases with depth resulting in more detailed interpretation needed at the lower stratigraphic units. Ghost function on petrel is a helpful tool to locate the active surface across faults and has been extensively used especially for Unit A-C.

Table 3.3: Shows the different seismic surfaces, polarity of the surface signal, quality of the reflector and further comments.

Seismic Surface	Reflector pick	Reflection quality	Comments on upper boundary
Top Unconformity	Peak	Strong, continuous	Unconformity
Top Zechstein Supergroup	Peak	Very Strong, continuous	Strong and undulating
Base Zechstein Supergroup	Trough	Strong, continuous	
Unit D	Trough	Strong, continuous	Unconformity
Unit C	Trough	Weak, disrupted	
Unit B	Trough	Intermediate, disrupted	
Unit A	Trough	Intermediate, disrupted	
Basement	Peak	Intermediate, disrupted	

When the interpreted grid for the surfaces was completed, a polygon around the grid was created to make surfaces. The surfaces were then revised, and some areas were not satisfactory, so the interpreted grid was refitted. This process was repeated until all surfaces were at a satisfactory quality. Time-structure maps were created from the surfaces.

The Basement is an intermediate peak and highly uneven. It is followed over most parts of the Sele High, though on the flanks it is mostly downthrown too deep or too far laterally to visible or within the 3D seismic data. The Lower and Mid Devonian are intermediate troughs that are disrupted and only visible on the northern and western parts of the high, even though they are truncating against Base Rotliegend on the northern part. Outside of the high they are too weak and deep to be visible on the seismic and are therefore not possible to track. Unit D is strong

continuous trough that lay unconformably over the lower stratigraphy and is interpreted over most of the study area. The Base Zechstein Supergroup separates the Rotliegend Group or lower stratigraphy's from the Zechstein Supergroup and is a strong continuous trough that is interpreted over most of the study area. Top Zechstein is a very strong and continuous undulating peak with packages above and below following its undulating character. It is interpreted over the entire study area. Top Zechstein has a higher A.I. difference in the southern part of the study area than in the northern part. There is an unconformity above the Top Zechstein, which is interpreted throughout the entire study area, corresponding to the Top Skagerrak Fm. It is a strong and continuous peak. The creation of time-thickness maps is the final step in the workflow. They are made by using the surface calculation operation in Petrel, which calculates the vertical time difference between two time-structure maps. Analyzing the time-thickness maps reveals sediment accumulation, depositional environment, and tectonostratigraphic information.

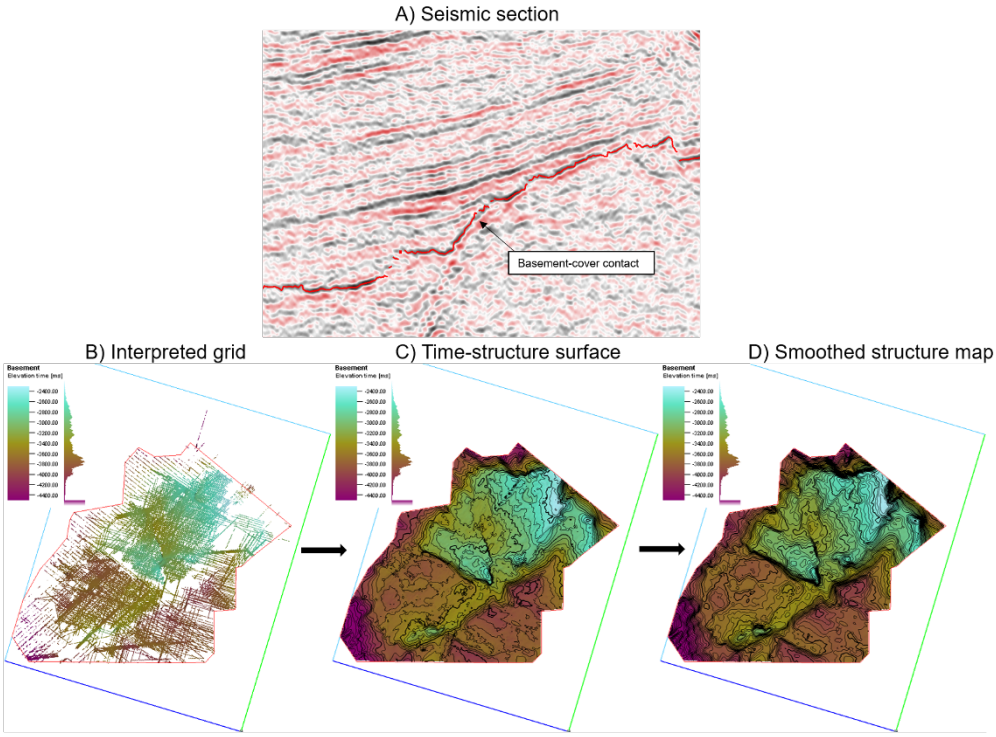

Figure 3.9. Diagram illustrating the four stages for surface interpretation and creation using the basement-cover contact as example. A) Interpretation in LO1101 inline 3602, B) interpreted grid, C) time-structure map, D) smoothed time-structure map. B-D use 'hawaii' color scale from Crameri et al. (2020).

4. Results

The main objective of this study is to establish an updated structural framework of the Sele High, analyze critical faults, assess pre- syn- and post-sedimentary packages and determine the distribution of evaporites. In this chapter, interpreted cross-sections, time-structure maps and time-thickness-maps are used to describe the pre-Triassic architecture of the Sele High. As there are no wells open to the public in the study area, a simplified interpretation of the basement-cover contact is, therefore, applied and is based on three factors; the high amplitude reflector at depth; its uneven character; and the lack of conform reflectors below. Several stratigraphic units which are interpreted lack definite ages as a consequence of the lack of well data on Sele High, so the prominent Zechstein Supergroup is used for time control on the stratigraphy. All figures in this section are presented in the time domain (i.e., elevation, depth, and thickness are given in ms TWT).

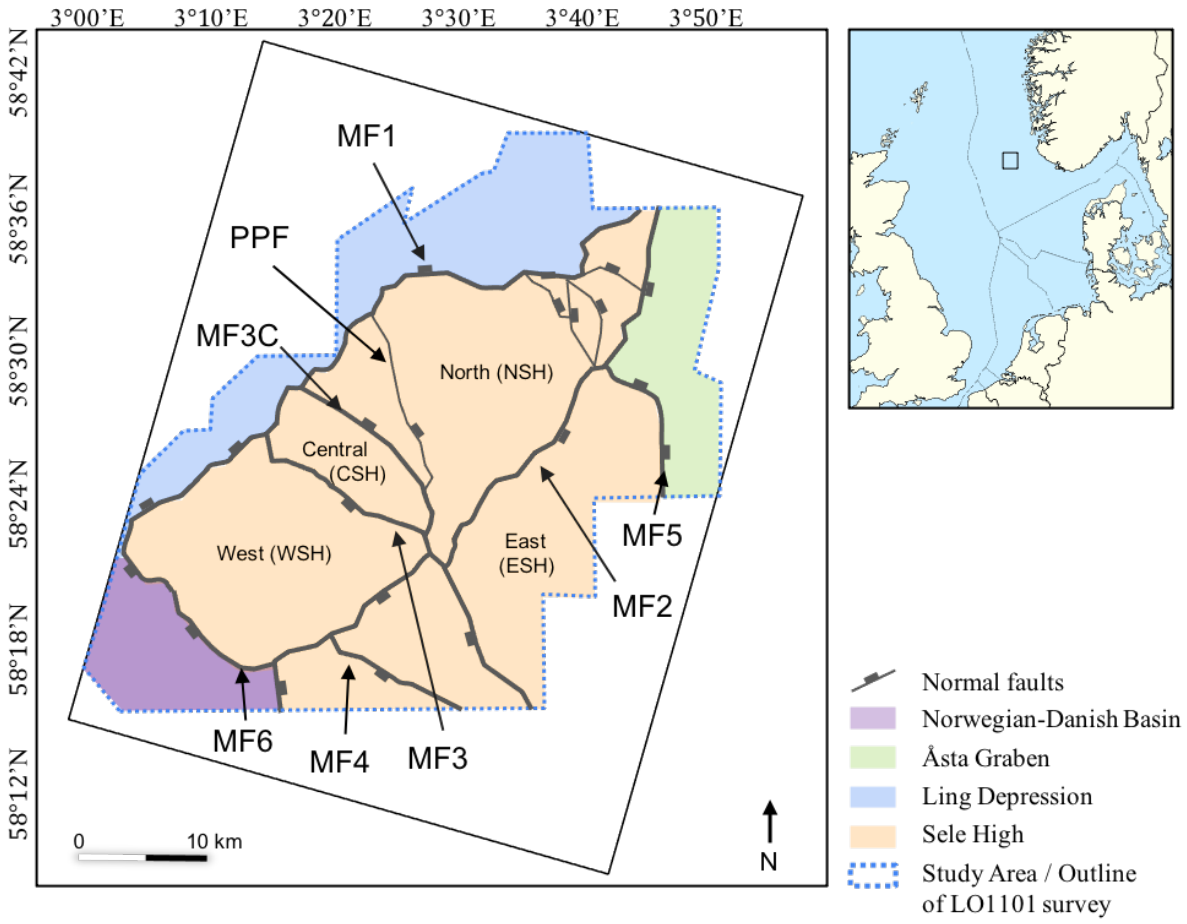

Figure 4.1: Outline of the 3D seismic data indicated by a blue stippled line with the structural elements within created from the Basement time-structure map. CSH, Central Sele High; NSH, North Sele High; ESH, East Sele High; WSH, West Sele High; MF1, master fault 1; MF2, master fault 2; MF3, master fault 3; MF3C, master fault 3 conjugate; MF4, master fault 4; MF5, master fault 5; MF6, master fault 6.

4.1 Structural elements, inheritance and subdivision

The stratigraphic and structural architecture of the Sele High is described and presented to elaborate on the structural evolution and the geological history of the study area and the North Sea in general. The outline of the 3D seismic survey and the different structural elements within is illustrated in Figure 4.1, as well as the position of the study area.

4.1.1 Ling Depression

The Ling Depression is a NE-SW-oriented structural feature in the North Sea which align with the NE-SW trending Hardangerfjord Shear Zone and the Lærdal-Gjende Fault Zone (Fazlikhani et al., 2017; Fossen and Hurich, 2005; Færseth et al., 1995; Phillips et al., 2016). The northeast Ling Depression connects with the Øygarden Fault Complex, the Stavanger Platform, and the Åsta Graben. In the Ling Depression, the basement is severely downthrown, and it separates the Sele High in the south from the Utsira High and Patch Bank Ridge in the north (Fig. 4.2 C-D). The southwest Ling Depression borders Norwegian-Danish Basin and Jæren High before it links up with the triple junction created by the trilete rift system in the North Sea. The Ling Depression is approximately 185 km long and 20-30 km wide, covering 4225 km^2 (NPD Factmap). In this study area a small portion of the Ling Depression is evident in the northwest of the Sele High (Figs. 4.1; 4.3 a-d; 4.4 g-j).

4.1.2 Norwegian-Danish Basin

The Norwegian-Danish Basin (NDB) has a long and complicated history originating from plate reorganization during Late Carboniferous-Early Permian (Ziegler, 1982). It is a massive structural feature stretching 600 km from the southeast, down beyond mainland Denmark, all the way until the Ling Depression in the northwest. The northeastern most part of the Norwegian-Danish Basin has an approximately 50 km long border to the southwestern Sele High (Fig. 4.2) (NPD Factmap). In the current study, only a small part of the Norwegian-Danish Basin is covered in the southwestern corner of the 3D seismic data, and only 15 km of their border is visible which is constituted by the master fault 6 (MF6) (Figs. 4.1; 4.2; 4.3 a; 4.4 f). The Norwegian-Danish Basin has several thick-skinned faults and salt diapirs (Fig. 4.2 A-B).

4.1.3 Åsta Graben

The Åsta Graben covers approximately 3.300 km^2 (NPD Factmap) and is a half-graben with a westward tilt (Fig. 4.2. B-D). It borders the Sele High to the west, Ling Depression to the north,

Stavanger Platform to the east and Egersund Basin to the south. The Åsta Graben has approximately a 45 km long border along the eastern Sele High (NPD Factmap). A small part of the Åsta Graben is visible in the northeastern corner of the study area (Figs. 4.1; 4.3 e; 4.4 i & j).

4.1.4 Sele High

The Sele High is a prominent basement culmination in the North Sea covering 1325 km^2 (NPD Fact Map) where the southern half is not visible in the 3D data. In this study the part of Sele High which is visible in the 3D data is subdivided into four parts. The subdivisions are delineated by the study of master faults and the subdivision is only clear in the Basement and Unit A-C levels.

North Sele High domain

In this study the Sele High is subdivided into four different parts. The North Sele High (NSH) is the northernmost part of Sele High and is delineated by MF1 in the north, MF2 in the east and south, and by MF3C and PPF in the west. In the NSH the Basement is situated between 2300-3400 ms TWT with a southeast dip (Fig. 4.3).

Central Sele High domain

The Central Sele High (CSH) is delineated by the faults MF1, MF3, MF3C and PPF (Fig. 4.1). It is the smallest of the subdivided areas. The CSH is prominent due to the presence of most elevated basement in the study region. The part in between MF3 and MF3C is a horst created by the two faults (Figs. 4.1; 4.3 a & b; 4.4 h).

East Sele High domain

The East Sele High (ESH) is the largest subdivision of the main structural elements, however it is also the area with the poorest resolution, resulting in some forced interpretation to be done. It is delineated by MF2 and MF5 and exceeds out the southern and eastern limit of the 3D seismic data (Fig. 4.1). It borders the Åsta Graben to the north, Norwegian-Danish Basin to the south and WSH to the west (Figs. 4.1; 4.3 b-e; 4.4 f-j).

West Sele High domain

The West Sele High (WSH) is delineated by MF1, MF2, MF3 and MF6 and borders the CSH to the north, ESH to the east, Norwegian-Danish Basin to the south and Ling Depression to the west (Figs. 4.1; 4.3 a & b; 4.4 f-h). The Basement-cover contact has a minor northeast tilt within the WSH.

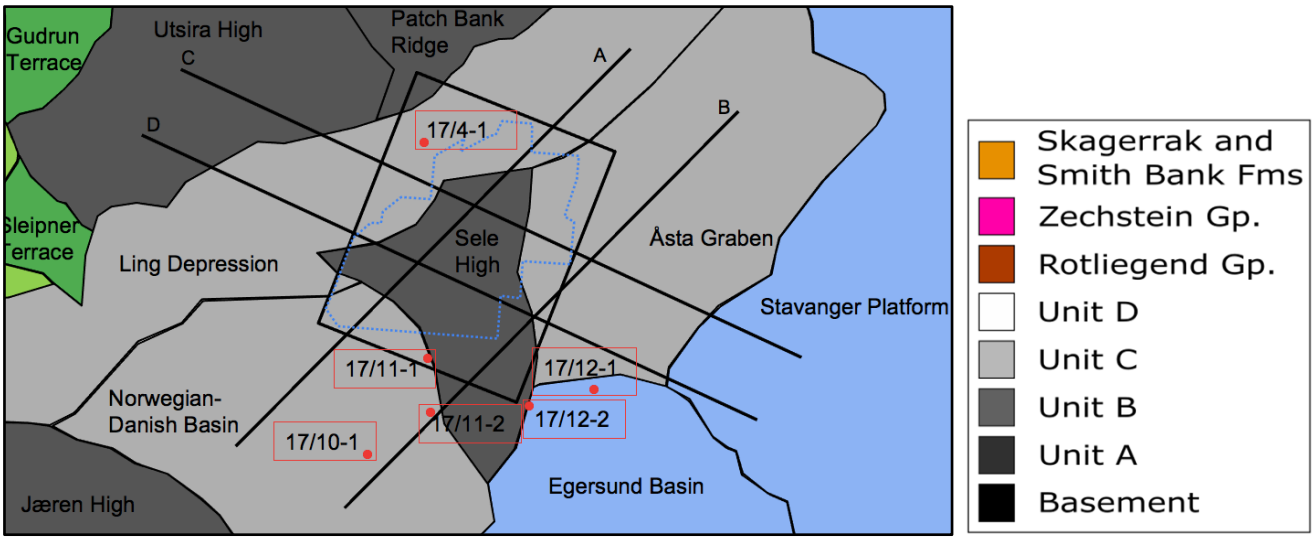

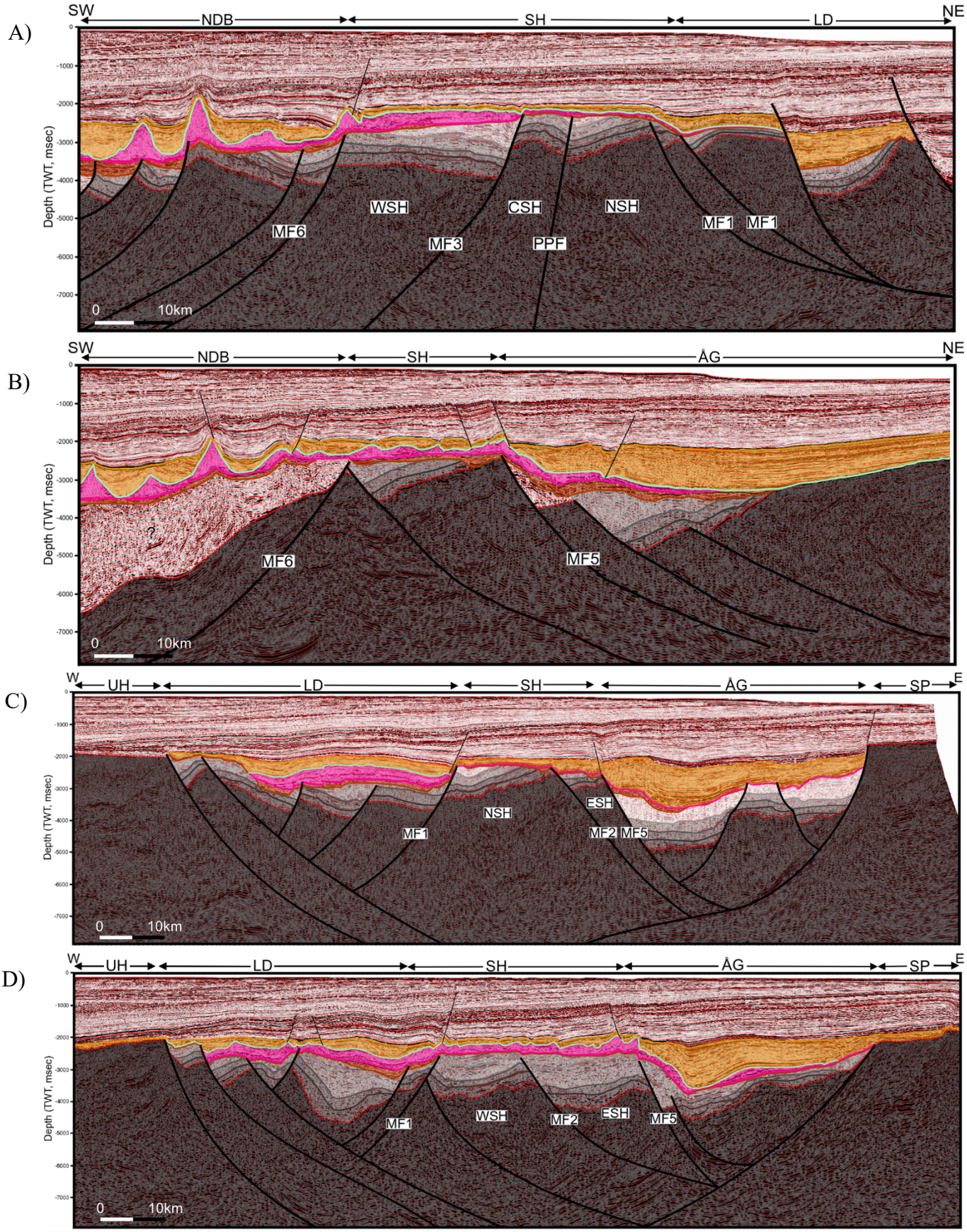

Figure 4.2: Regional view of and around the Sele High in the Norwegian Central North Sea with coverage of the 3D seismic data, and the four 2D lines. Wells open to public and used in this study are highlighted with red rectangles. SH, Sele High; UH, Utsira High; SP, Stavanger Platform; ESG, East Sele High; NSH, North Sele High; WSH, West Sele High; CSH, Central Sele High; ÅG, Åsta Graben; LD, Ling Depression; NDB, Norwegian-

Danish Basin; MF1, master fault 1; MF2, master fault 2; MF3, master fault 3; MF5, master fault 5; MF6, master fault 6.

4.2 Pre-Jurassic Stratigraphy

4.2.1 Skagerrak and Smith Bank Formations

The Skagerrak and Smith Bank formations are interpreted together and is the uppermost stratigraphy interpreted in this study. The formations were deposited during Early to Middle Triassic in a continental setting (NPD Factpage Smith Bank Fm). The Skagerrak Formation conformably overlay the Smith Bank Formation. The upper boundary of the Skagerrak Formation is an unconformity throughout the study area and are superimposed by Middle Jurassic rocks (Well 17/4-1, 17/11-1, and 17/11-2) (Fig. 4.2). The Skagerrak Formation consists of interbedded shales, siltstones, sandstones and conglomerates where the color is dominantly shades of brown and red, but dark and light grey beds do occur.

The Smith Bank Formation consists of mainly silty claystone with a few thin interbedded layers of sandstone (NPD Factpage Smith Bank Fm). There are also minor components of dark shale, conglomerate, limestone, dolomite and marl. The Smith Bank Formation was deposited during the earliest Triassic and conformably superimpose the Zechstein Supergroup (Fig. 2.10) which is confirmed by several wells in the Norwegian-Danish Basin to the south of the study area (Wells; 17/10-1, 17/11-1, 17/11-2, 17/12-1, and 17/12-2) (Fig. 4.2). The top boundary of either Skagerrak or Smith Bank, where Skagerrak is eroded, is also invariably coincident with the uppermost occurrence of red beds in this area.

4.2.2 Zechstein Supergroup

The Zechstein Supergroup is a marine evaporitic unit composed of mainly halite, anhydrite, carbonates and sulfates, deposited during the Late Permian (Fig. 2.10) (Heeremans et al., 2004; Jackson and Lewis, 2013). The Zechstein Supergroup underlays the Smith Bank Fm. (NPD Factpages Smith Bank Fm) and superimpose the Rotliegend Group or crystalline basement according to NPD, finding of this thesis will show that both are true, but will also argue that it locally superimposes older stratigraphic units. The Zechstein Supergroup was deposited in the Permian basins over NW Europe and the composition changes from halite-rich in the deeper parts of the basin to anhydrite- and carbonate-rich in the shallower parts of the basin (Fig. 3.10) (Stewart and Clark, 1999). Fluctuations in the sea level, driven by melting on growth of the

Permian ice sheets, gave rise to three or four depositional cycles of the Zechstein Supergroup (Glennie et al., 2003).

4.2.3 Rotliegend Group

The second dominant stratigraphic group deposited during the Permian is the Rotliegend Group. The base of Rotliegend Group is often an unconformity associated with the Carboniferous hiatus and usually superimpose strata of Devonian, Silurian or Caledonian crust in the NCS (Glennie et al., 2003). The Rotliegend Group is lowermost stratigraphy deposited during the Permian (Fig. 2.10). It consists mainly of continental red-beds such as fluvial, aeolian and sabkha deposits, and in the lowermost part volcanic rocks are common (NPD Factpages Rotliegend Group). The Rotliegend Group is very similar to the Old Red Group of the Devonian which originates from the fact that it is often formed by recycled Devonian deposits (Glennie et al., 2003).

4.2.4 Carboniferous stratigraphy

The Carboniferous is poorly understood in the Norwegian North Sea as there is no finding of strata from this period, a consequence of the Carboniferous hiatus. At the beginning of Carboniferous a transgression entering from the south occurred altering the depositional environment from the continental red beds to an broader spectrum of sediments containing marine, deltaic, continental and fluvial (Anderton, 1979; Bruce and Stemmerik, 2003)

4.2.5 Devonian stratigraphy

During Devonian the NW Europe was an onshore landscape with deposition of continental red beds, dubbed the Old Red Group. In Early Devonian extension and collapse of the Caledonides created numerous basins with internal drainage and alluvial and lacustrine depositional environments (Fig. 2.7) (Marshall and Hewett, 2003). In this period the Lower Old Red Group was deposited subsequent to the uplift and erosion of Caledonian Orogeny; hence the base of the group is a basement-cover contact. The deposition became more widespread during Mid-Devonian, stretching from the western Norway to Moray Firth and eastern Greenland (Fig. 2.2).

4.2.6 Basement

The main parts of the basement are crystalline gneiss pre-dating the Caledonides. However, the basement also consists of metamorphosed rocks of continental margin and oceanic basin

affinity and metamorphosed metasedimentary rocks (e.g., mica schist; quartzite; greenschist) (NPD Factpages Basement). The basement is partly intruded by granitoids.

4.3 Master faults

The master faults are thick-skinned faults which offsets the basement and effect the Pre-Permian stratigraphy and mainly terminate towards the Base Zechstein Supergroup.

4.3.1 Master fault 1 (MF1)

MF1 is the northwesternmost fault in the study area, separating the Sele High and the Ling Depression (Fig.4.1). Together with MF2, it is the longest fault in the study area. The normal fault has a general NE-SW trend, dipping to the northwest. However, in the north, just past where it intersects with PPF it turns, striking E-W, dipping towards the north, before it again turns, striking NE-SW, dipping towards the northwest.

In all the transects where it is visible, it is impossible to detect where MF1 dies out in the Basement as it propagates too deep or horizontally out of the 3D seismic cube. From the time-structure maps and the transects, it is also noticeable that it offsets all the stratigraphy interpreted in this study (Figs. 4.3 a-d; 4.4 g-j; 4.5-4.12). The MF3, MF3C, MF6, and PPF all die out in the northwest when they link up with MF1.

4.3.2 Master fault 2 (MF2)

The MF2 mirrors the MF1 by also trending NE-SW, but is dipping to the SE, i.e., opposite to MF1 (Fig. 4.1). The MF1 and MF2 are the longest fault in the study area. MF2 separates the subsegments WSH and NSH from the ESH (Fig. 4.1). The northernmost part of MF2, beyond the intersection with MF5, separates NSH from Åsta Graben (Fig. 4.1).

The southernmost part of MF2 links up with the NW-SE trending MF6 (Fig. 4.4 f). Just north of this intersection, the MF2 links up with MF4 in the south of the study area, creating a ramp-flat-ramp structure (Fig. 4.3 b). The Figure 4.3 c is an inline that crosses the triple junction of MF2, MF3, and MF3C. The MF3 and MF3C both terminate and link up with MF2. However, they affect the MF2, creating a ramp-flat-ramp structure (Fig. 4.3 c) and making it take an eastward step before continuing propagating to the northeast (Fig. 4.1). Further to the north, the MF2 links up with MF5, where they separate the Sele High and the Åsta Graben. The MF2

mainly offsets the Basement and Unit A-D (Figs. 4.3 b-d: 4.4 f-j: 4.9-4.12), but also locally offset the Base Zechstein Supergroup (Fig. 4.7), Top Zechstein Supergroup and Base Smith Bank FM (Fig. 4.6). MF1 and MF2 create a horst where WSH, CSH, and NSH are situated.

4.3.3 Master fault 3 (MF3)

The MF3 is a normal fault striking southeast, indicating its dip to the southwest. It is much shorter than the aforementioned master faults. It is also limited westward by the MF1 and eastward by MF2 (Figs. 4.1 and 4.3 c). The MF3 separates the subsegments CSH to the north and ESH to the south (Fig. 4.1).

The MF3 continues out of the 3D and 2D seismic at depth (Figs. 4.2, 4.3 a-b and 4.4 c). Together with MF3C, the fault creates a horst situated in the CSH. MF3 offset the Basement and Unit A-D (Figs. 4.9: 4.10-4.12).

4.3.4 Master fault 3 conjugate (MF3C)

The MF3C is a normal fault striking northwest, dipping towards the northeast, which mirrors MF3 and the two create a horst (Fig. 4.1). The MF3C is limited to the west by MF1 and by MF3 in the east. In depth, the fault extends out of the 3D seismic (Figs. 4.3 a and 4.4 c), except where it terminates towards PPF (Fig. 4.3 b). The MF3C offsets the Basement and Unit A-D (Figs. 4.3 a-b: 4.4 c: 4.9: 4.10- 4.12).

4.3.5 Master fault 4 (MF4)

The MF4 is a normal fault striking to the southeast dipping southwest and situated within the ESH (Fig. 4.1). The fault is limited westward by the MF2 and continues out of the 3D seismic cube in the southeast (Fig.4.1). The MF4 offset the Basement and Unit A-D (Figs. 4.3 b-c: 4.9: 4.10-4.12).

4.3.6 Master fault 5 (MF5)

The MF5 is a normal fault and western half of the fault strikes east before bending southwards changing the strike to north (Fig. 4.1). The MF5 dips to the northeast and separates the ESH and Åsta Graben. The fault is limited westwards by the MF2 (Fig. 4.4 j), and eastwards, it continues out of the 3D seismic data. The area where MF5 is situated has relatively poor resolution resulting that no surfaces are interpreted across the entire MF5, except for the Top

Smith Bank Fm and Basement. The MF5 offset the Basement, Unit A-D, Zechstein Supergroup, and Base Smith Bank (Fig. 4.4 j).

4.3.7 Master fault 6 (MF6)

The MF6 is a normal fault striking southeast and dips towards the southwest (Fig. 4.1). It is limited westward by MF1 and eastwards by MF2. The MF6 separates the ESH and the Norwegian-Danish Basin. It has created an offset in the Basement, Unit A-D (Fig. 4.4 f), and Base Zechstein (Fig. 4.3 a). The MF6 reaches too far laterally to be tracked entirely within the 3D seismic data.

4.3.8 Pre-Permian fault (PPF)

The PPF is a vertical fault striking northwest-southeast and separates the CSH from the NSH (Figs. 4.1: 4.3 b: 4.4 i). It terminates towards the MF1 in the north, and MF3C in the south and at depth. The fault has offset the Basement-cover contact and Unit A-D.

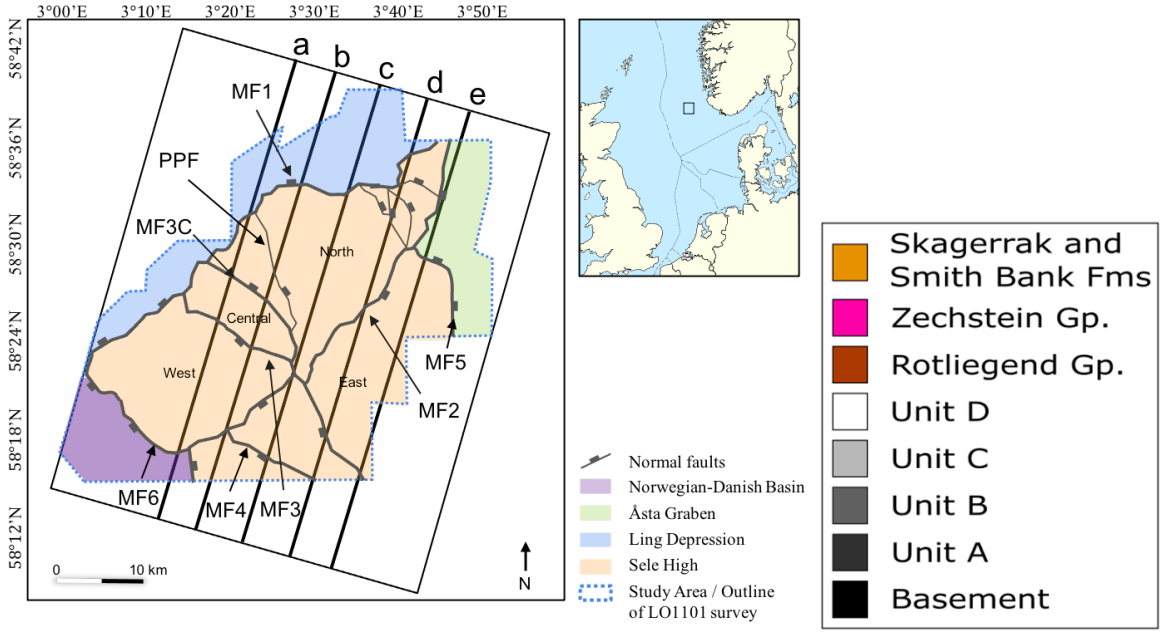
3°00'E
3°10'E
3°20'E
3°30'E
3°40'E
3°50'E
58°42'N
58°36'N
58°30'N
58°24'N
58°18'N
58°12'N
a
b
c
d
e
MF1
PPF
MF3C
North
Central
West
East
MF5
MF2
MF6
MF4
MF3
0
10 km
N
Normal faults
Norwegian-Danish Basin
Åsta Graben
Ling Depression
Sele High
Study Area / Outline of LO1101 survey
Skagerrak and Smith Bank Fms
Zechstein Gp.
Rotliegend Gp.
Unit D
Unit C
Unit B
Unit A
Basement

a)

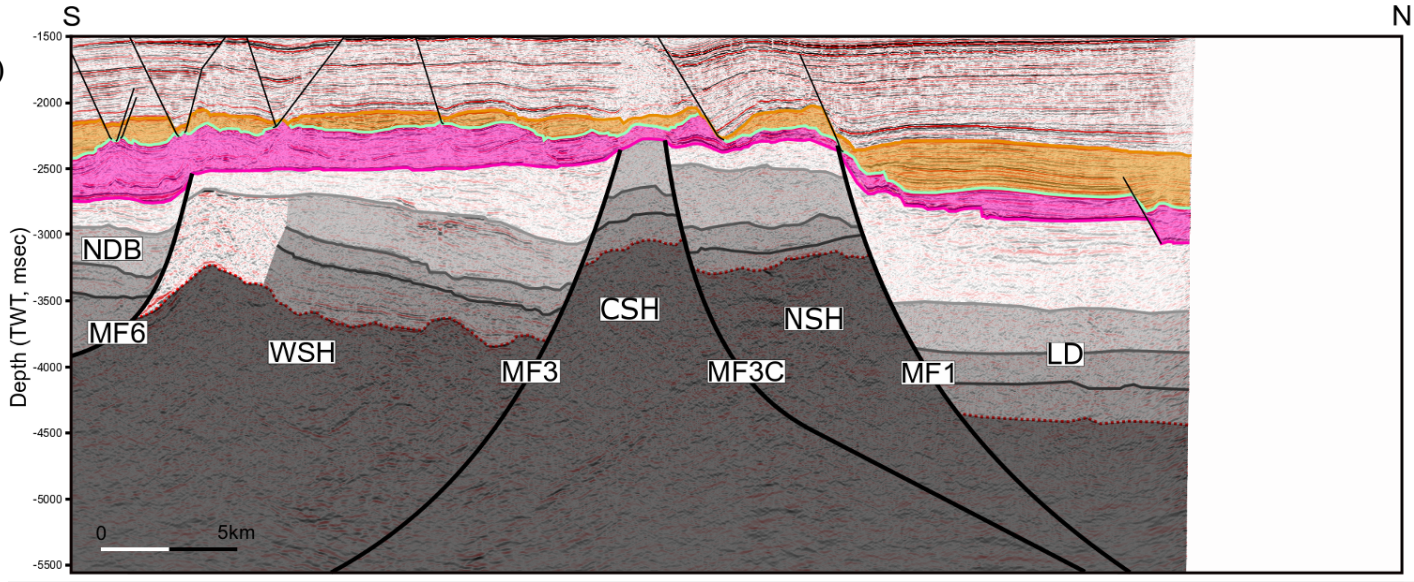
S
N
Depth (TWT, msec)
-1500
-2000
-2500
-3000
-3500
-4000
-4500
-5000
-5500
NDB
MF6
WSH
MF3
CSH
MF3C
NSH
MF1
LD
0
5km

b)

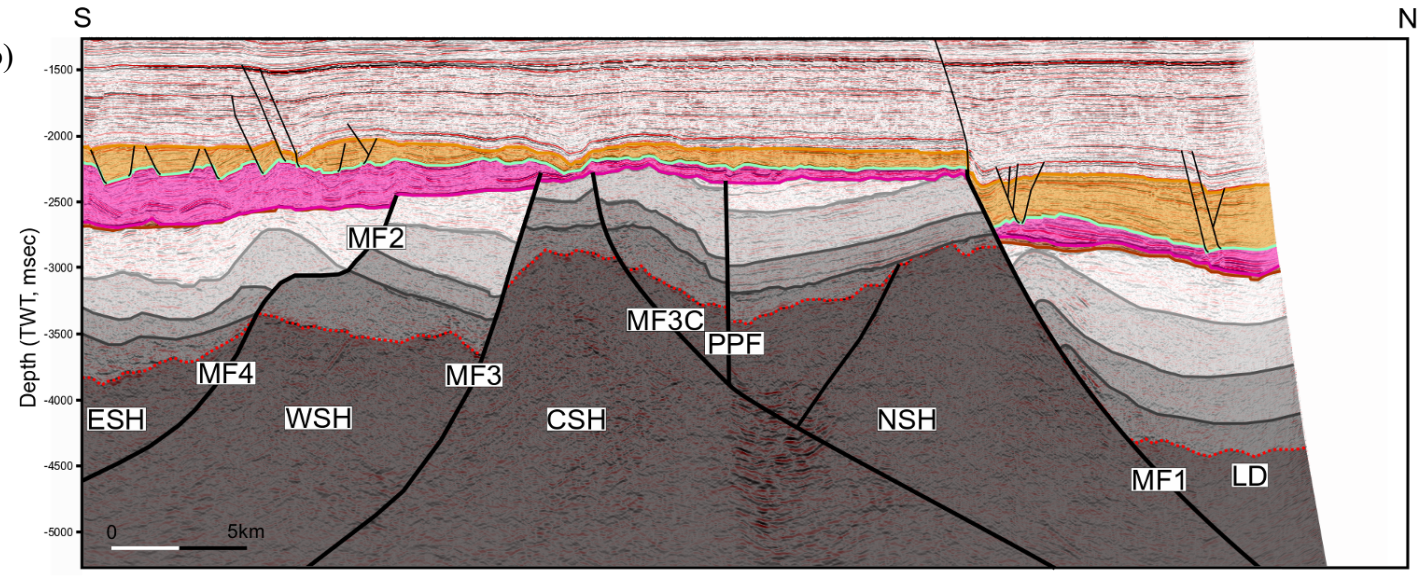
S
N
Depth (TWT, msec)
-1500
-2000
-2500
-3000
-3500
-4000
-4500
-5000
MF2
MF4
MF3
MF3C
PPF
ESH
WSH
CSH
NSH
MF1
LD
0
5km

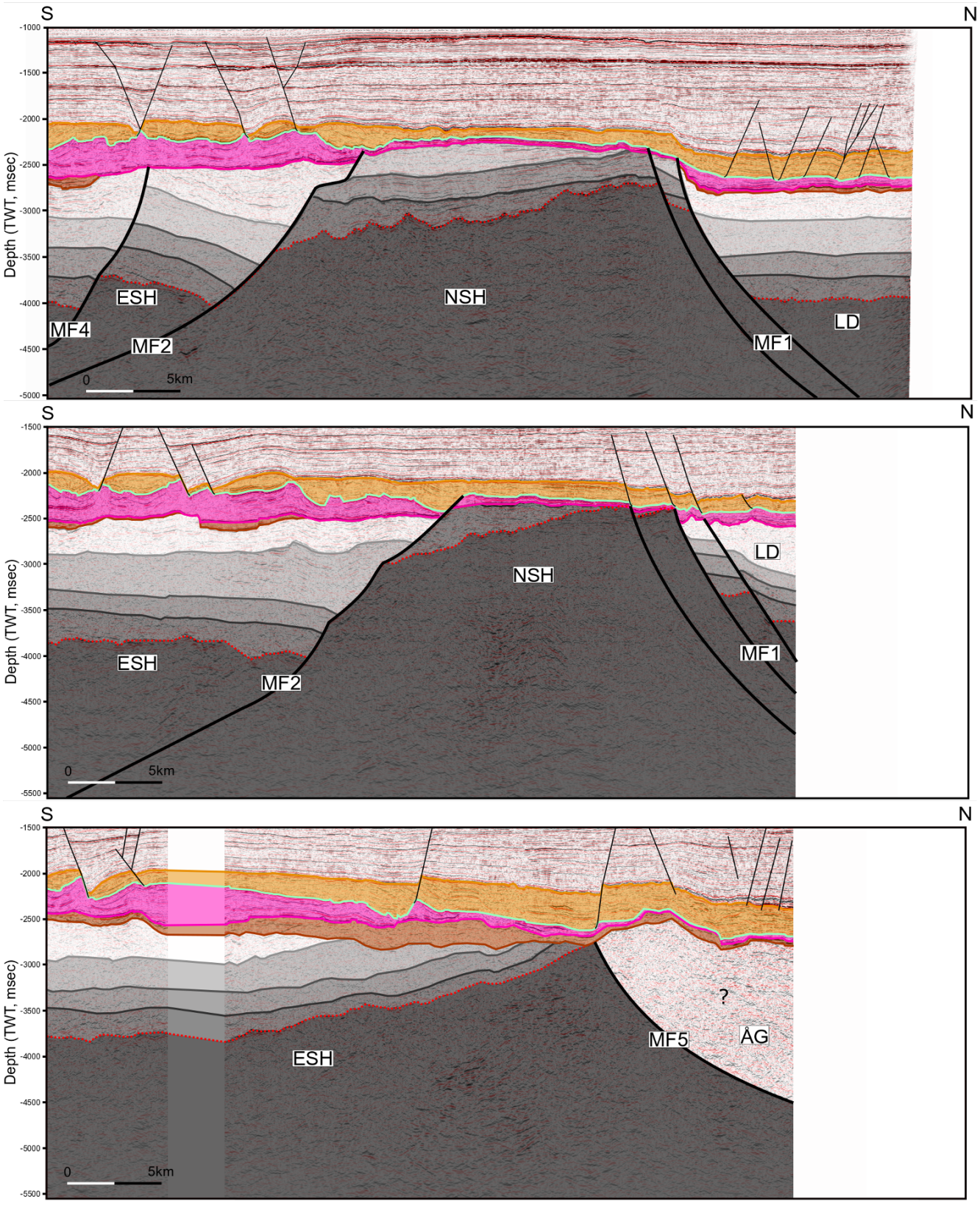

Figure 4.3: Overview of the study area around the Sele High in the Norwegian Central North Sea with structural elements, coverage of the seismic data, and the five inlines highlighted, showing where they are located in the study area and illuminating which structural elements each section cross. a-e) interpreted inlines form the 3D seismic data set oriented NNE-SSW, shown from westernmost to easternmost section. ESH, East Sele High; NSH, North Sele High; WSH, West Sele High; CSH, Central Sele High; ÅG, Åsta Graben; LD, Ling Depression; NDB, Norwegian-Danish Basin; MF1, master fault 1; MF2, master fault 2; MF3, master fault 3; MF3C, master fault 3 conjugate; MF4, master fault 4; MF5, master fault 5; MF6, master fault 6.

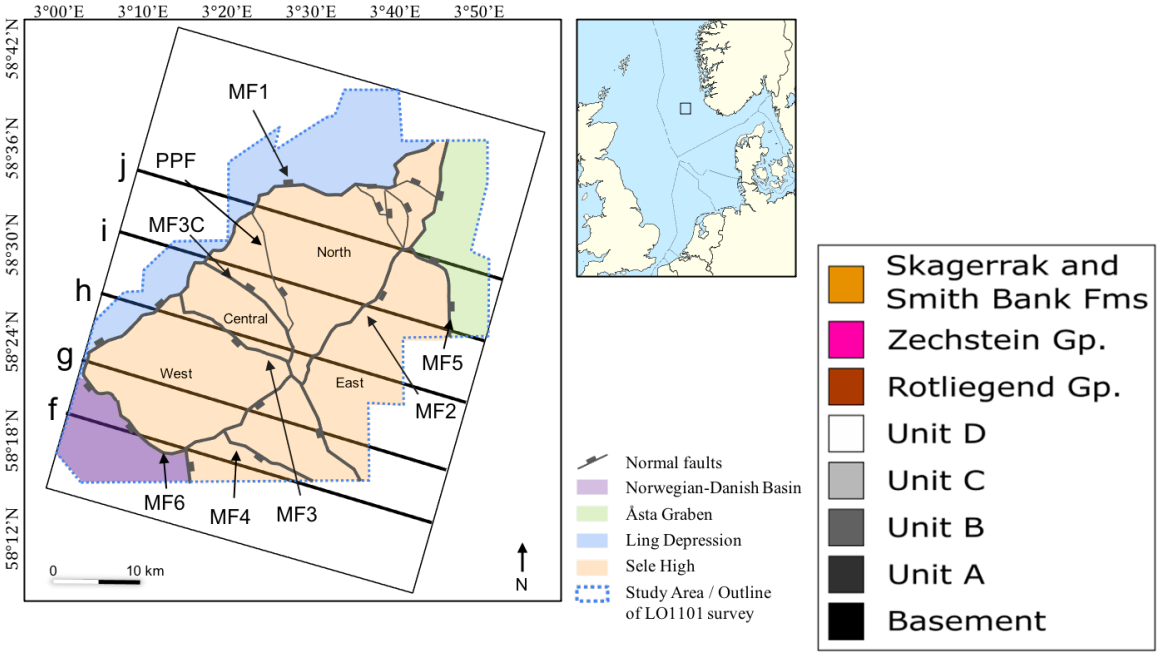
3°00'E
3°10'E
3°20'E
3°30'E
3°40'E
3°50'E
58°42'N
58°36'N
58°30'N
58°24'N
58°18'N
58°12'N
MF1
PPF
MF3C
North
Central
West
East
MF5
MF2
MF6
MF4
MF3
j
i
h
g
f
0
10 km
N
Normal faults
Norwegian-Danish Basin
Åsta Graben
Ling Depression
Sele High
Study Area / Outline of LO1101 survey
Skagerrak and Smith Bank Fms
Zechstein Gp.
Rotliegend Gp.
Unit D
Unit C
Unit B
Unit A
Basement

f)

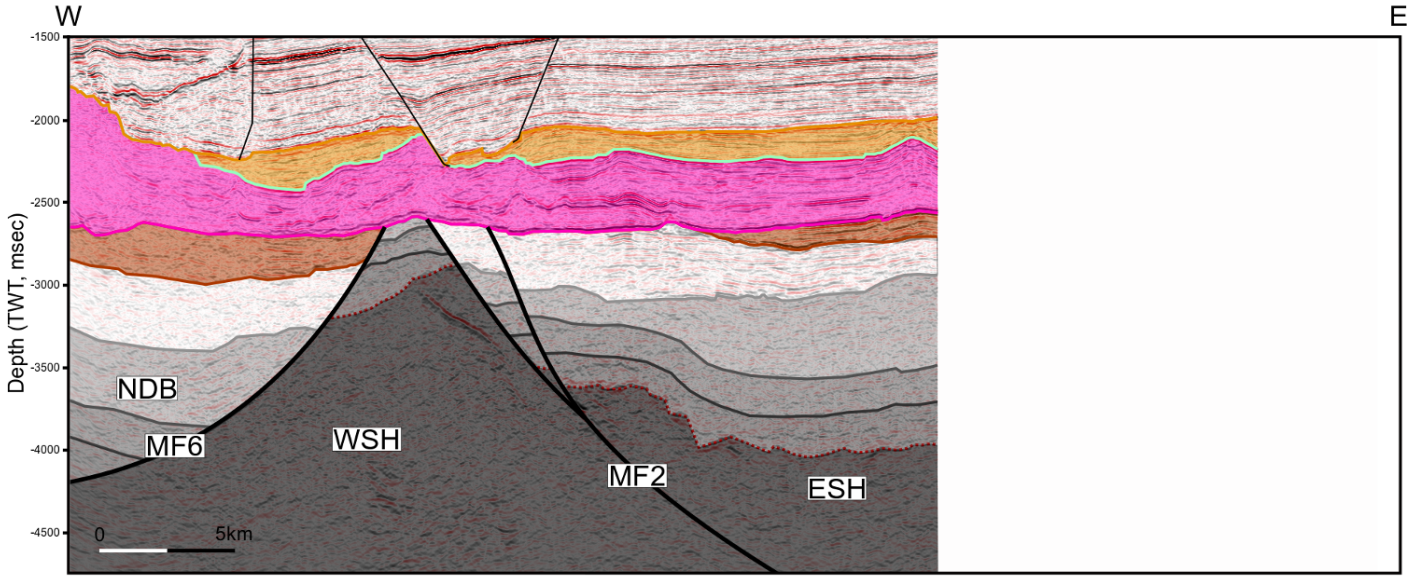
W
E
Depth (TWT, msec)
-1500
-2000
-2500
-3000
-3500
-4000
-4500
NDB
MF6
WSH
MF2
ESH
0
5km

g)

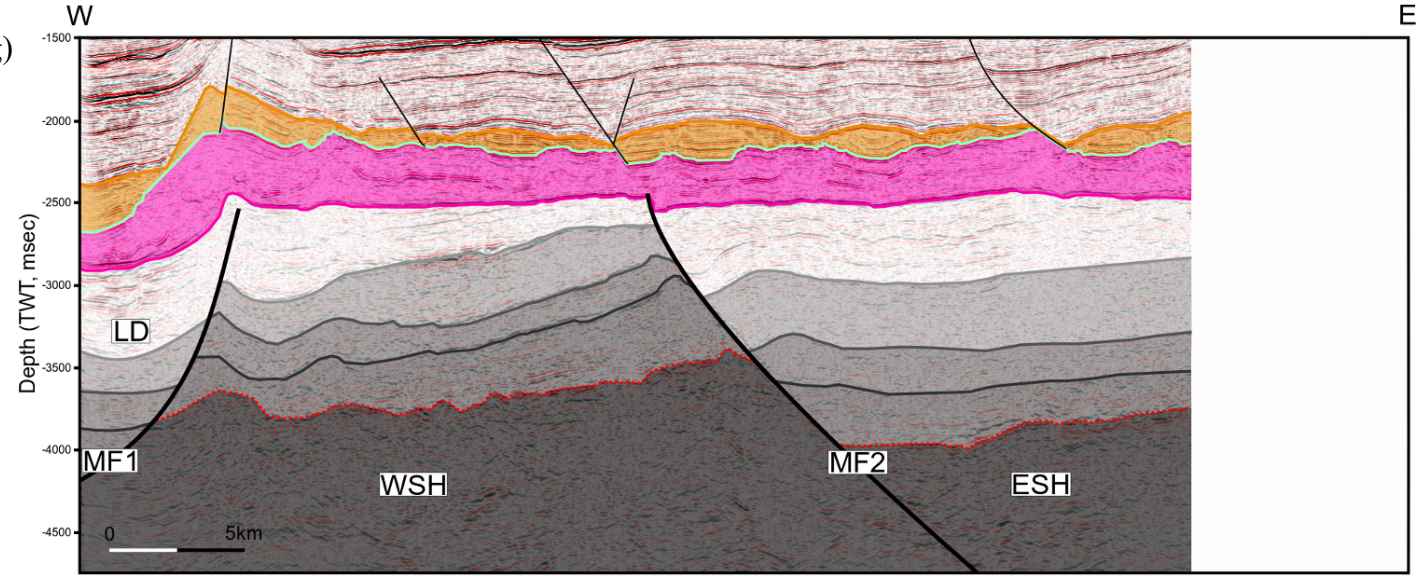
W
E
Depth (TWT, msec)
-1500
-2000
-2500
-3000
-3500
-4000
-4500
LD
MF1
WSH
MF2
ESH
0
5km

h)

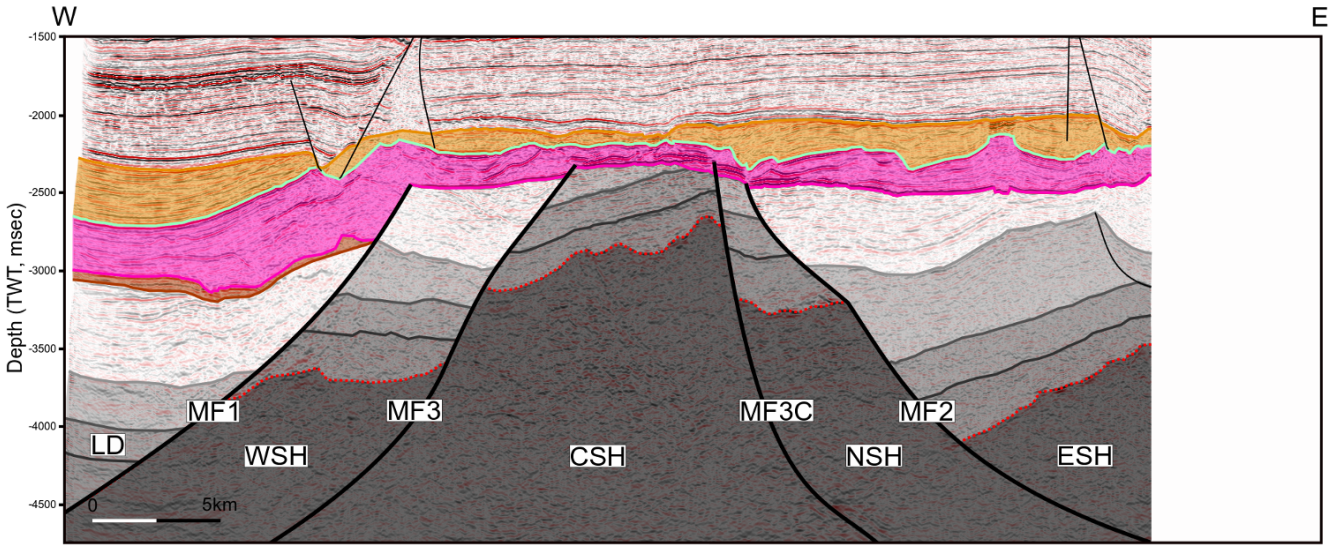

i)

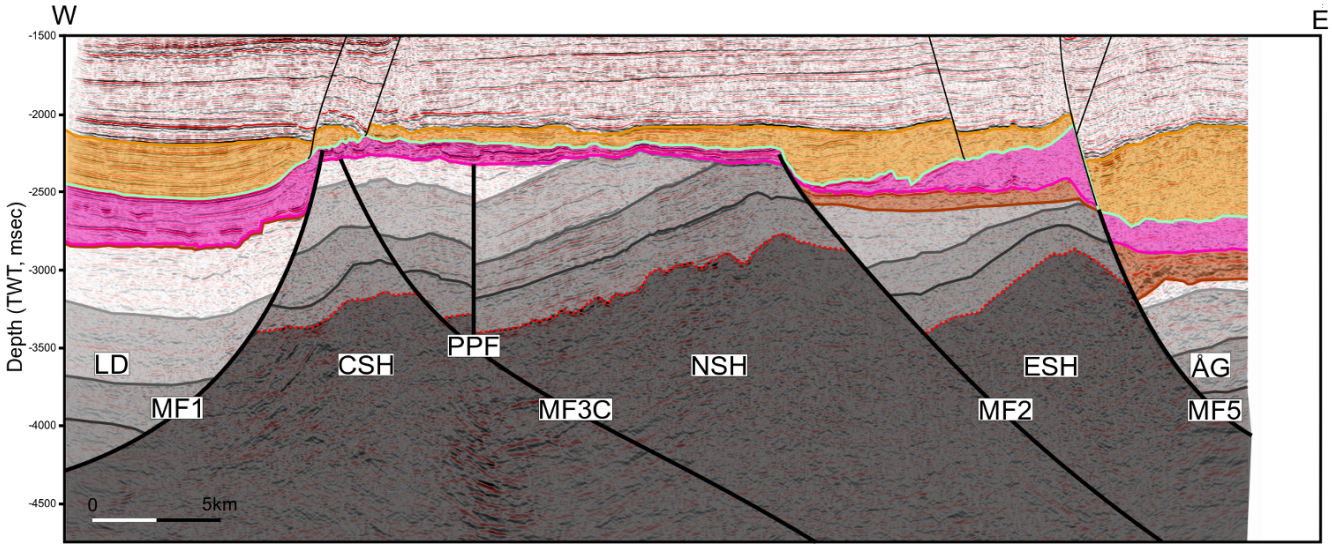

j)

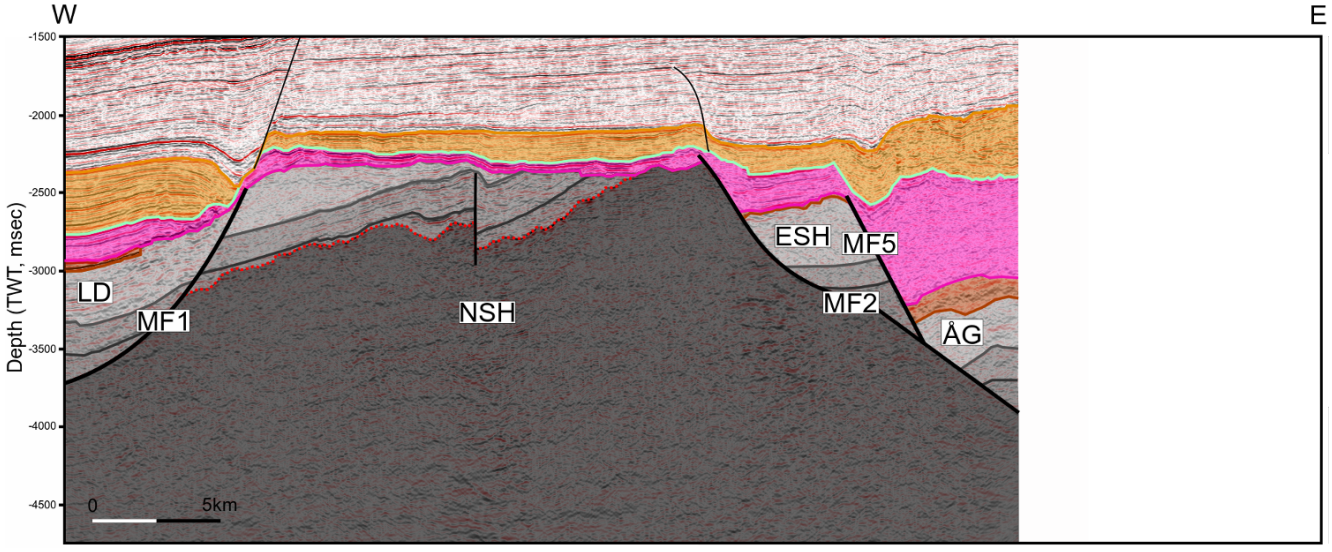

Figure 4.4: Overview of the study area around the Sele High in the Norwegian Central North Sea with structural elements, coverage of the seismic data, and the five crosslines highlighted, showing where they are located in the study area and illuminating which structural elements each section cross. a-e) interpreted crosslines form the 3D seismic data set oriented WNW-ESE, shown from southernmost to northernmost section. ESH, East Sele High; NSH, North Sele High; WSH, West Sele High; CSH, Central Sele High; ÅG, Åsta Graben; LD, Ling Depression; NDB, Norwegian-Danish Basin; MF1, master fault 1; MF2, master fault 2; MF3, master fault 3; MF3C, master fault 3 conjugate; MF4, master fault 4; MF5, master fault 5; MF6, master fault 6; PPF, Pre-Permian fault.

4.4 Present-day structural configuration of the Sele High

4.4.1 Top Skagerrak Fm. (time-structure map)

The Skagerrak and Smith Bank formations are the uppermost stratigraphic units interpreted in this study. The time-structure map of Top Skagerrak Fm. is capped at 1950 and 2450 ms TWT so that the structures are better visualized and that the scale is not overly fixated on the highest and lowest parts (Fig. 4.5). The most elevated parts of the surface lie in the Sele High and Åsta Graben sitting in the interval between 1950-2100 ms TWT and are generally flat (Figs. 4.3 and 4.4). The surface sits more profound in the Ling Depression and the Norwegian-Danish Basin reaching below 2450 ms TWT. The MF1 creates an offset in the surface separating the Sele High and the Ling Depression in contrast to the other master faults where we do not see any offset except in the northernmost and southernmost parts of MF2 and some at MF5.

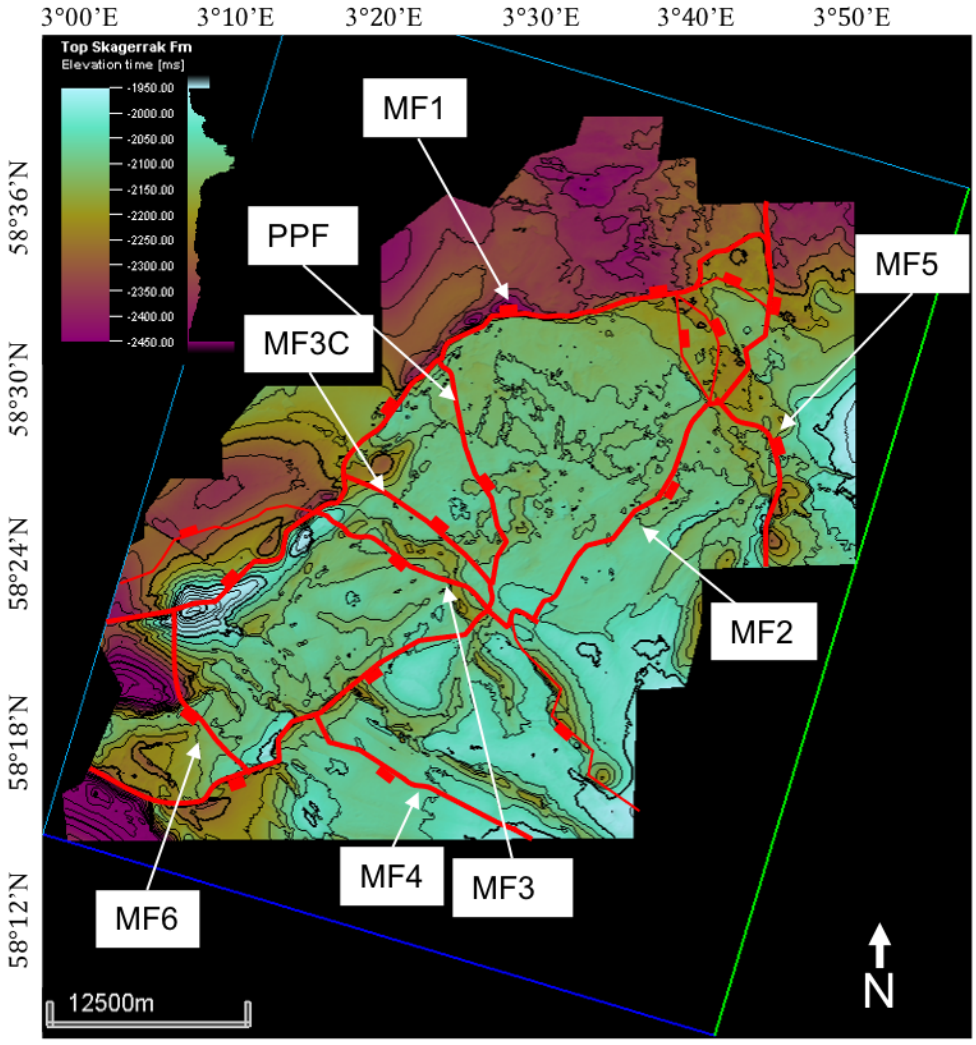

Figure 4.5: Time-structure map of the Smith Bank Fm. MF1, master fault 1; MF2, master fault 2; MF3, master fault 3; MF3C, master fault 3 conjugate; MF4, master fault 4; MF5, master fault 5; MF6, master fault 6; PPF, Pre-Permian fault.

4.4.2 Top Zechstein Supergroup (time-structure map)

The Top Zechstein Supergroup is the second uppermost surface interpreted in this study. The time-structure map of this surface is capped at 2000 and 2800 ms TWT to make the structures easier to see and prevent the scale from being excessively focused on the highest and lowest points (Fig. 4.6).

The highest parts of this surface are in the Sele High, where most are in the interval 2100-2250 ms TWT. The surface is generally flat in the Sele High except for two domes in the southern part of WSH, elevated above 2000 ms TWT, and the northern part of ESH, where the surface is lower, at 2300-2400 ms TWT. As in the Top Skagerrak Fm., the MF1 offset the Top Zechstein Supergroup from the Sele High to the Ling Depression, in the Sele High it lies in 2600 to down below 2800 ms TWT in the Ling Depression. The part of MF2 which separates NSH and ESH creates an offset in this surface in contrast to the Top Skagerrak Fm. that did not have an offset at this interval (Figs. 4.5 and 4.6). The part of MF2 which separates WSH and ESH does not show any offset before the area where MF4 connects with the MF2 (Fig. 4.3 b). In addition, the MF3 causes minor offset at this surface whereas MF3C, MF4, MF5 and PPF do not cause any offset (Fig. 4.6).

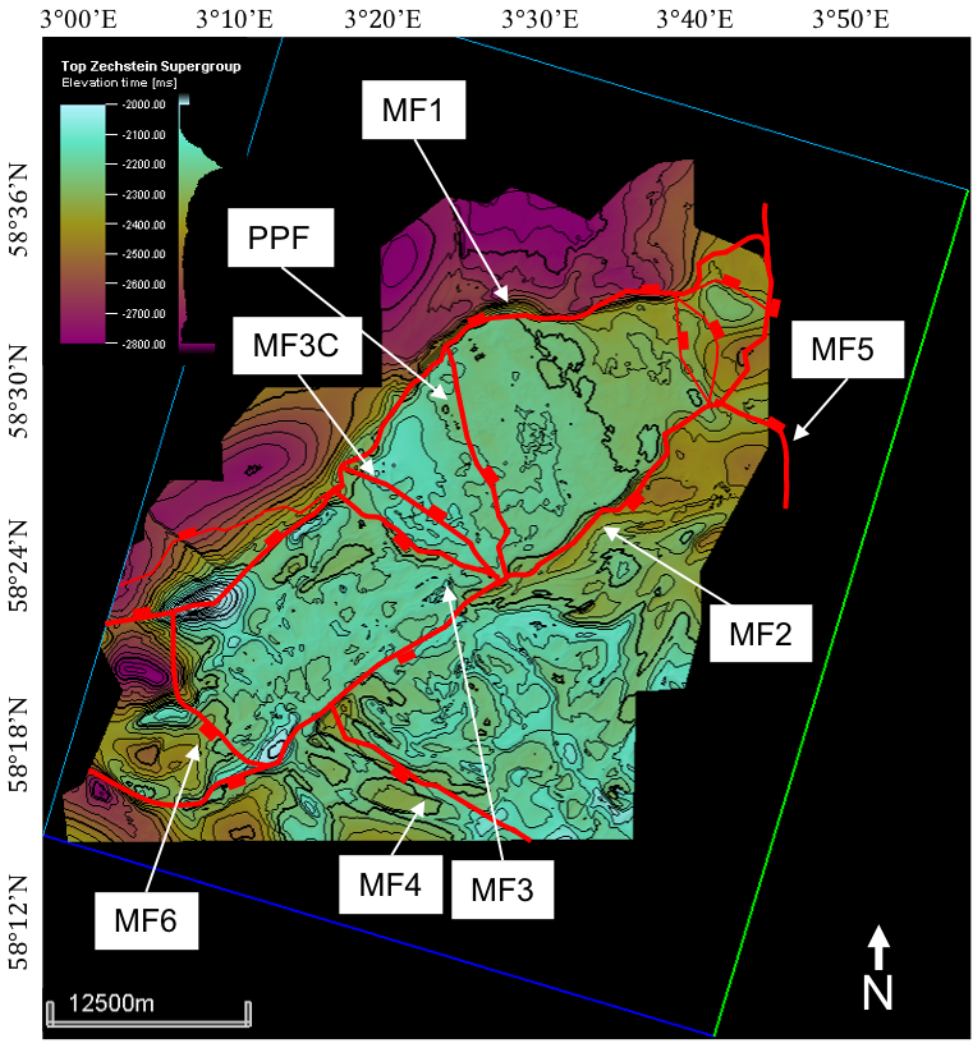

Figure 4.6: Time-structure map of the Top Zechstein Group, which also corresponds to the Base Smith Bank Fm. MF1, master fault 1; MF2, master fault 2; MF3, master fault 3; MF3C, master fault 3 conjugate; MF4, master fault 4; MF5, master fault 5; MF6, master fault 6; PPF, Pre-Permian fault.

4.4.3 Base Zechstein Supergroup (time-structure map)

The Base Zechstein Supergroup is the third highest surface interpreted in this study. The Base Zechstein Supergroups time-structure map is capped at 2200 and 3100 ms TWT to exclude the outliers and enhance structural visualization (Fig. 4.7).

This surface has the structurally highest area in the NSH and CSH ranging from 2200 to 2300 ms TWT. In the ESH and WSH, the Base Zechstein Supergroup sits lower at 2350-2600 ms TWT. The surface sits much deeper in the Ling Depression, reaching below 3100 ms TWT (Figs. 4.3 a-c and 4.4 g-j). The surface is also deeper in the Norwegian-Danish Basin and the parts of the Åsta Graben, which were interpretable compared to the Sele High (Fig. 4.7). The MF1, MF2, and MF3 offset the Base Zechstein Supergroup, with the most significant offset at MF1 separating the Sele High and the Ling Depression. The MF3 connects with MF1 to the west where MF1 splays and creates another fault that offsets the Base Zechstein Supergroup level.

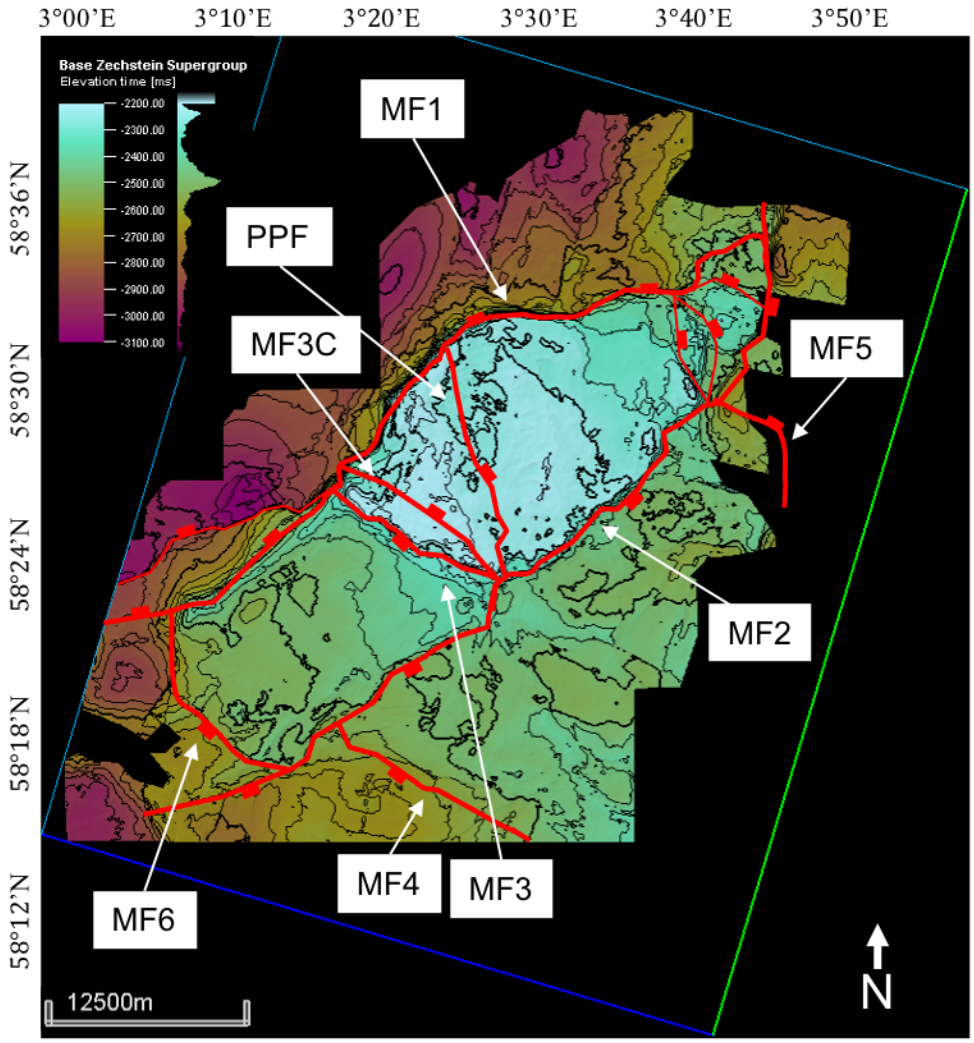

Figure 4.7 Time-structure map of the Base Zechstein Group. MF1, master fault 1; MF2, master fault 2; MF3, master fault 3; MF3C, master fault 3 conjugate; MF4, master fault 4; MF5, master fault 5; MF6, master fault 6; PPF, Pre-Permian fault.

4.4.4 Top Unit D (time-structure map)

The Top Unit D is the fourth highest surface interpreted in this region and is not possible to correlate with any known stratigraphic level; therefore, the name Unit D in the current study. The time-structure map of the Unit D is capped at 2200 and 3100 ms TWT to cutoff the outliers and better visualize the structures (Fig. 4.8).

Top Unit D is very similar to Base Zechstein Supergroup level (Fig. 4.7) and is tracked where the lower surfaces are truncating towards it. As the previous surface, the NSH and CSH are the highest structural areas in the interval 2200-2300 ms TWT (Fig. 4.8). This surface, as the previous, shows offset at MF1, MF2, and MF3 while the MF3C and MF4 do not affect it.

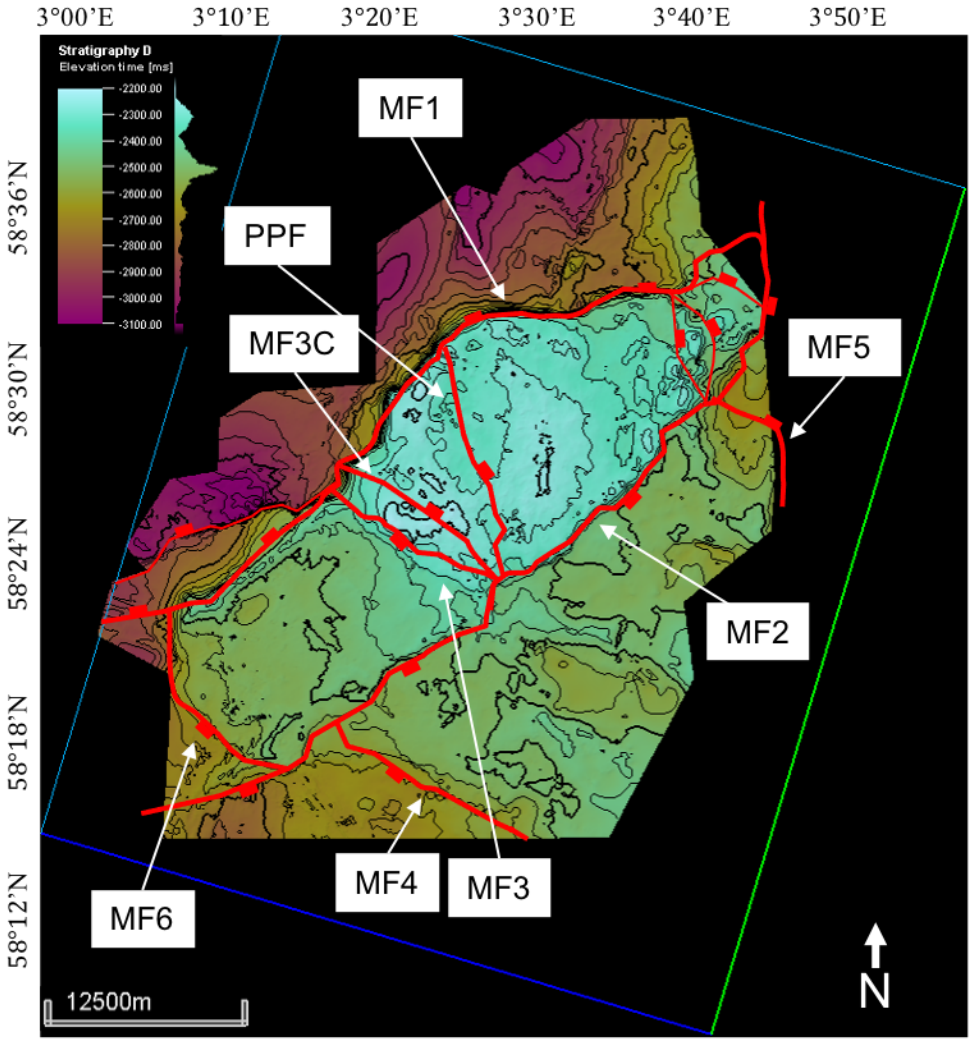

Figure 4.8: Time-structure map of the Top Unit D, which is an unconformity throughout the study area. MF1, master fault 1; MF2, master fault 2; MF3, master fault 3; MF3C, master fault 3 conjugate; MF4, master fault 4; MF5, master fault 5; MF6, master fault 6; PPF, Pre-Permian fault.

4.4.5 Top Unit C (time-structure map)

Top Unit C is the fourth lowest surface interpreted in this study and does not correlate with any known stratigraphic level; therefore, the name Unit C. The Top Unit C's time-structure map is capped at 2300 and 3200 ms TWT for visualization purposes (Fig. 4.9).

This and the lower interpreted surfaces, except for the Basement-cover contact, are smaller than the aforementioned surfaces as they are not possible to track in the Ling Depression, Åsta Graben, Norwegian Danish Basin, and the eastern parts of the ESH in the 3D seismic due to the depth and cover which reduces the seismic signal (Figs. 4.9-4.11). The most elevated parts of this surface are flat, much like a plateau, and are situated in the NSH and CSH, in the interval 2300-2330 ms TWT (Fig. 4.9). However, in the western part of NSH, the surface dips towards the west and reaches 2700 ms TWT (Figs. 4.4 i). In the WSH, the surface is deeper in the interval 2600-3100 ms TWT with a deepening westward trend (Fig. 4.4 g). In the ESH the Top Unit C is situated even deeper at 2850-3200 ms TWT and are segmented by the MF4. At this surface, we can also see that all the master faults and the PPF create an offset except for MF3C, which is within the plateau at CSH.

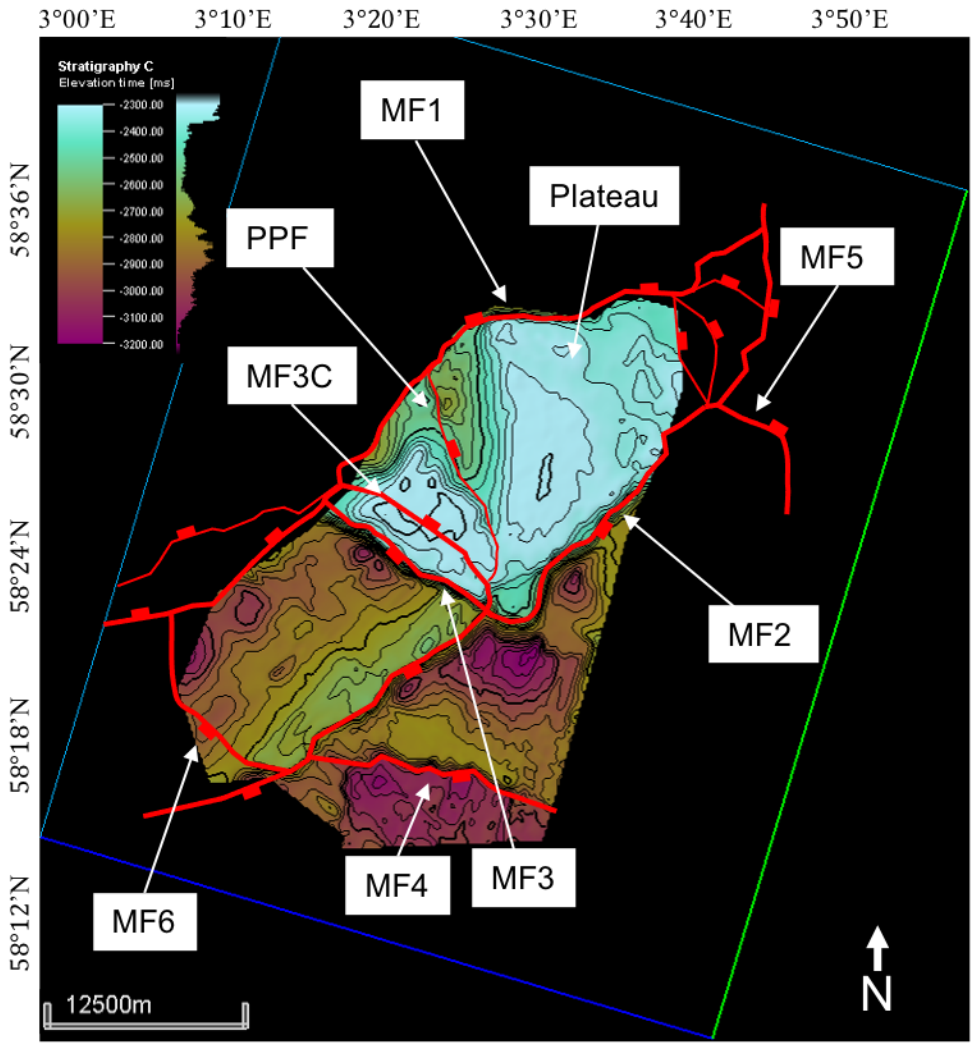

Figure 4.9: Time-structure map of the Top Unit C. MF1, master fault 1; MF2, master fault 2; MF3, master fault 3; MF3C, master fault 3 conjugate; MF4, master fault 4; MF5, master fault 5; MF6, master fault 6; PPF, Pre-Permian fault.

4.4.6 Top Unit B (time-structure map)

The Top Unit B is the third lowest surface interpreted in this study and does not correlate with any known stratigraphic level; therefore, the name Unit B. The surface is in the interval 2300-3600 ms TWT (Fig. 4.10).

At this surface, the CSH and northeastern part of NSH are the highest structural areas reaching 2300 ms TWT. The shallowest part of the Top Unit B in NSH is flat (Plateau), much like in Top Unit C but to a lesser extent (Figs. 4.9-4.10). From the high northeast of NSH, the Top Unit B has a southwest dip going from 2300 in the northeast to 2950 ms TWT in the southwest (Figs. 4.4 i-j). In the WSH, the surface has a northwest dip, going from 2750 in the southeast to 3500 ms TWT in the northwest (Fig. 4.4 g). In the ESH, the Top Unit B is more complicated as the surface reaches 2800 ms TWT in the northeast, but are in general situated much deeper,

reaching down to 3600 ms TWT, this may be explained by the proximity to the MF5 which record most of the displacement (Fig. 4.4 i-j). All master faults do offset this surface (Fig. 4.10).

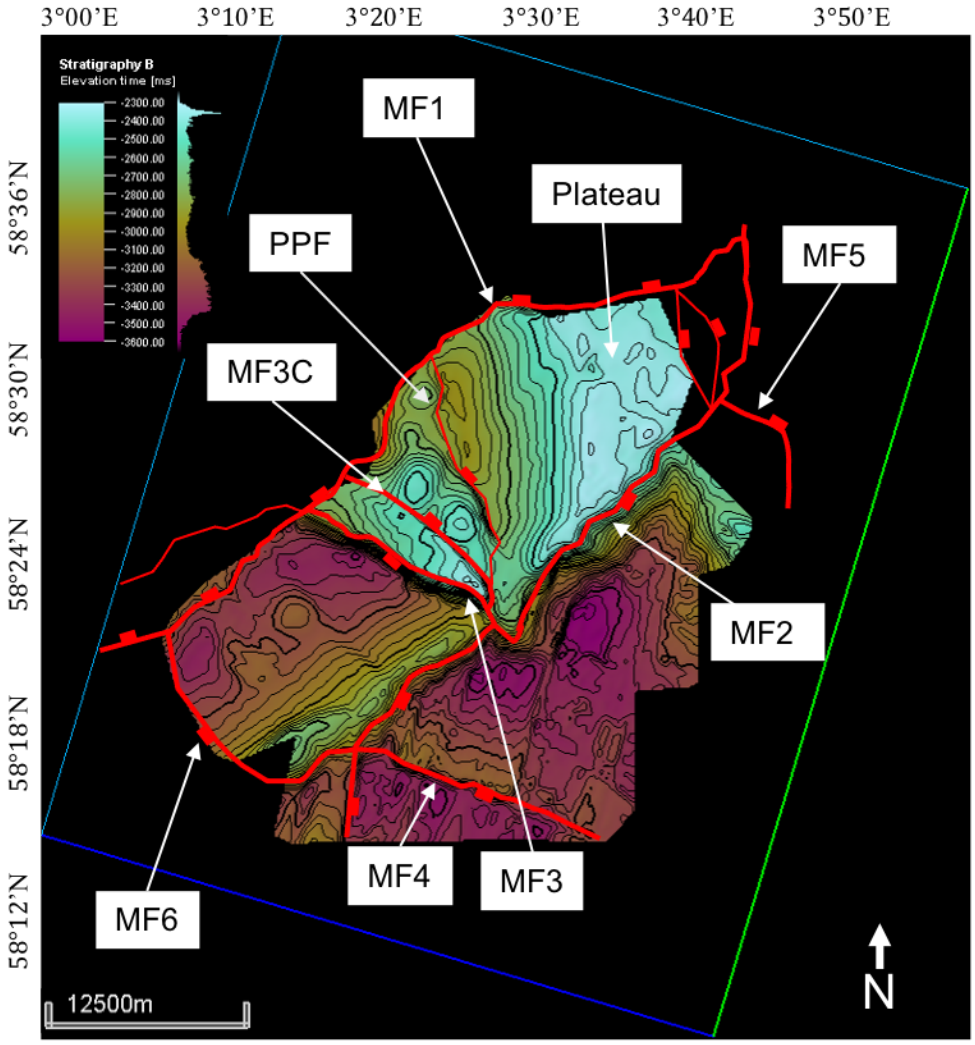

Figure 4.10: Time-structure map of the Top Unit B. MF1, master fault 1; MF2, master fault 2; MF3, master fault 3; MF3C, master fault 3 conjugate; MF4, master fault 4; MF5, master fault 5; MF6, master fault 6; PPF, Pre-Permian fault.

4.4.7 Top Unit A (time-structure map)

Top Unit A is the second lowest surface interpreted in this study and does not correlate with any known stratigraphic level; therefore, the name Unit A. The Top Unit A is in the interval 2300-3800 ms TWT (Fig. 4.11).

The highest parts of this surface are in the CSH and northeast of NSH. The higher parts of NSH are also flat, like Top Unit B and C but to a lesser extent (Figs. 4.9-4.11). The surface in the NSH dips from 2300 in the northeast to 3200 ms TWT in the southwest (Fig. 4.4 i-j). In the WSH, the surface dips towards the northwest from 3000 in the southwest to 3500 ms TWT (Fig. 4.4 g). The WSH is generally situated deeper than the other parts of the Sele High, reaching

down to 3800 ms TWT in the central part and on the downthrown side of the MF4 (Fig. 4.11). From the upthrown side of MF4, the surface has a northward dip. All the master faults create an offset in this stratigraphic level.

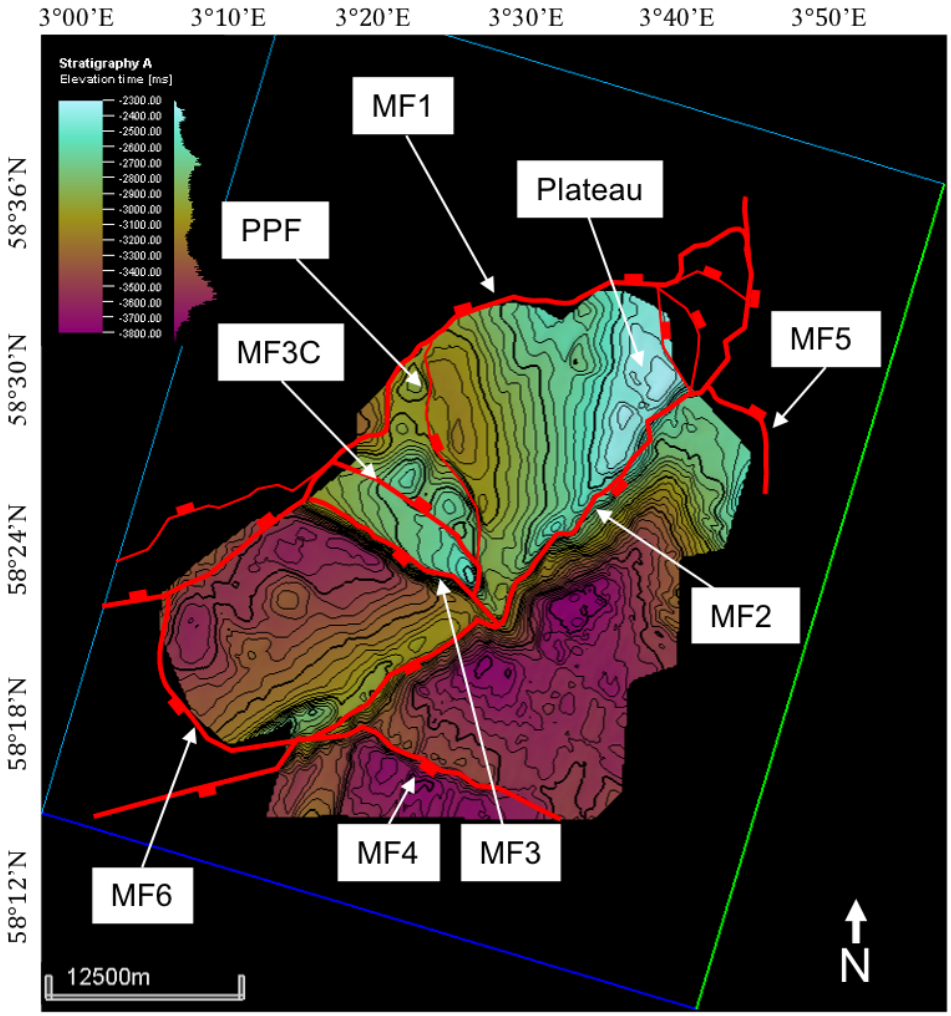

Figure 4.11: Time-structure map of the Top Unit A. MF1, master fault 1; MF2, master fault 2; MF3, master fault 3; MF3C, master fault 3 conjugate; MF4, master fault 4; MF5, master fault 5; MF6, master fault 6; PPF, Pre-Permian fault.

4.4.8 Basement

The Basement-cover contact is the lowest interpreted surface. It is capped at 2300 and 4500 ms TWT so that the structures are better visualized and that the scale is fixated on the outliers (Fig. 4.12).

The peak of this surface is in the northeastern corner of NSH, reaching just above 2300 ms TWT (Figs 4.3 d and 4.12). From this point, the Basement has a southwest deepening trend and reaches 3400 ms TWT towards the PPF (Figs. 4.3 b: 4.4 i and 4.12). Between the MF3 and MF3C, the Basement has a west-east inclination going from 2660 ms TWT in the east, down

to 3130 ms TWT in the west, adjacent to MF1 (Fig. 4.12). In the WSH, the Basement has two NE-SW trending ridges that are primarily controlled by the MF1 and MF2. The one to the west is deeper and lies around 3700 ms TWT compared to the 3400 ms TWT for the shallower eastern ridge. At the southern part of the eastern ridge, there is a culmination along the MF2 between the intersection of MF4 and MF6. The lowest part of WSH can be found just east of the small ridge, following the same trend. This gives the Basement at WSH a west-skewed saucer shape (Fig. 4.12). The Basement has a culmination in the northern part of ESH, adjoining MF5, which reaches 2530 ms TWT (Fig. 4.3 e). Southwards from this culmination, it is rapidly deepening to 4000 ms TWT. The footwall of MF4 reaches 3700 ms TWT and has a northward dip reaching 4030 ms TWT (Fig. 4.12). The downthrown side sits at 4050 ms TWT adjacent to MF4 before shallowing southwards. The Basement is downfaulted from the Sele High to its adjacent structural elements, reaching deeper than 4400 ms TWT in the Ling Depression and Norwegian-Danish Basin (Figs 4.3 and 4.4). For Åsta Graben the Basement is faulted out of the 3D cube.

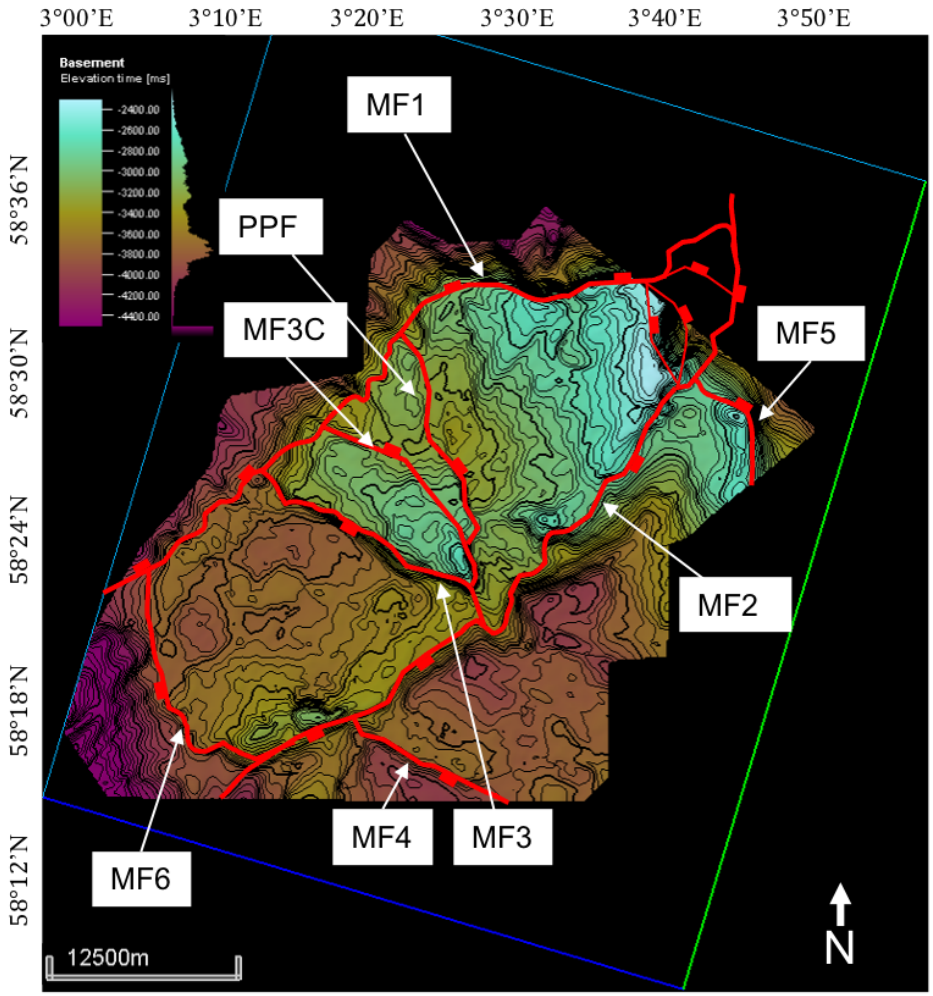

Figure 4.12: Time-structure map of the Basement-cover contact. MF1, master fault 1; MF2, master fault 2; MF3, master fault 3; MF3C, master fault 3 conjugate; MF4, master fault 4; MF5, master fault 5; MF6, master fault 6; PPF, Pre-Permian fault.

4.5 Tectonostratigraphic development of the Sele High

4.5.1 Thickness of the Skagerrak and Smith Bank Formations

The thickness of Skagerrak and Smith Bank Fm is between 0 and 500 ms TWT (Fig. 4.13). In the NSH, the formation has a thickening trend towards the northeast, going from 50 ms TWT in the southwest to 150 ms TWT in the northeast. In the CSH, the formation is between 0-100 ms TWT, with a large area with 0 ms TWT thickness just south of MF1. In WSH, the Smith Bank has an undulating thickness from northwest to southeast. Also, in the southern part of ESH, there is an undulating thickness at a northeast-southwest trend, more or less perpendicular to MF4. In the northern part of ESH, the thickness increases to 400 ms TWT. In the Ling Depression, the Smith Bank is much thicker than on the Sele High. Along MF1, the thickness is around 0 ms TWT, and across MF1, the thickness changes from around 50 to 350 ms TWT from the upthrown to the downthrown side. This is also seen across MF2 but only in the part separating NSH and ESH.

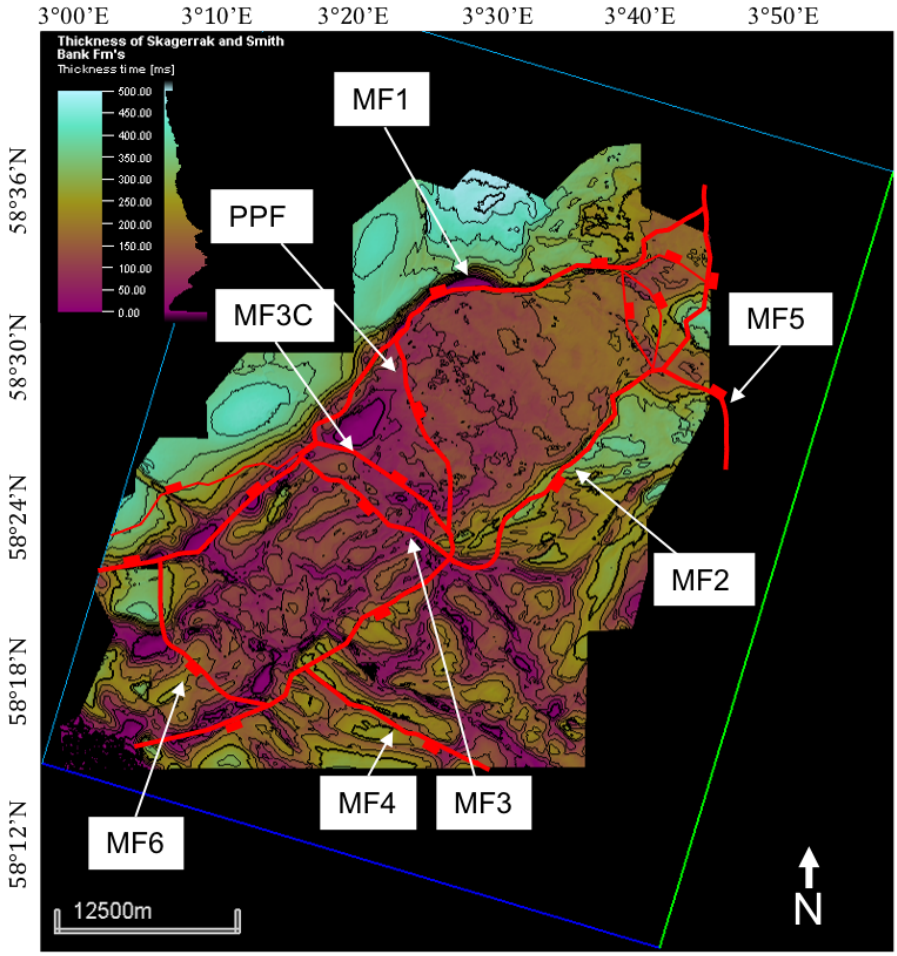

Figure 4.13. Time-thickness map of the Skagerrak and Smith Bank Formations. MF1, master fault 1; MF2, master fault 2; MF3, master fault 3; MF3C, master fault 3 conjugate; MF4, master fault 4; MF5, master fault 5; MF6, master fault 6; PPF, Pre-Permian fault.

4.5.2 Thickness Zechstein Supergroup

The Thickness of the Zechstein Supergroup is capped at 0 and 500 ms TWT (Fig. 4.14). The thickness of the Zechstein Supergroup is 0 ms TWT for large portions of the CSH, NSH, northern Ling Depression, and northern WSH. In the southern part, the thickness increases, giving a general trend of thickness increasing from north to south. In the WSH and ESH, the thickness of the Zechstein Supergroup is between 200 and up above 500 ms TWT. Across the splay of MF1, the group is thicker on the downthrown side than the upthrown. In the southern part of MF1, where it links with MF6, the Zechstein Supergroup forms a dome and reaches to a thickness of above 750 ms TWT (Fig. 4.14).

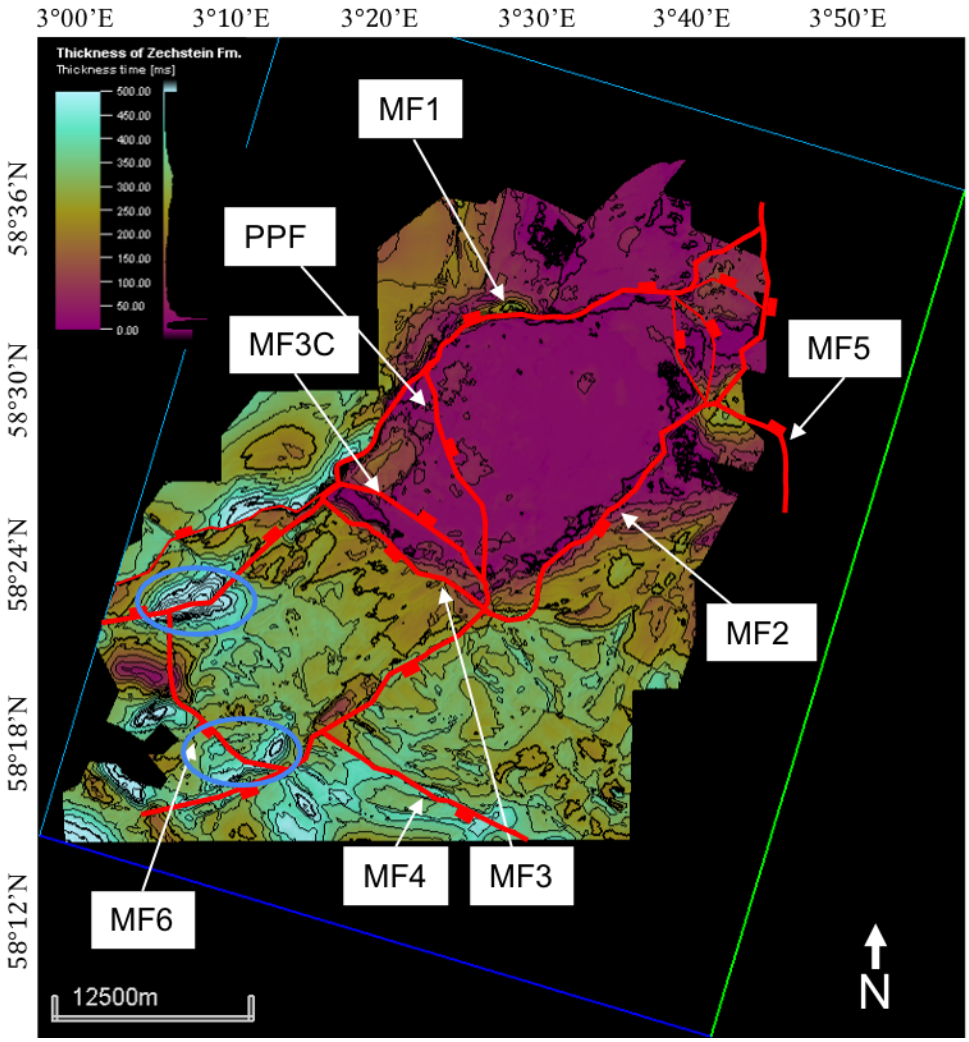

Figure 4.14. Time-thickness map of the Zechstein Group. Domes in encircled in blue. MF1, master fault 1; MF2, master fault 2; MF3, master fault 3; MF3C, master fault 3 conjugate; MF4, master fault 4; MF5, master fault 5; MF6, master fault 6; PPF, Pre-Permian fault.

4.5.3 Thickness Unit D

The thickness of Unit D is capped at 0 and 600 ms TWT (Fig. 4.15). The thickness is zero for most of the NSH and CSH area, equivalent to the plateau area from the time-structure map of Unit C (Fig. 4.9). In ESH, the unit has a northwest thickening trend, being 100 ms TWT thick in the southeast reaching 500 ms TWT in the northwest (Fig. 4.15). In the WSH, the thickness is between 250 and 650 ms TWT with a south-to-north thickening trend abrupted by MF4. There is a thickness offset across all the master faults except MF3C.

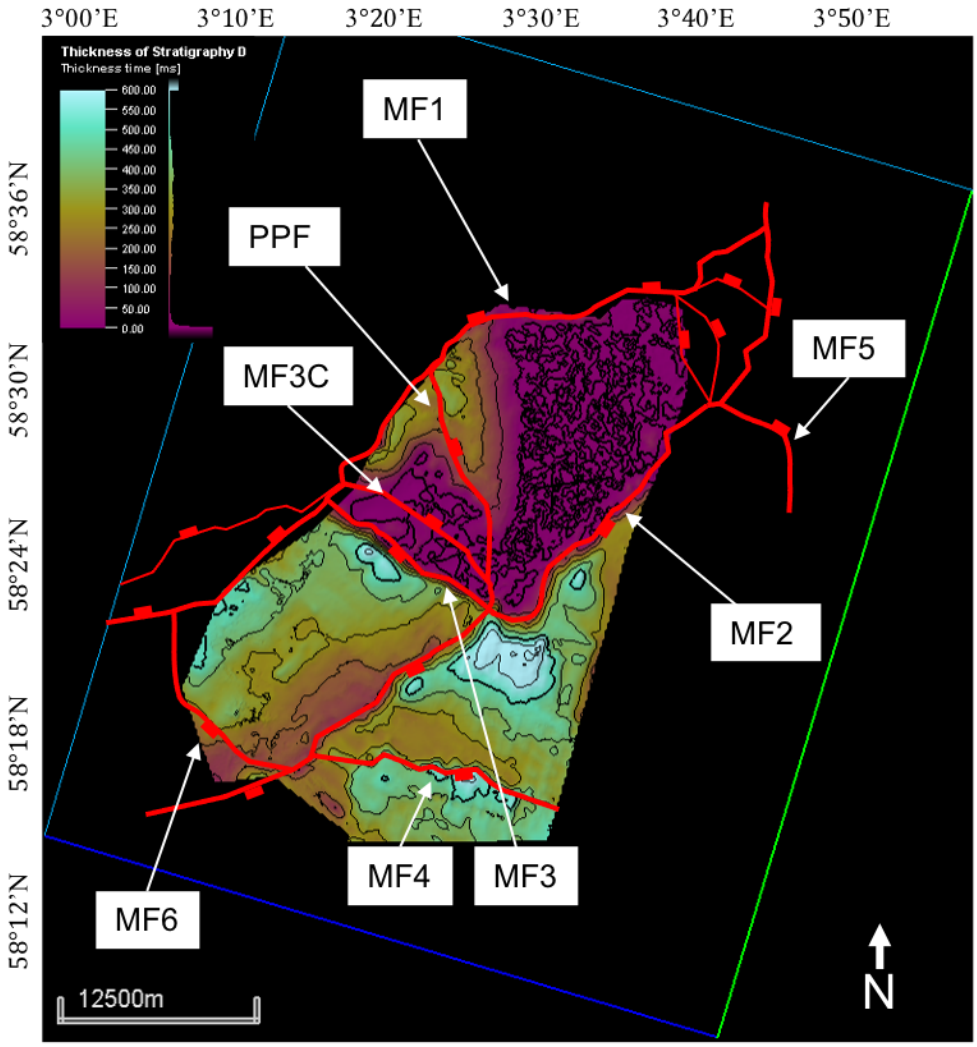

Figure 4.15. Time-thickness map of the Unit D. MF1, master fault 1; MF2, master fault 2; MF3, master fault 3; MF3C, master fault 3 conjugate; MF4, master fault 4; MF5, master fault 5; MF6, master fault 6; PPF, Pre-Permian fault.

4.5.4 Thickness Unit C

The thickness of Unit C is capped at 0 and 600 ms TWT (Fig. 4.16). The plateau area from the time-structure map of Top Unit B is located in the northeastern part of NSH, in this area the thickness is zero for Unit C (Fig. 4.10). The thickness in NSH is increasing towards PPF reaching 450 ms TWT. It is thinner on the southern side of PPF. In CSH the thickness is zero in the southeastern corner increasing westwards between MF3 and MF3C. Unit C thickens from the upthrown (CSH) to the downthrown (WSH) side of MF3. In the WSH, the thickness varies from 0 along MF2 to 600 ms TWT in the northeast.

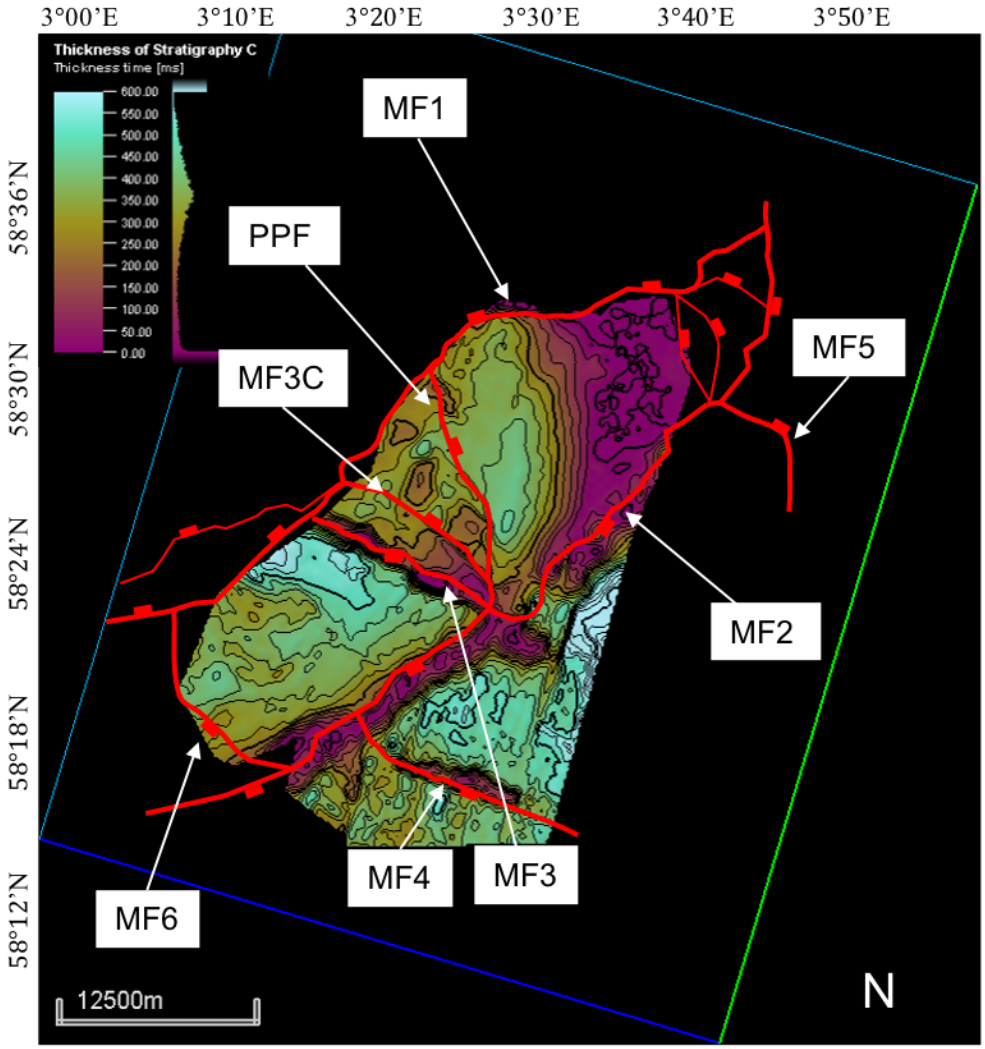

Figure 4.16. Time-thickness map of the Unit C. MF1, master fault 1; MF2, master fault 2; MF3, master fault 3; MF3C, master fault 3 conjugate; MF4, master fault 4; MF5, master fault 5; MF6, master fault 6; PPF, Pre-Permian fault.

4.5.5 Thickness Unit B

Unit B's thickness is capped at 0 ms TWT. In the NSH, the thickness is zero in the northeastern corner, corresponding to the plateau area from the time-structure map of Top Unit A (Fig. 4.11). From the northeast corner the unit rapidly thickens westwards to 250 ms TWT (Fig. 4.17). Continuing westwards in the NSH the unit thins from the 250 to 200 ms TWT adjacent to MF1 (Fig. 4.4 j). For the CSH, ESH and WSH the thickness of Unit B is fairly homogenous at around 200 only abrupted below the faults where the thickness decreases to zero.

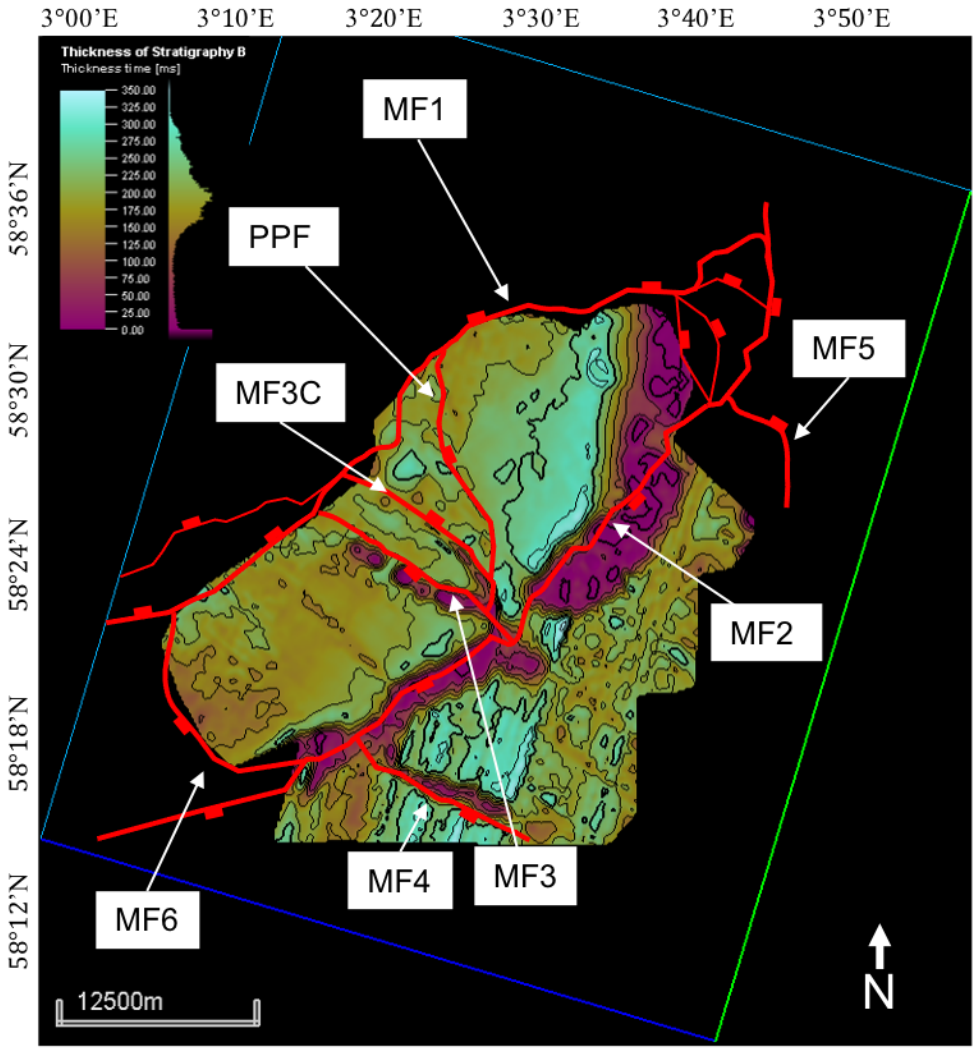

Figure 4.17. Time-thickness map of the Unit B. MF1, master fault 1; MF2, master fault 2; MF3, master fault 3; MF3C, master fault 3 conjugate; MF4, master fault 4; MF5, master fault 5; MF6, master fault 6; PPF, Pre-Permian fault.

4.5.6 Thickness Unit A

The Unit A is the lowermost sequence interpreted in this study. Its thickness is capped at 0 and 550 ms TWT (Fig. 4.18). In NSH, the unit reaches a thickness of right above 400 ms TWT in the southeastern part before decreasing towards the northwest, becoming thinner than 50 ms TWT close to MF1. In the CSH, the unit is mainly in the interval 100-300 ms TWT with no clear trend, though one dome lies north of MF3C reaching above 550 ms TWT. Close to MF1 and MF3 in the WSH, the thickness is generally thinner than the rest of the WSH, yet opposite is correct close to MF2. There is no clear trend for ESH, but the thickness is mainly between 150-350 ms TWT, except along MF2, MF3 and MF4, where it is primarily zero.

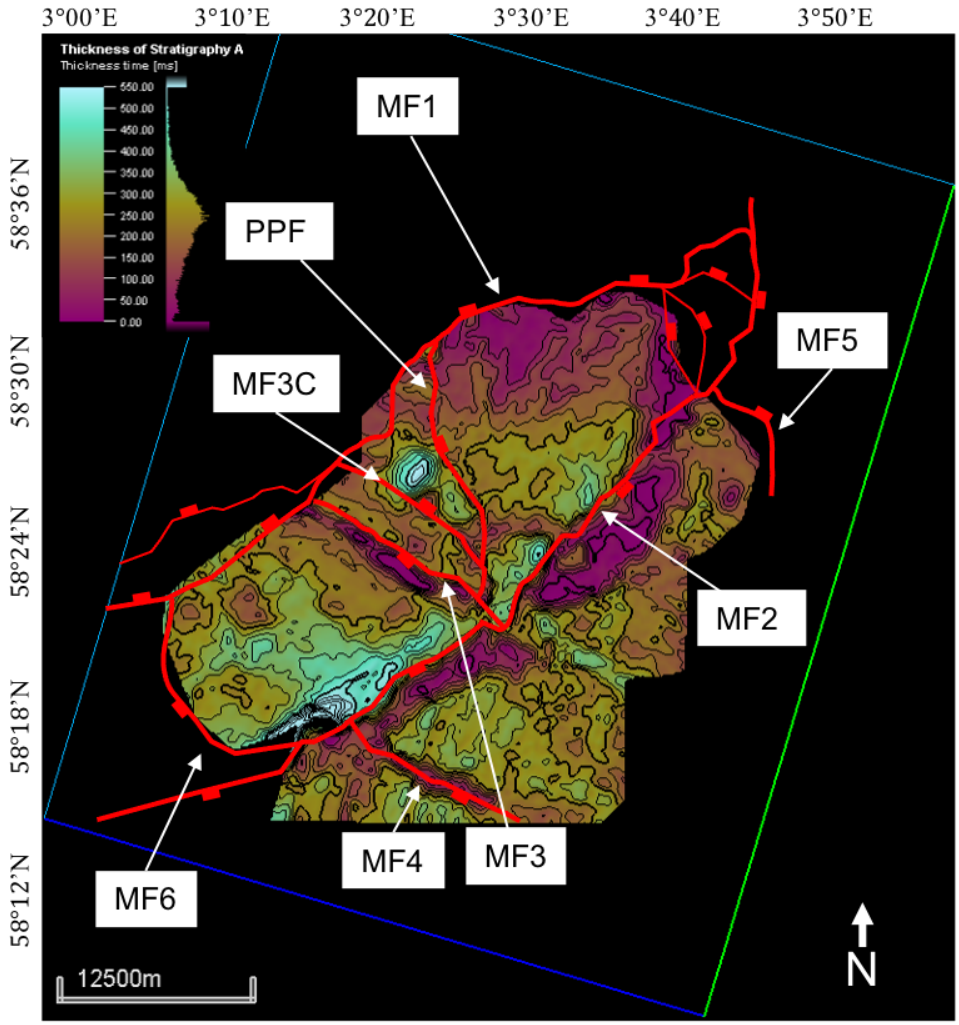

Figure 4.18. Time-thickness map of the Unit A. MF1, master fault 1; MF2, master fault 2; MF3, master fault 3; MF3C, master fault 3 conjugate; MF4, master fault 4; MF5, master fault 5; MF6, master fault 6; PPF, Pre-Permian fault

4.5.7 Thickness from Unconformity to Basement

The thickness from the Unconformity to the Basement correlates with the thickness of Unit A to D combined (Fig. 4.19). The thickness varies from 0 to 1600 ms TWT throughout the study area. In the NSH, there is a clear southwest thickening trend, going from 0 to 1000ms TWT. In the CSH, the thickness varies from 600 to 1000 ms TWT, and the thickness declines towards MF1 between the intersection of MF3 and MF3C. In the WSH, the thickness is between 1100 to 1300 ms TWT with a slight thickening trend to the northwest. It is thinner along MF1 and MF2 in the WSH, with the thinnest part coming above the culmination along MF2 seen in the time-structure map of the Basement (Fig. 4.12). On the ESH, the thickest part is close to MF2, reaching above 1500 ms TWT before it pinches out northwards towards MF5.

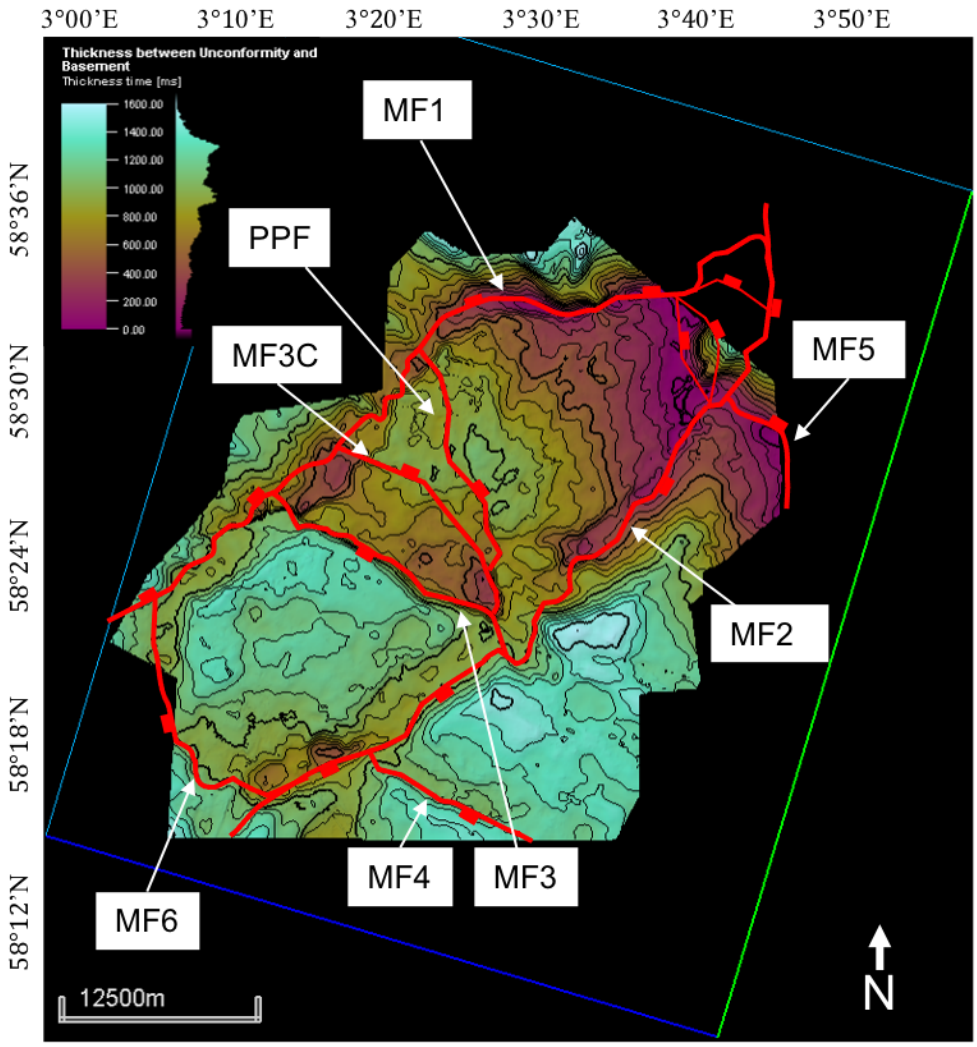

Figure 4.19. Time-thickness map of the Pre-Permian stratigraphy. MF1, master fault 1; MF2, master fault 2; MF3, master fault 3; MF3C, master fault 3 conjugate; MF4, master fault 4; MF5, master fault 5; MF6, master fault 6; PPF, Pre-Permian fault.

5. Discussion

Several tectonic events throughout geological time have formed the present day Sele High and the North Sea Basin. The regional tectonic events that have broadly affected the North Sea are as follows:

- Collapse of the Caledonian orogeny created a major extension event with distinct intermountain basin systems. An overall transtensional setting for the system has been proposed (e.g., Dewey and Strachan, 2003; Osmundsen and Andersen, 2001), with inter-linked extensional detachments and NE-SW oriented steep shear zones setting up current boundaries of preserved Devonian basins (e.g., Fossen, 1992; Norton, 1986).
- Compression and inversion as far field effects of the Variscan Orogeny, attributed to Late Carboniferous to Early Permian (Coward et al., 1989; Ziegler, 1992).
- Rifting phase 1 (RP1): Late Permian – Early Triassic extension with an E-W extensional direction.
- Rifting phase 2 (RP2): Late Jurassic – Early Cretaceous extension with an NW-SE extensional direction.
- Late Cretaceous inversion associated with the Alpine orogeny.

A detailed comparative analysis of the current study findings and regional events affecting the entire North Sea Basin has been established to understand the Sele High evolution, which is part of a larger and more complex geological puzzle (Fig. 5.1). The detailed analysis and description of key profiles were described in chapter 4 focusing on structural geometries, faults and stratigraphy. Now these results will be comprehensively discussed and compared with previous work to elaborate on the geological evolution of the Sele High and see if the observations of this study comply or contradicts with earlier findings. The discussion will follow geological time and are subdivided to three parts; Top Basement to Saliaan Unconformity; Base Rotliegend to Mid-Jurassic Unconformity; and post Mid-Jurassic Unconformity.

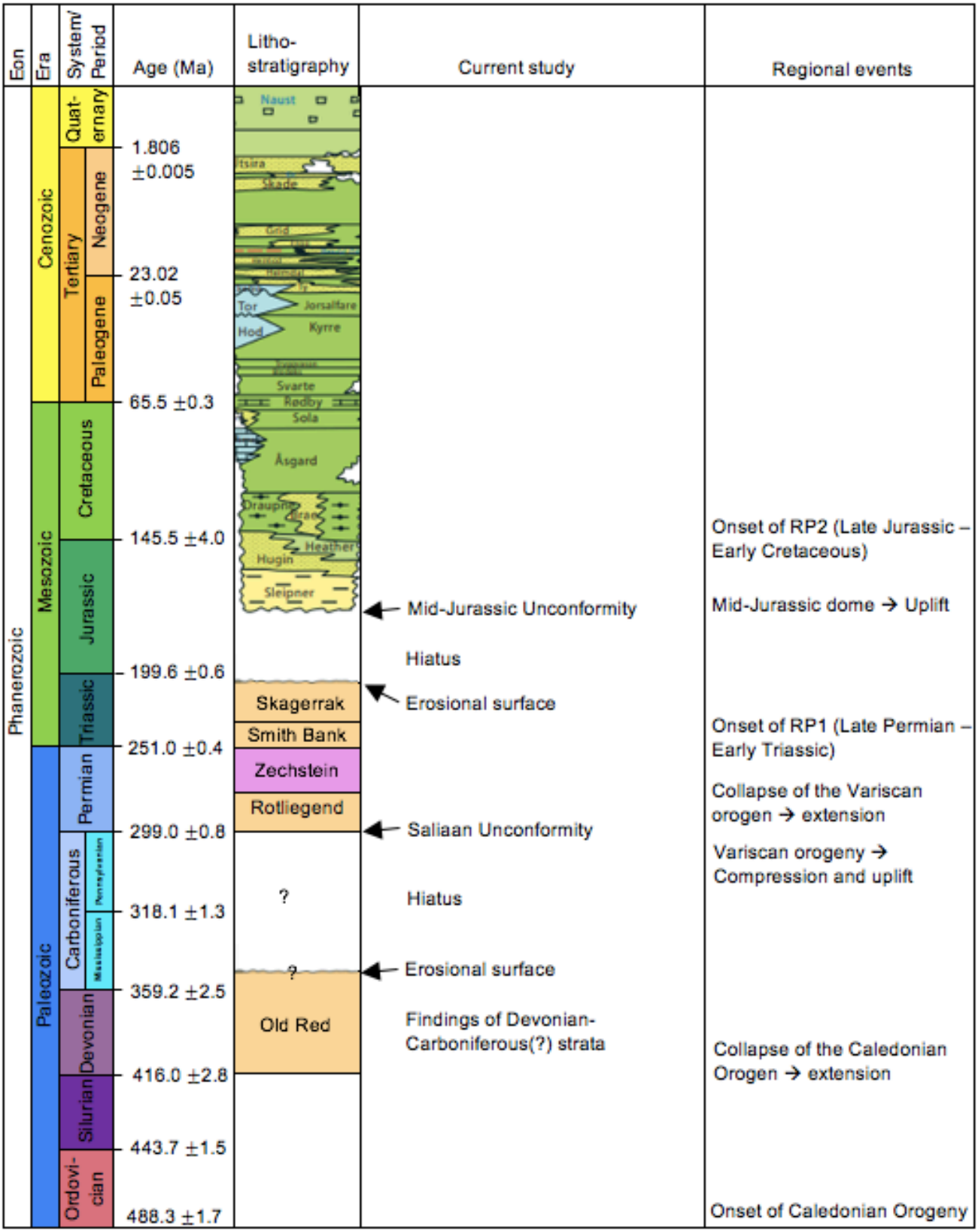

Figure 5.1. Overview of the Geological time together with lithostratigraphy of the study area, current study findings and the regional events of the North Sea.

5.1 Top Basement – Saalian Unconformity

5.1.1 Devonian

The NE-SW oriented extension caused by the Caledonian collapse in Early Devonian created several shear zones (e.g., Fossen, 1992; Norton, 1986). The Ling Depression, just north of the study area is situated above one of the shear zones created, namely the Hardangerfjord Shear Zone (Fig. 5.2) (Fossen and Hurich, 2005). The Devonian subaerial basins of UK are related to regional NW-SE extension (McClay et al., 1986; Norton et al., 1987). The Devonian basins seen onshore western Norway are created by linked half-grabens which are consistently west dipping, matching the trend of the preceding compressional structures indicating reactivation on the décollement and anisotropy induced by the Caledonian collision (Norton et al., 1987). Earlier work on the Sunnfjord region of western Norway exhibit N-S shortening characterized by thrusting from transpression or compression during Late Devonian, which developed to N-S shortening with an E-W extension during Early Carboniferous (Braathen, 1999). During this last stage strike-slip faults developed in some of the Devonian basins in western Norway.

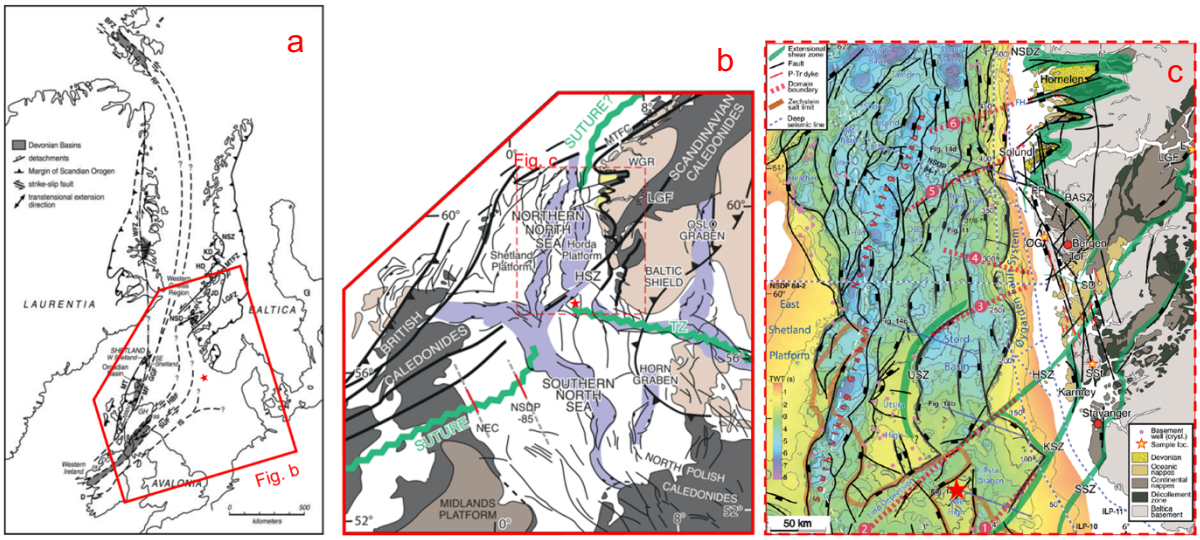

Figure 5.2. Tectonic overview of the Caledonides step-by-step zooming in on western Norway and NCS. Sele High is marked with a red star in all figures. HSZ, Hardangerfjord shear zone; KSZ, Karmøy Shear Zone; MTFC, Møre-Trøndelag Fault Complex; MTFZ, Møre-Trøndelag Fault Zone; TZ, Tornquist Zone; SSZ, Stavanger Shear Zone; BASZ, Bergen Arc Shear Zone; WGR, Western Gneiss Region; NSDZ, Nordfjord-Sogn Detachment Zone; LGF, Lærdal-Gjende Fault; USZ, Utsira Shear Zone. Modified from (Dewey and Strachan, 2003; Fazlikhani et al., 2017; Fossen, 2016).

5.1.2 Carboniferous

The Carboniferous is the least understood period as there is no findings offshore on the NCS. However, there are a lot of findings in UK part of the North Sea. Earlier work on the Orcadian Basin (Armitage et al., 2021; Coward et al., 1989; Dichiarante et al., 2020), Mid North Sea

High Region (Brackenridge et al., 2020), Fladen Ground Spur and Kraken High (Patruno and Reid, 2017) are all interpreted to be subjected to inversion and uplift during Late Carboniferous - Early Permian and attributed to far-field effects of The Variscan Orogeny (Glennie and Underhill, 1998; Seranne, 1992). What is clear from the NCS and North Sea in general is that it is missing several kilometers of Devonian and Carboniferous strata (Figs. 5.7 and 5.8) (Coward, 1993; Coward et al., 1989; Seranne, 1992; Ziegler, 1992). This hiatus was created from erosion following the uplift and is frequently referred to as the Base Permian Unconformity, the Variscan Unconformity or the Saalian Unconformity.

5.1.3 Observations from Basement to Saliaan Unconformity

In the study area, the Unit A superimposes the basement and follow the trend of the basement-cover contact. The Units B and C conformably superimpose Unit A displaying that all are deposited in succession without interruption. The Units A-C are heavily faulted throughout the study area but do not show any clear thickening across the master faults emphasizing that the strata were deposited pre-rifting of the master faults (Figs. 4.3-4.4 and 4.15-4.18). The ages of these units are somewhat uncertain, but the newly drilled well (i.e., Well 17/8-1, drilled within the NSH) could confirm the age of the interpreted Units A-D, however the data will not become public before 23.10.2023. The oldest penetrated age is indicated as Devonian supporting Devonian age for at least some of these Units. Furthermore, the well 17/12-2, located in the northwestern corner of Egersund Basin close to the border of Sele High, penetrated sandstone below the Rotliegend Group, believed to be of Devonian age. The Units A-D truncate towards the Base Rotliegend and the Base Zechstein groups in various places of the available 3D and 2D seismic data (Figs. 4.2-4.4). The extent of Unit D is very limited and the areas where interpreted the strata within are disordered making interpretations difficult. However, Unit D seem to have growth wedges towards the master faults (Fig. 5.4) implying syn-rift deposition, hence the faults where created simultaneously as deposition of Unit D.

The Units A-C form an anticlinal shape adjacent to MF1 (Fig. 5.3). This structure is ambiguous and may be achieved in both contractional and extensional regime; snakehead from contractional inversion; or as a rollover anticline in between two normal faults (i.e., MF1 and one drawn in figure 5.3 a). However, there are some indications that points to the former being the case. In both cases there will be friction between the strata and the fault surface working against the direction of movement. In the extensional setting this would lead the strata to onlap

the fault, as the rollover anticline interpreted in the ESH towards MF2 and MF4 (Figs. 4.3 b and 5.4). Nevertheless, the strata seem to downlap on the fault, which indicate contraction as the friction would hold the linking point between fault and strata back as it gets pushed up steepening the strata towards the fault (Fig. 5.3). In addition, the strata seem to bend horizontally inside the black box indicated by light blue lines, which is unlikely if there are a normal fault going through. Therefore, it seems the Units A-C underwent N-S to NNE-SSW contraction which likely are interlinked with the inversion and uplift seen several places in the UK North Sea associated with far-field effects of the Variscan Orogeny in Late Carboniferous – Early Permian. However, as the Rotliegend Group of Early Permian unconformably superimpose these units the timing of the inversion and uplift must be Pre-Permian.

The transect k stretches SW-NE through the 3D seismic data. It crosses the MF3, MF3C and PPF sub-perpendicular, making it optimal for investigating these faults. The PPF is a sub-horizontal fault striking SSE-NNW (160°-340°) where the northeastern side is downthrown. In the northeast of NSH a similar fault to the PPF is observed (Figs. 5.5 and 5.6). The PPF are not affecting the stratigraphy above the Saliaan Unconformity, meaning it occurred before the deposition of these. Between the MF3C and PPF the unit A and B forms an anticline (Figs. 5.5 and 5.6) somewhat similar to the snake-head inversion structure (Fig. 5.3). The contraction of Late Carboniferous has an oblique angle on the MF3C and PPF and it seems this created a transpressional setting on the MF3C resulting in inversion of the fault and creation of a strike-slip fault (PPF) to compensate for the horizontal component. The horizontal component may be responsible for the bulge seen on MF2 where it links up with MF3 (Fig. 4.12). Considering this and the geometries of the PPF and compression direction it seems likely that the PPF is a right-lateral strike-slip fault.

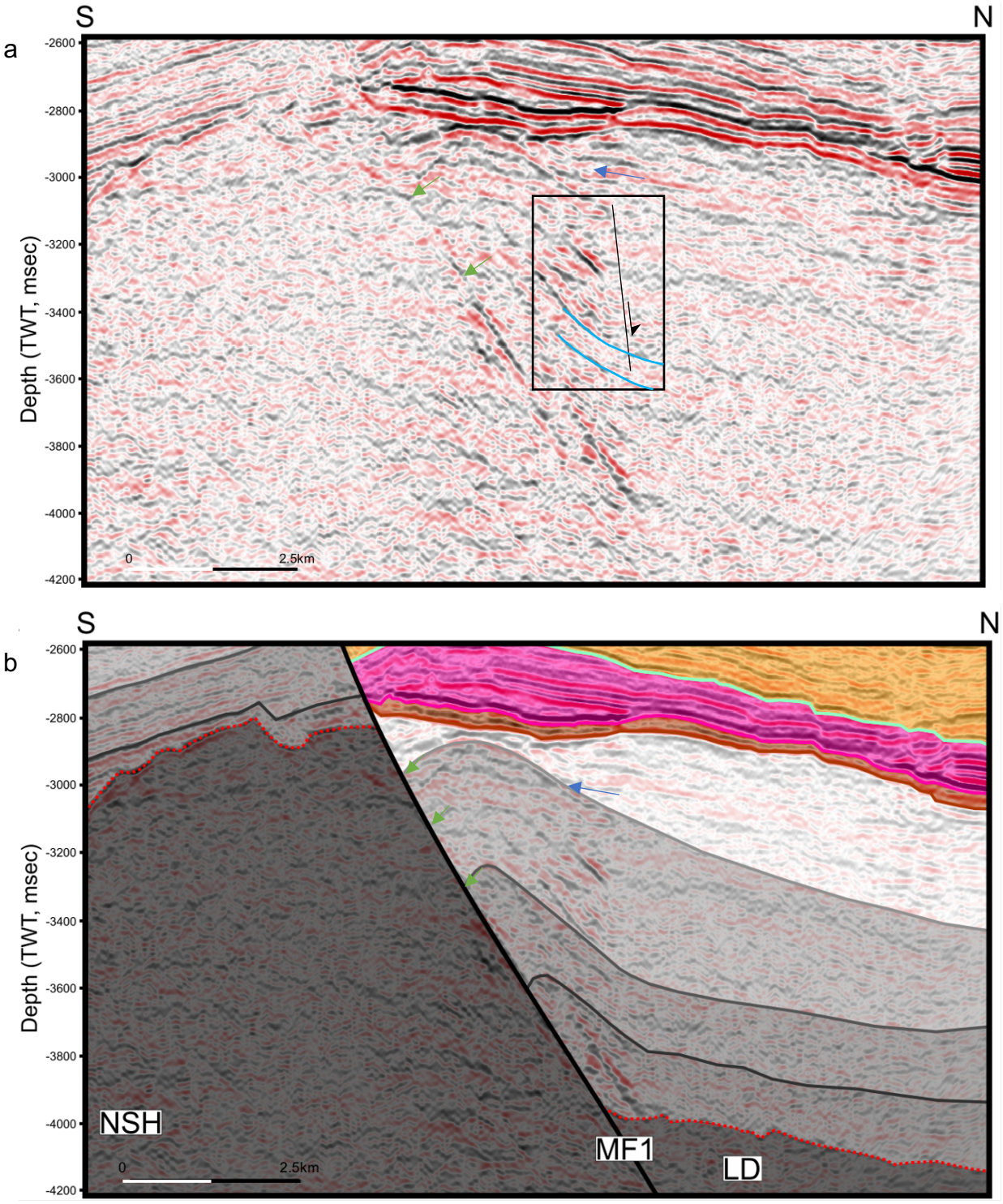

Figure 5.3. Zoomed in on the MF1 from figure 4.3 b, with inversion structure on the MF1. a) is an uninterpreted section with box containing position of possible normal fault and bending strata indicated by light blue lines. b) is interpreted section. Onlap indicated by blue arrow and downlap indicated by green arrow. The figure 4.3 b has a 35-degree angle on the PPF. NSH, North Sele High; MF1, master fault 1; LD, Ling Depression.

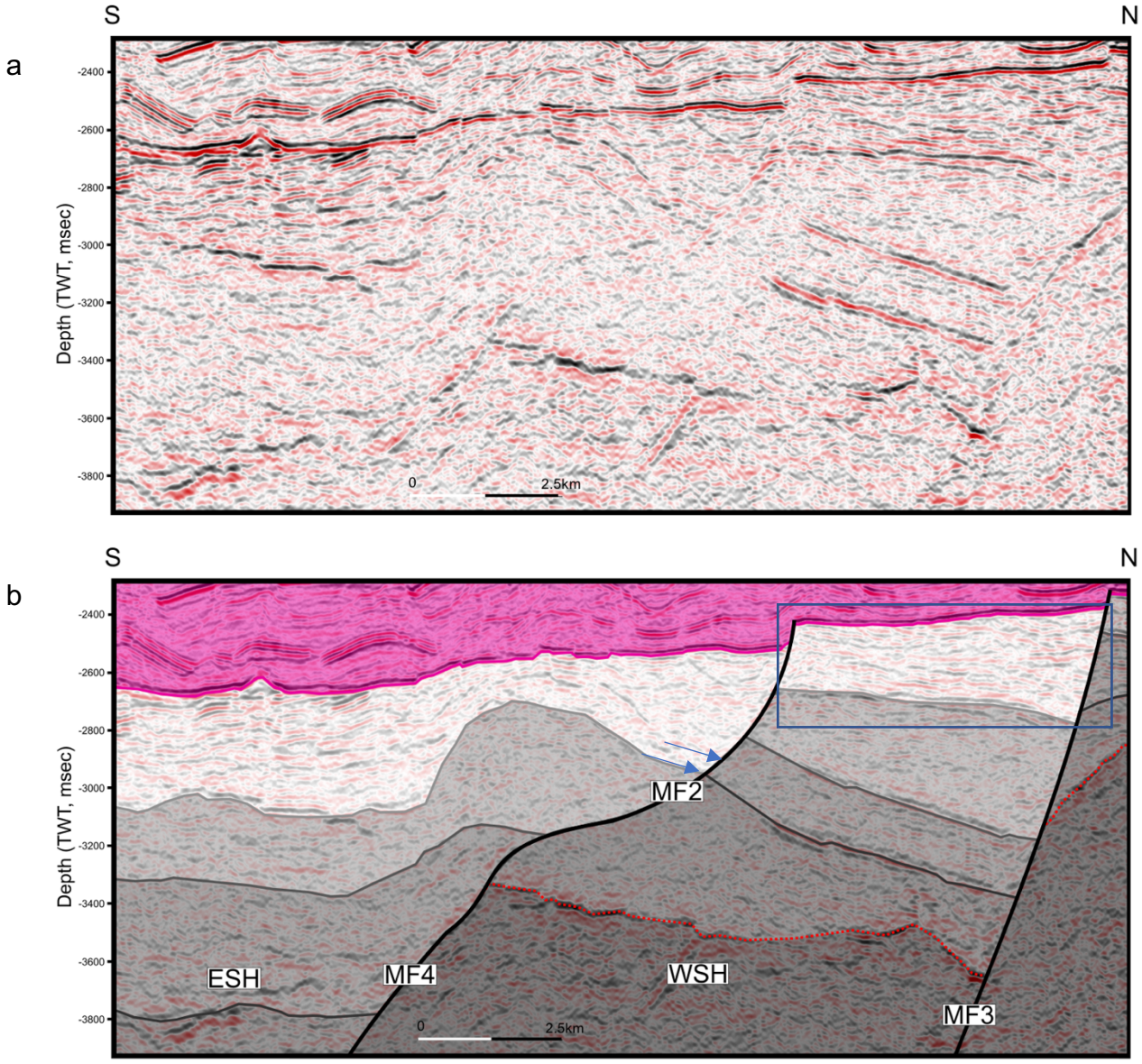

Figure 5.4. Zoomed in on MF4 and MF2 from figure 4.3 b and displays a rollover anticline which onlaps the MF2. Blue arrows indicate onlapping. ESH, East Sele High; WSH, West Sele High; MF2, master fault 2; MF4, master fault 4.

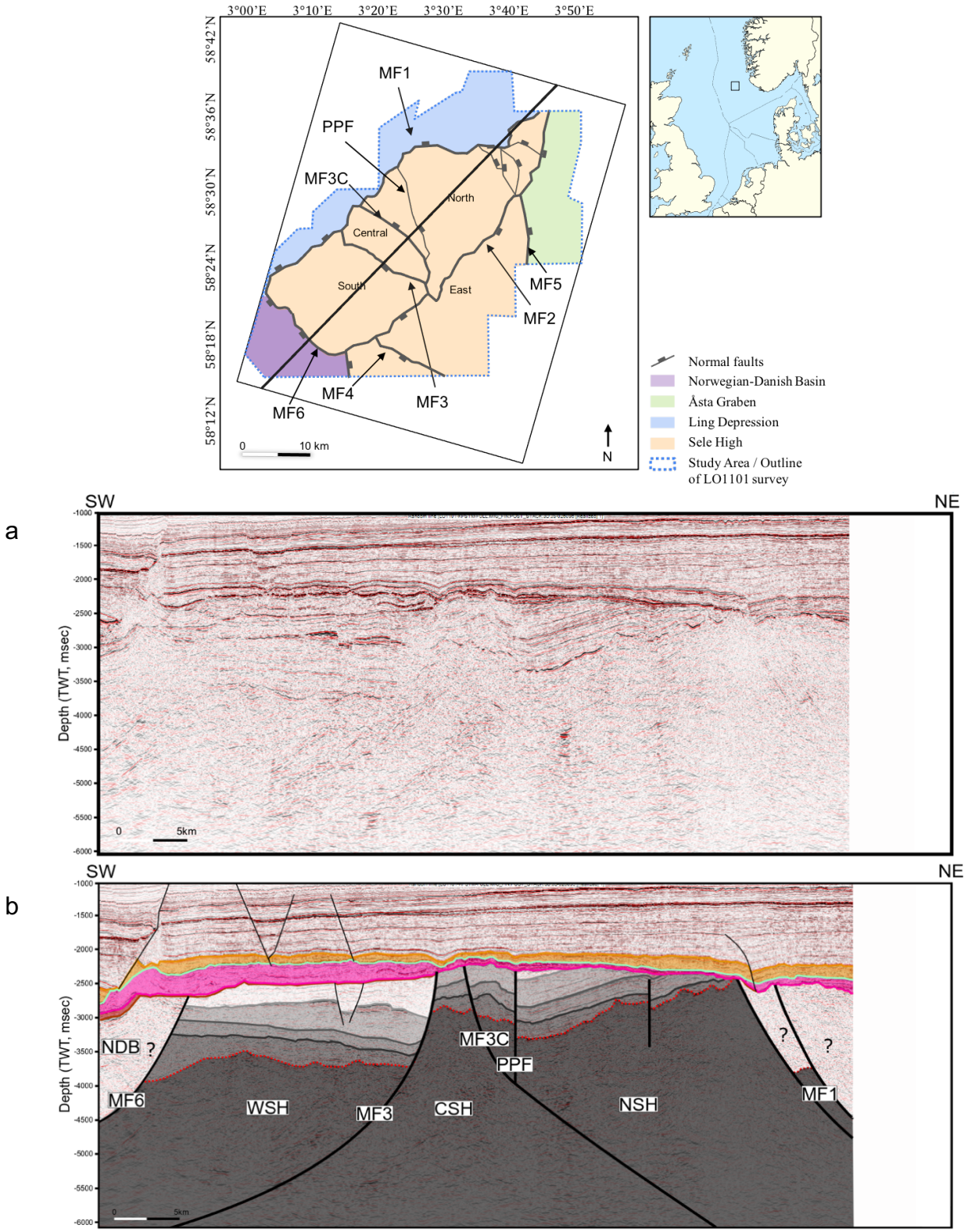

Figure 5.5. Transect k is an arbitrary line stretching SW-NE throughout the 3D seismic data. It crosses the MF3, MF3C and PPF sub-perpendicular, which is better for illustrating the faults. NDB, Norwegian-Danish Basin; WSH, West Sele High; CSH, Central Sele High; NSH, North Sele High; MF1, master fault 1; MF3, master fault 3; MF3C, master fault 3 conjugate; MF6, master fault 6; PPF, Pre-Permian fault.

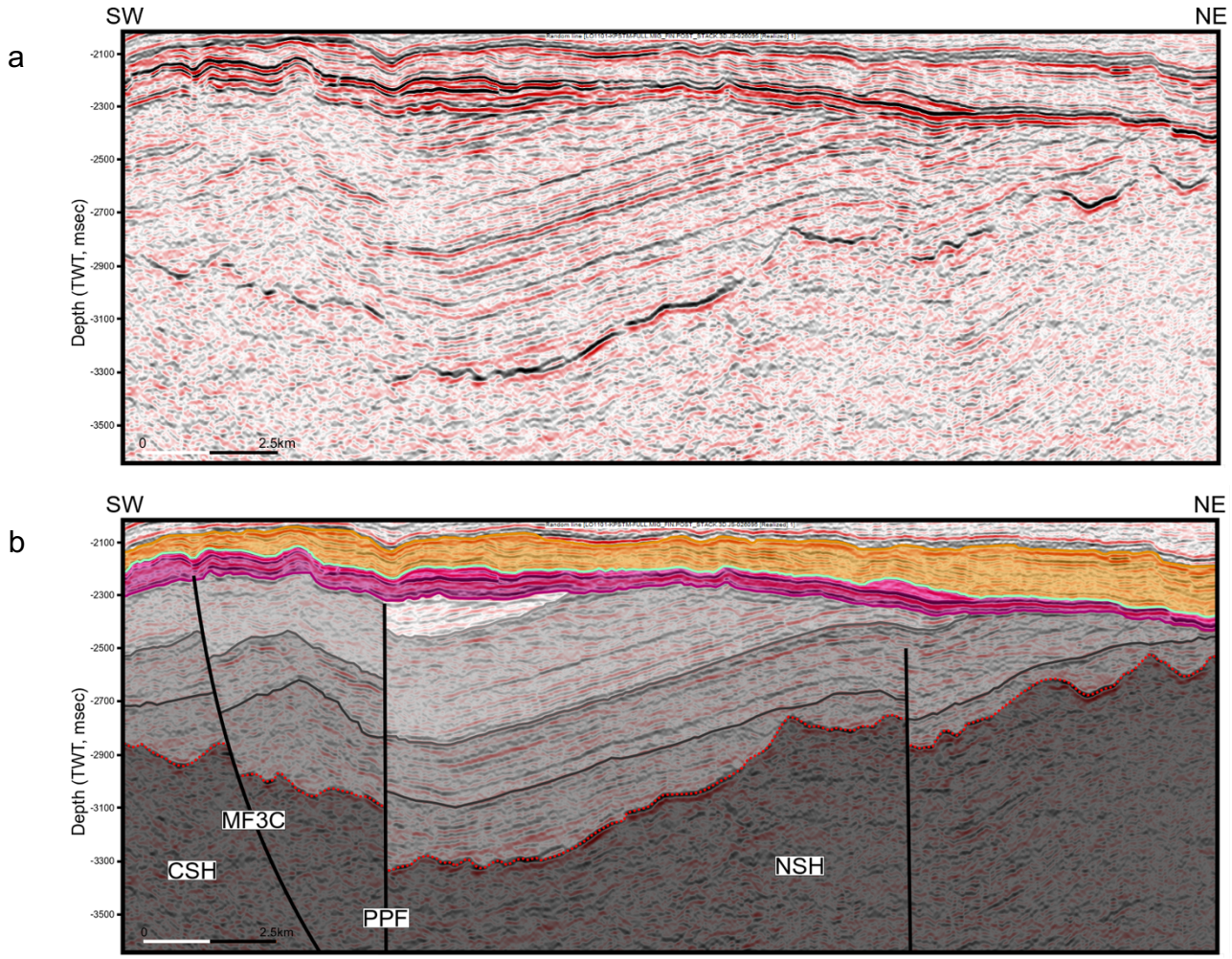

Figure 5.6. Close-up on the NSH and CSH from figure 5.5. CSH, Central Sele High; MF3C, master fault 3 conjugate; PPF, Pre-Permian Fault; NSH, North Sele High.

5.2 Saliaan Unconformity – Mid Jurassic

5.2.1 Earliest Permian – Late Permian

During the Early Permian extension occurred in NW Europe, likely a response to the Variscan collapse, creating several normal faults in the Central North Sea, such as the Sele High and Stavanger fault systems (Jackson and Lewis, 2013, 2016; Sørensen et al., 1992). The extension abated at the end of the Early Permian, thermal subsidence followed creating the North and South Permian Basins (Phillips et al., 2016; Ziegler, 1992) where the study area is located within the northeastern edge of the North Permian Basin. The Permian basins was infilled with Rotliegend and Zechstein groups.

5.2.2 Late Permian – Early Triassic

In Late Permian – Early Triassic, RP1 occurred having a E-W extensional direction (Færseth, 1996). This regional event created and reactivated N-S trending normal faults in the current study area and North Sea in general, to form the foundation for the Viking Graben as well as the continuous Åsta Graben and Horda Platform basin (Fig. 2.4) (Færseth, 1996; Jackson and Lewis, 2013, 2016; Sørensen et al., 1992). The rifting also initiated movement in the buoyant Zechstein Supergroup.

5.2.3 Middle Triassic – Late Jurassic

The RP1 diminished in the Middle Triassic initiating a period of tectonic quiescence and thermal subsidence (Roberts et al., 1993). The thermal subsidence and the consecutive sedimentary infill and loading lead to a broad basin to develop over the North Sea (Bartholomew et al., 1993). In the transition of Early to Middle Jurassic a thermal upwelling occurred, centered around the North Sea triple junction, causing widespread erosion to the Early Jurassic and Triassic sediments (Fig. 2.5) (Underhill and Partington, 1993). The dome collapsed at the Middle to Late Jurassic transition which led to a fast transgression and the Egersund Fm is situated above the unconformity.

5.2.4 Observations from Saliaan Unconformity – Mid-Jurassic Unconformity

The rifting of Early Permian seems to have affected some of the N-S striking faults of the Sele High, creating some accommodation room for the Rotliegend Group above the hanging wall. The interpretation of Rotliegend in the Sele High is debatable but are made on the basis that there are some reflectors bellow the Zechstein Supergroup which do not look like typical evaporitic reflectors and are conformable with the Zechstein Supergroup though uncomfortably superimpose the lower units. Outside the Sele High, such as in the NDB, LD and ÅG, Rotliegend are thicker and therefore easier to distinguish form the Zechstein giving a more confident interpretation together with well data confirming Rotliegend bellow Zechstein Supergroup (i.e., well 17/4-1 penetrating 163 meters of Early Permian Rotliegend Group before terminating and well 17/12-2 penetrating a 7-meter-thick succession of Rotliegend before possibly Devonian Sandstones). The Zechstein Group, Smith Bank and Skagerrak Fm's are generally thicker on the downthrown side of the N-S trending faults in this study (i.e., MF1,

MF2, MF5) (Figs. 4.4, 4.13 and 4.14) which indicate reactivation during RP1. However, as the Top Skagerrak surface is an unconformity it is not clear if the thickness difference of Smith Bank and Skagerrak is caused by syn-rift deposition or if they are deposited pre-rift and eroded post-rift. With regard to this Smith Bank and Skagerrak Fm's are deposited during Early and Middle Triassic which makes it likely they are both deposited syn-rift in the early stages and post-rift later on. In the transition between Early and Middle Jurassic thermal upwelling centered on the triple junction resulted in regional uplift and erosion of the study area (Fig. 4.2) causing the Egersund Fm of Callovian to Kimmeridgian to unconformably superimpose the Smith Bank and Skagerrak Fm's, thus a hiatus from Middle Triassic to Middle/Late Jurassic.

The Zechstein Supergroup as an evaporitic sequence can be subdivided in to 4 zones (Fig. 3.3). The NSH, CSH and northernmost LD seem to represent the marginal part of the Zechstein deposition (i.e., Zone 1) assessed from the limited deposition and minimal to no halokinesis (Figs. 4.3-4.4 and 4.14). The Zechstein Supergroup in the WSH and ESH have some influence from halokinesis also effecting the Smith Bank and Skagerrak Fm's above suggesting a higher halite concentration (Zone 2) (Figs. 4.3-4.4). In the neighboring areas, the Zechstein Supergroup is generally thicker on the western side of Sele High than the eastern side. In the southwestern part of the Ling Depression, there is a thick succession of Zechstein Supergroup exceeding 1200 meters, however it appears rather undisturbed by halokinesis (Zone 3/4) (Fig. 4.2 C-D). The thickness and halite content gradually decrease towards the northeast (Zone 1) (Fig. 4.2 A). In the Norwegian-Danish Basin to the south the succession is similar in thickness however with extensive halokinesis creating large diapers and close to creating welds (Zone 3/4) (Fig. 4.2 A-B). Åsta Graben exhibits less deposition but is clearly impacted by halokinesis (Zone 2/3) (Fig. 4.2 B-D). The Zechstein Supergroup also prohibit the master faults to propagate to the supra-Zechstein stratigraphy's but are however in some areas soft-linked with faults above.

5.3 Succeeding the Mid-Jurassic Unconformity

5.3.1 Late Jurassic – Early Cretaceous

A renewed rift phase (RP2) started in the Late Jurassic and lasting until the Early Cretaceous (e.g., Phillips et al., 2019). It had an E-W extension direction and localized in the center of RP1, the Viking Graben, reactivating and creating new faults (e.g., Færseth, 1996; Klemperer, 1988). The todays trilete rift system where created during this rift phase (Davies et al., 2001). The

rifting occurred simultaneously as eustatic sea level rose inducing rapid subsidence of an upward-deepening marine succession where the sedimentary load resulted in rapid growth of the salt diapirs in the Sele High area (Jackson and Lewis, 2013; Sørensen et al., 1992).

5.3.2 Cenozoic

At the Cenozoic the North Sea was a wide epicontinental basin centered above the Viking Graben. The period saw two phases of uplift, the first caused by the Iceland plume during Late Paleocene to Early Eocene effected the entire North Sea but the western side to an greater extent resulting in tilting and erosion (Faleide et al., 2002). The second is related to the isostatic response of the unloading caused by glacial erosion and melting of the Scandinavian ice sheet at the Pliocene – Pleistocene transition, which also feed the North Sea basin (Faleide et al., 2002). Cenozoic reaches an approximate thickness of 2.5 km.

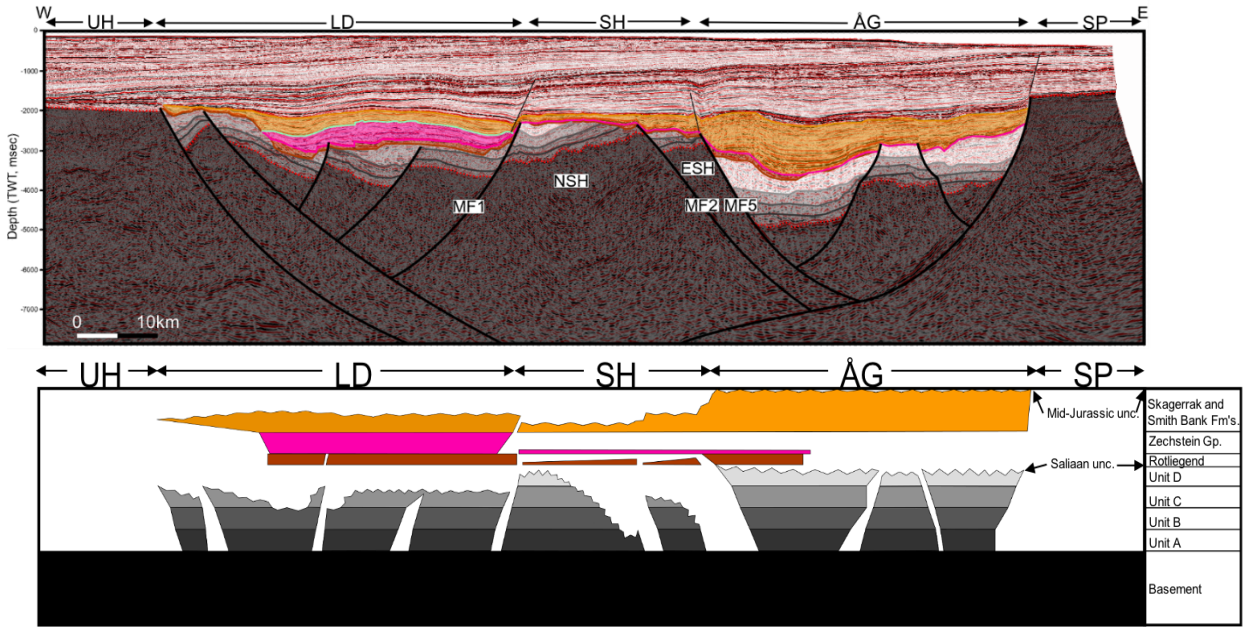

Figure 5.7. The 2D line C with wheeler diagram, displaying how much of each unit is present. The two unconformities (i.e., Mid-Jurassic and Saliaan) are also indicated by a rough surface. UH, Utsira High; LD, Ling Depression; SH, Sele High; ÅG, Åsta Graben; SP, Stavanger Platform; NSH, North Sele High; ESH, East Sele High; MF1, master fault 1; MF2, master fault 2; MF5, master fault 5.

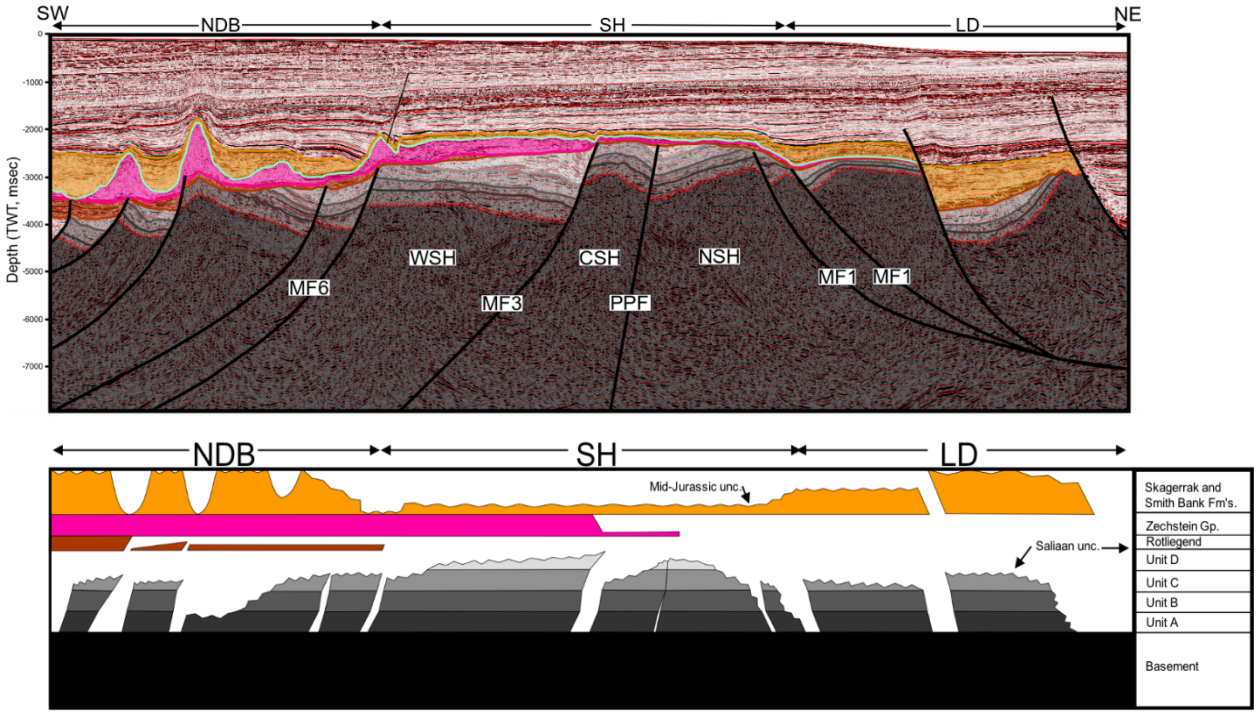

Figure 5.8. The 2D line A from figure 4.2 with wheeler diagram displaying how much of each unit is present. The two unconformities (i.e., Mid-Jurassic and Saliaan) are also indicated by a rough surface. NDB, Norwegian-Danish Basin; SH, Sele High; LD, Ling Depression; WSH, West Sele High; CSH, Central Sele High; NSH, North Sele High; MF1, master fault 1; MF3, master fault 3; MF6, master fault 6; PPF, Pre-Permian Fault.

5.4 The Evolution of Sele High (Devonian – Mid Jurassic)

In this chapter two simplistic 2D evolutionary models of the Sele High are proposed. The two transects used for the models are chosen because of its perpendicular orientation on the main structural elements of the Sele High. The evolution is presented in five stages (Figs. 5.9-5.10):

1) Devonian: Deposition of Unit A-C, likely the Old Red Group which conformably superimpose the basement. The deposition probably occurred in a broad basin as Devonian units are also identified outside the Sele High, such as Ling Depression, Åsta Graben, Norwegian-Danish Basin (Fig. 4.2) and Egersund Basin (Well 17/12-2).
2) Late Devonian – Late Carboniferous: Rifting creating the thick-skinned master faults (MF1, MF2, MF3, MF3C, MF5 and MF6) and syn-rift deposition of Unit D and possibly other units.
3) Late Carboniferous: Compression caused by far-field effects of the Variscan Orogeny causing inversion on MF3C and creation of the PPF in a transpression regime. The compression also induced uplift and erosion of Unit A-D and possibly other units deposited in stage 2. Erosion of these units are seen in the Sele High and neighboring areas (Fig. 4.2). Creating a hiatus from Upper Devonian/Lower Carboniferous to the Lower Permian – Saliaan Unconformity.
4) Early Permian – Early Jurassic: Subdivided in three parts; i) Early Permian Extension and subsequent thermal subsidence in Mid Permian with deposition of Rotliegend and Zechstein Groups; ii) Late Permian – Early Triassic (RP1) continuous deposition of Zechstein Supergroup, Smith Bank and Skagerrak Fm's, faulting and sediment loading probably lead to the mobilization of salt; iii) Mid Triassic – Mid Jurassic thermal subsidence following RP1 and continuous deposition of sediments.
5) Mid Jurassic doming: Thermal doming centered bellow the triple junction in the North Sea caused widespread uplift and erosion of the North Sea, resulting in a hiatus from Middle Triassic to Middle/Late Jurassic in the Sele High and neighboring areas – Mid Jurassic Unconformity.

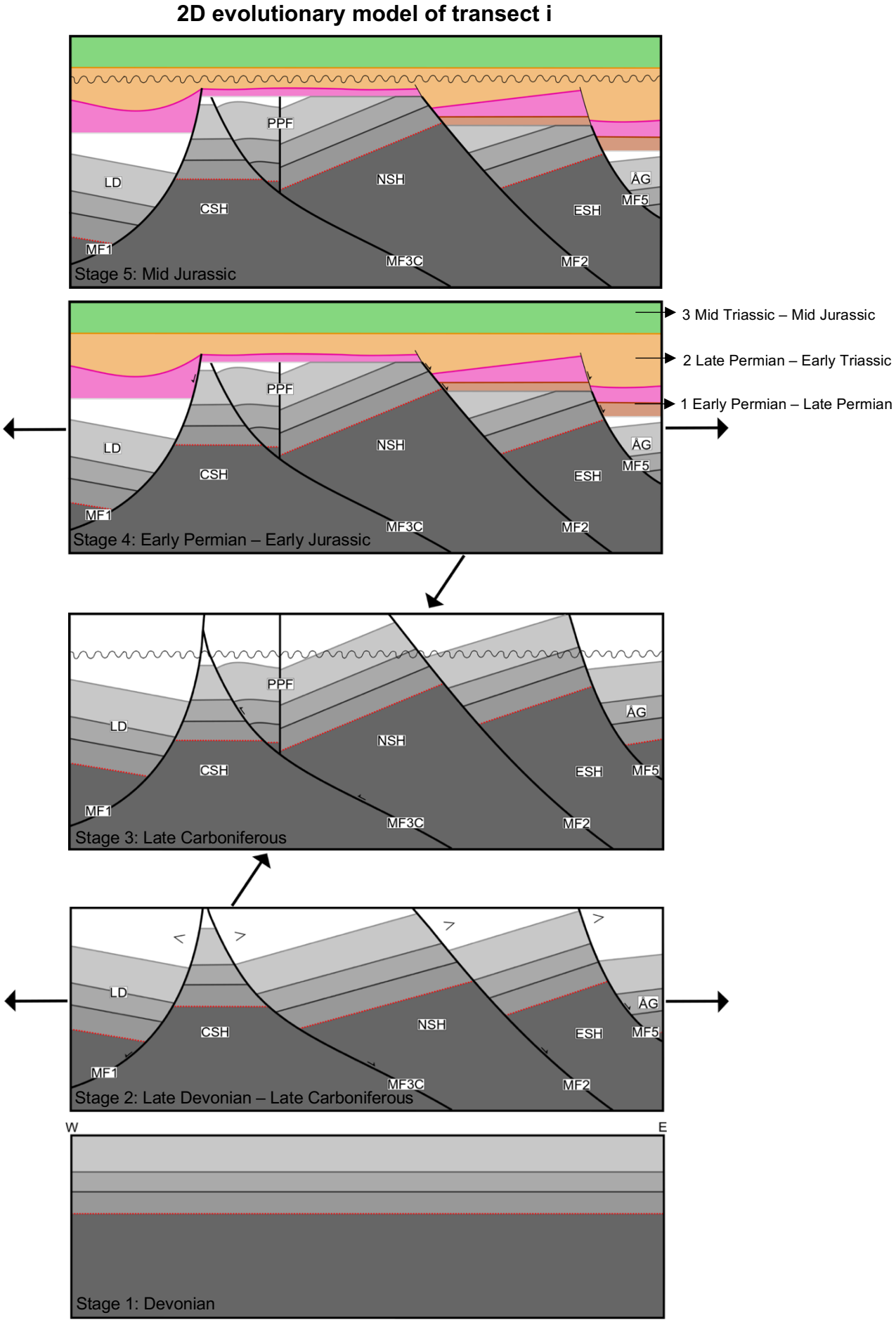
2D evolutionary model of transect i
PPF
LD
CSH
NSH
ESH
AG
MF5
MF1
MF3C
MF2
Stage 5: Mid Jurassic
3 Mid Triassic – Mid Jurassic
2 Late Permian – Early Triassic
1 Early Permian – Late Permian
Stage 4: Early Permian – Early Jurassic
Stage 3: Late Carboniferous
Stage 2: Late Devonian – Late Carboniferous
W
E
Stage 1: Devonian

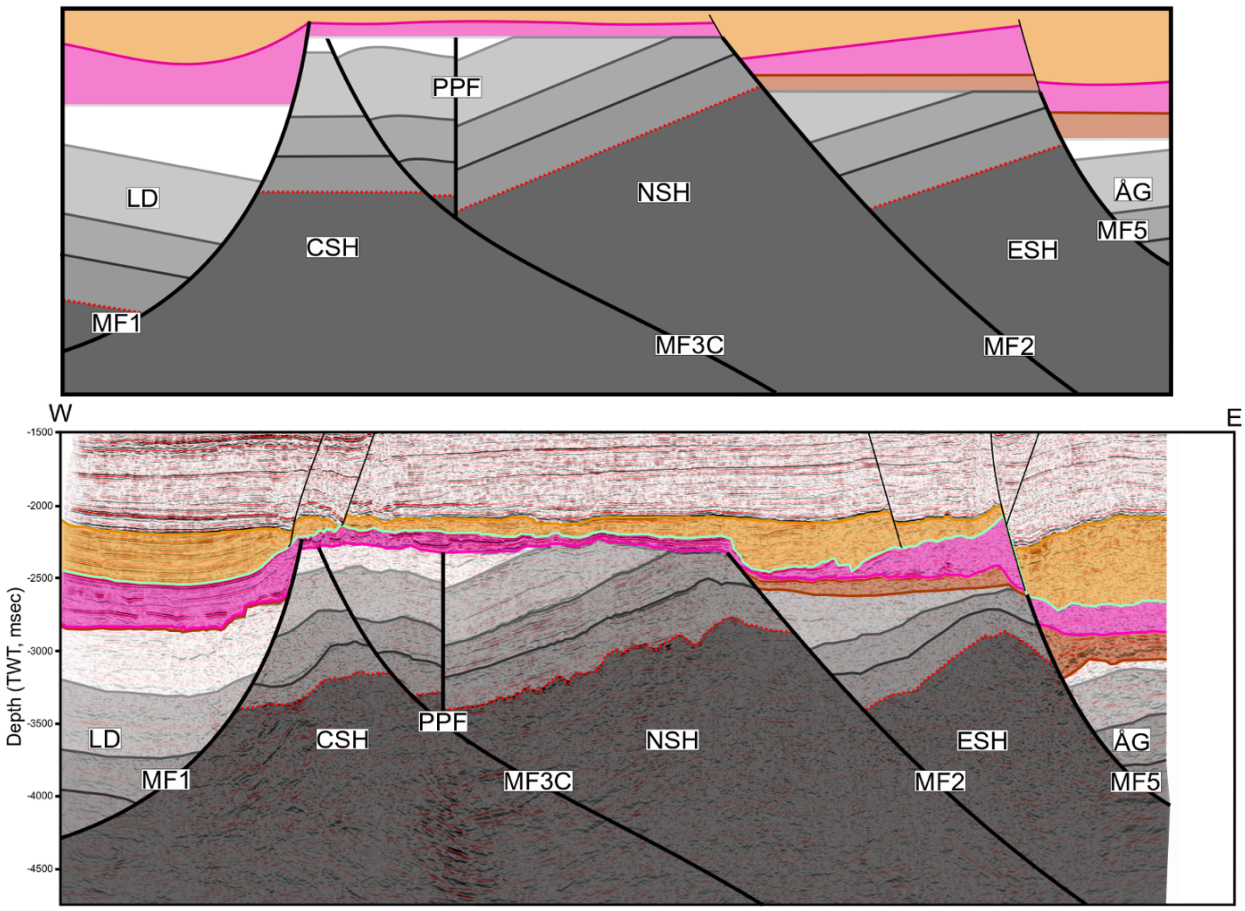

Figure 5.9. A five step 2D evolutionary model of transect i (location and orientation of transect seen in figure 4.4). Last picture is how Sele High looked like in the Late Jurassic, transect i is put bellow for comparison. LD, Ling Depression; ÅG, Åsta Graben; ESH, East Sele High; CSH, Central Sele High; NSH, North Sele High; MF1, master fault 1; MF3C, master fault 3 conjugate; MF5, master fault 5; PPF, Pre-Permian fault.

2D evolutionary model of transect k

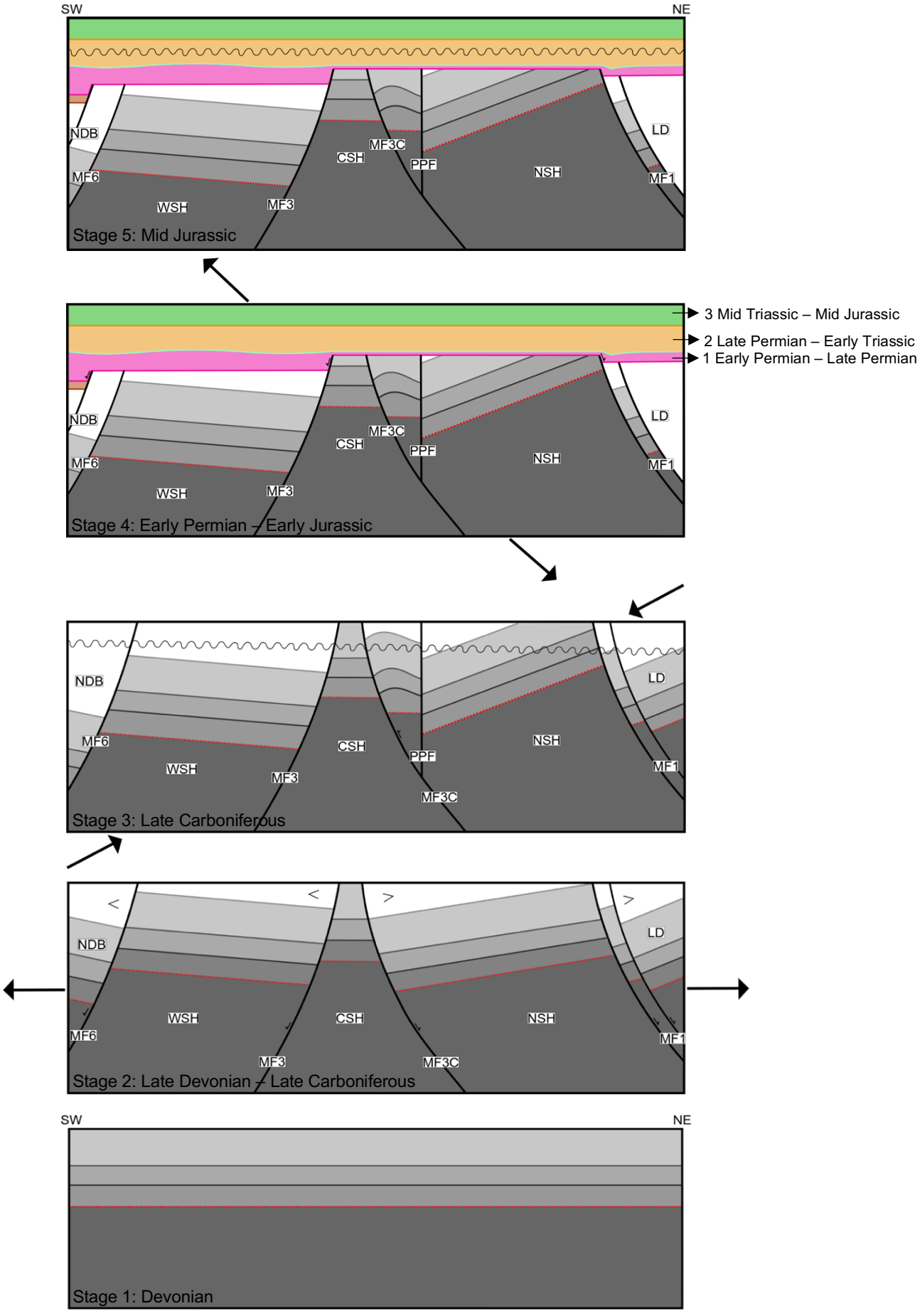

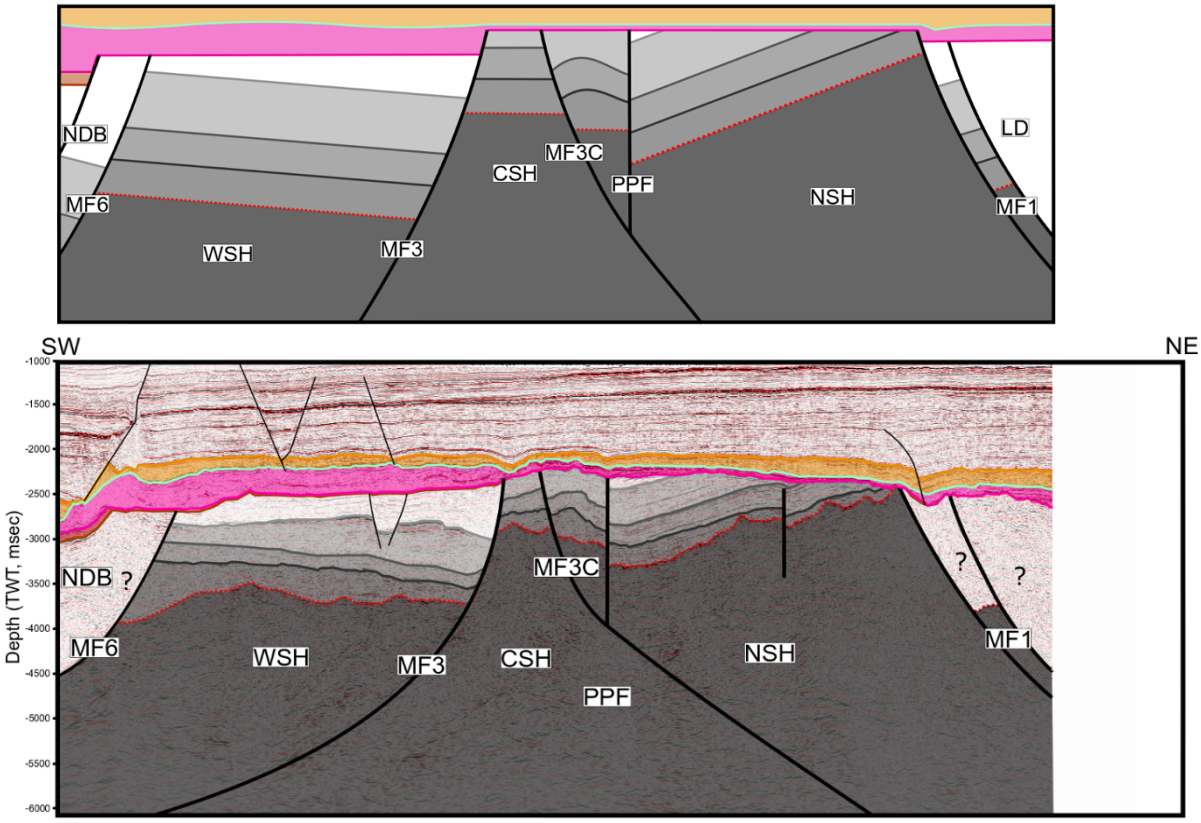

Figure 5.10. A five step 2D evolutionary model of transect k (location and orientation of transect seen in figure 5.5). Last picture is how Sele High looked like in the Late Jurassic, transect k is put bellow for comparison. NDB, Norwegian-Danish Basin; WSH, West Sele High; CSH, Central Sele High; NSH, North Sele High; MF1, master fault 1; MF3, master fault 3; MF3C, master fault 3 conjugate; MF6, master fault 6; PPF, Pre-Permian fault.

6. Conclusion

The Pre-Permian history of the North Sea within the Norwegian Continental Shelf (NCS) is poorly understood due to a complex history of rifting, thermal cooling, sedimentation, subsidence and erosion resulting in limited quality and quantity of geological and geophysical data. However, pre-existing structures exert a significant influence on later evolution making the earlier developments important for understanding of the Post-Permian evolution. Therefore, the basement highs are of great importance, offering better resolution and accessibility to the older stratigraphy with less overprint from younger stratigraphy. In consideration of this, the research questions were to i) generate a seismic-stratigraphic framework of the Sele High, ii) assess the spatial and temporal evolution of faults, iii) analyze the tectonostratigraphic evolution of Sele High with emphasize on the Pre-Permian evolution, and iv) distribution and role of different Zechstein facies.

The first objective was done by creating a detailed 3D geomodel of the Sele High, utilizing the LO1101 3D seismic survey and five CFI-NSR04 2D seismic lines in Petrel. The second objective was achieved through analysis of time-structure maps, time-thickness maps and fault orientations. The third objective was assessed by combining the results of the previous two objectives and study previous work in other areas to establish a tectonostratigraphic evolution of the Sele High. The key conclusion from detailed analysis following the listed objectives are:

- **Devonian:** Deposition of Unit A-C, likely the Old Red Group which conformably superimpose the basement. The deposition probably occurred in a broad basin as Devonian units are also identified outside the Sele High, such as Ling Depression, Åsta Graben, Norwegian-Danish Basin and Egersund Basin (Well 17/12-2).

- **Late Devonian – Late Carboniferous:** Rifting creating the thick-skinned master faults (MF1, MF2, MF3, MF3C, MF5 and MF6) and syn-rift deposition of Unit D and possibly other units.

- **Late Carboniferous:** Compression caused by far-field effects of the Variscan Orogeny causing inversion on MF3C and creation of the PPF in a transpression regime. The compression also induced uplift and erosion of Unit A-D and possibly other units deposited in stage 2. The erosion of these units is seen in the Sele High

and neighboring areas which creates a hiatus from Upper Devonian/Lower Carboniferous to the Lower Permian – Saliaan Unconformity.

- **Early Permian – Early Jurassic:** It can be subdivided in three parts; 1) Early Permian Extension and subsequent thermal subsidence in Mid Permian with deposition of Rotliegend and Zechstein Groups; 2) Late Permian – Early Triassic (RP1) continuous deposition of Zechstein Supergroup, Smith Bank and Skagerrak Fm's, faulting and sediment loading probably lead to the mobilization of salt; 3) Mid Triassic – Mid Jurassic thermal subsidence following RP1 and continuous deposition of sediments.

- **Mid Jurassic doming:** Thermal doming centered below the triple junction in the North Sea caused widespread uplift and erosion of the North Sea, resulting in a hiatus from Middle Triassic to Middle/Late Jurassic in the Sele High and neighboring areas – Mid Jurassic Unconformity.

The fourth and final objective was done by assessing the Zechstein Supergroup thickness and the extent of halokinesis. The key conclusions are:

- The Sele High was structurally higher than the surrounding areas resulting in marginal deposition of Zechstein Supergroup evaporites on the high (i.e., Zone 1-2). Some higher concentrations of halite are identified in ESH and WSH compared to the CSH and NSH.

- Basinal deposition of Zechstein Supergroup are seen on the western side of the Sele High (i.e., NDB and southwestern LD, Zone 3-4).

- The border of basinal and marginal deposition of Zechstein Supergroup are seen in Åsta Graben (i.e., Zone 2-4).

References

Andersen, T. B., 1998, Extensional tectonics in the Caledonides of southern Norway, an overview: Tectonophysics, v. 285, no. 3-4, p. 333-351.

Andersen, T. B., and Jamtveit, B., 1990, Uplift of deep crust during orogenic extensional collapse: A model based on field studies in the Sogn-Sunnfjord Region of western Norway: Tectonics, v. 9, no. 5, p. 1097-1111.

Andersen, T. B., Jamtveit, B., Dewey, J. F., and Swensson, E., 1991, Subduction and eduction of continental crust: major mechanisms during continent-continent collision and orogenic extensional collapse, a model based on the south Norwegian Caledonides: Terra nova (Oxford, England), v. 3, no. 3, p. 303-310.

Andersen, T. B., Torsvik, T. H., Eide, E. A., Osmundsen, P. T., and Faleide, J. I., 1999, Permian and Mesozoic extensional faulting within the Caledonides of central south Norway: Journal of the Geological Society, v. 156, no. 6, p. 1073-1080.

Anderson, E. M., 1905, The dynamics of faulting: Transactions of the Edinburgh Geological Society, v. 8, no. 3, p. 387-402.

Anderton, R., 1979, A Dynamic stratigraphy of the British Isles : a study in crustal evolution, London, Allen & Unwin.

Armitage, T. B., Watts, L. M., Holdsworth, R. E., and Strachan, R. A., 2021, Late Carboniferous dextral transpressional reactivation of the crustal-scale Walls Boundary Fault, Shetland; the role of pre-existing structures and lithological heterogeneities: Journal of the Geological Society, v. 178, no. 1, p. 1.

Badley, M., Price, J., Dahl, C. R., and Agdestein, T., 1988, The structural evolution of the northern Viking Graben and its bearing upon extensional modes of basin formation: Journal of the Geological Society, v. 145, no. 3, p. 455-472.

Badley, M. E., Egeberg, T., and Nipen, O., 1984, Development of rift basins illustrated by the structural evolution of the Oseberg feature, Block 30/6, offshore Norway: Journal of the Geological Society, v. 141, no. 4, p. 639-649.

Bartholomew, I. D., Peters, J. M., and Powell, C. M., 1993, Regional structural evolution of the North Sea: Oblique slip and the reactivation of basement lineaments: Geological Society, London, Petroleum Geology Conference Series, v. 4, no. 1, p. 1109-1122.

Beamish, D., and Smythe, D. K., 1986, Geophysical images of the deep crust: the Iapetus suture: Journal of the Geological Society, v. 143, no. 3, p. 489-497.

Bell, R. E., Jackson, C. A. L., Whipp, P. S., and Clements, B., 2014, Strain migration during multiphase extension: Observations from the northern North Sea: Tectonics, v. 33, no. 10, p. 1936-1963.

Biddle, K. T., and Rudolph, K. W., 1988, Early Tertiary structural inversion in the Stord Basin, Norwegian North Sea: Journal of the Geological Society, v. 145, no. 4, p. 603-611.

Bird, P. C., Cartwright, J. A., and Davies, T. L., 2014, Basement reactivation in the development of rift basins; an example of reactivated Caledonide structures in the West Orkney Basin: Journal of the Geological Society, v. 172, no. 1, p. 77-85.

Brackenridge, R. E., Underhill, J. R., Jamieson, R., and Bell, A., 2020, Structural and stratigraphic evolution of the Mid North Sea High region of the UK Continental Shelf: Petroleum Geoscience, v. 26, no. 2, p. 154-173.

Brown, A. R., 2011, Interpretation of three-dimensional seismic data, Tulsa, Okla, American Association of Petroleum Geologists Society of Exploration Geophysicists, AAPG memoir.

Bruce, D., and Stemmerik, L., 2003, The Millennium atlas Ch. 7. Carboniferous: petroleum geology of the central and northern North Sea. Evans, D, Graham, C, Armour, A, and Bathurst, P (editors and co-ordinators). London, Geological Society of London, 83-90.

Braathen, A., 1999, Kinematics of post-Caledonian polyphase brittle faulting in the Sunnfjord region, western Norway: Tectonophysics, v. 302, no. 1-2, p. 99-121.

Braathen, A., and Erambert, M., 2014, Structural and metamorphic history of the Engebøfjellet Eclogite and the exhumation of the Western Gneiss Region, Norway: Norwegian Journal of Geology/Norsk Geologisk Forening, v. 94, no. 1.

Braathen, A., Osmundsen, P. T., and Gabrielsen, R. H., 2004, Dynamic development of fault rocks in a crustal-scale detachment: An example from western Norway: Tectonics, v. 23, no. 4.

Campbell, I. H., 2003, Constraints on continental growth models from Nb/U ratios in the 3.5 Ga Barberton and other Archaean basalt-komatiite suites: American Journal of Science, v. 303, no. 4, p. 319-351.

Cartwright, J., and Huuse, M., 2005, 3D seismic technology: the geological 'Hubble': Basin Research, v. 17, no. 1, p. 1-20.

Cawood, P. A., Hawkesworth, C., and Dhuime, B., 2013, The continental record and the generation of continental crust: Bulletin, v. 125, no. 1-2, p. 14-32.

Chauvet, A., and Séranne, M., 1994, Extension-parallel folding in the Scandinavian Caledonides: Implications for late-orogenic processes: Tectonophysics, v. 238, no. 1, p. 31-54.

Clark, J. A., Stewart, S. A., and Cartwright, J. A., 1998, Evolution of the NW margin of the North Permian Basin, UK North Sea: Journal of the Geological Society, v. 155, no. 4, p. 663-676.

Clemson, J., Cartwright, J. A., and Booth, J., 1997, Structural segmentation and the influence of basement structure on the Namibian passive margin: Journal of the Geological Society, v. 154, no. 3, p. 477-482.

Copestake, P., Sims, A., Crittenden, S., Hamar, G., Ineson, J., Rose, P., and Tringham, M., 2003, The Millennium atlas Ch. 12. Lower Cretaceous: petroleum geology of the central and northern North Sea. Evans, D, Graham, C, Armour, A, and Bathurst, P (editors and co-ordinators). London, Geological Society of London, 191-212.

Corti, G., 2009, Continental rift evolution: from rift initiation to incipient break-up in the Main Ethiopian Rift, East Africa: Earth-Science Reviews, v. 96, no. 1-2, p. 1-53.

Coward, M. P., 1993, The effect of Late Caledonian and Variscan continental escape tectonics on basement structure, Paleozoic basin kinematics and subsequent Mesozoic basin development in NW Europe: Geological Society, London, Petroleum Geology Conference series, v. 4, no. 1, p. 1095-1108.

Coward, M. P., Dewey, J. F., Hempton, M., and and Holroyd, J., 2003, The Millennium atlas Ch. 2. Tectonic evolution: petroleum geology of the central and northern North Sea. Evans, D, Graham, C, Armour, A, and Bathurst, P (editors and co-ordinators). London, Geological Society of London, 17-34.

Coward, M. P., Enfield, M. A., and Fischer, M. W., 1989, Devonian basins of Northern Scotland: extension and inversion related to Late Caledonian -- Variscan tectonics: Geological Society special publication, v. 44, no. 1, p. 275-308.

Crameri, F., Shephard, G. E., and Heron, P. J., 2020, The misuse of colour in science communication: Nature communications, v. 11, no. 1, p. 5444-5444.

Daly, M. C., Chorowicz, J., and Fairhead, J. D., 1989, Rift basin evolution in Africa: the influence of reactivated steep basement shear zones: Geological Society special publication, v. 44, no. 1, p. 309-334.

Davies, R. J., O'Donnell, D., Bentham, P. N., Gibson, J. P. C., Curry, M. R., Dunay, R. E., and Maynard, J. R., 1999, The origin and genesis of major Jurassic unconformities within the triple junction area of the North Sea, UK: Geological Society, London, Petroleum Geology Conference Series, v. 5, no. 1, p. 117-131.

Davies, R. J., Turner, J. D., and Underhill, J. R., 2001, Sequential dip-slip fault movement during rifting; a new model for the evolution of the Jurassic trilete North Sea rift system: Petroleum geoscience, v. 7, no. 4, p. 371-388.

Deegan, C. E., and Scull, B. J., 1977, A Standard lithostratigraphic nomenclature for the central and northern North Sea, London, H.M.S.O., Report (Natural Environment Research Council. Institute of Geological Sciences).

Denham, L. R., and Sheriff, R. E., 1981, What is horizontal resolution?

Dewey, J. F., 1988, Extensional collapse of orogens: Tectonics, v. 7, no. 6, p. 1123-1139.

Dewey, J. F., and Strachan, R. A., 2003, Changing Silurian-Devonian relative plate motion in the Caledonides; sinistral transpression to sinistral transtension: Journal of the Geological Society, v. 160, no. 2, p. 219-229.

Dhuime, B., Hawkesworth, C. J., Delavault, H., and Cawood, P. A., 2017, Continental growth seen through the sedimentary record: Sedimentary Geology, v. 357, p. 16-32.

Dichiarante, A. M., McCaffrey, K. J. W., Holdsworth, R. E., Bjørnarå, T. I., and Dempsey, E. D., 2020, Fracture attribute scaling and connectivity in the Devonian Orcadian Basin with implications for geologically equivalent sub-surface fractured reservoirs: Solid earth (Göttingen), v. 11, no. 6, p. 2221-2244.

Dickinson, B., 1996, The Puffin Field: the appraisal of a complex HP-HT gas-condensate accumulation: Geological Society special publication, v. 114, no. 1, p. 299-327.

Doré, A. G., 1992, Synoptic palaeogeography of the Northeast Atlantic Seaway: late Permian to Cretaceous: Basins on the Atlantic Seaboard: Petroleum Geology, Sedimentology and Basin Evolution, v. 62, no. 1, p. 421-446.

Doré, A. G., Lundin, E. R., Fichler, C., and Olesen, O., 1997, Patterns of basement structure and reactivation along the NE Atlantic margin: Journal of the Geological Society, v. 154, no. 1, p. 85-92.

Eide, E. A., Osmundsen, P. T., Meyer, G. B., Kendrick, M. A., and Corfu, F., 2002, The Nesna Shear Zone, north-central Norway: an 40 Ar/39 Ar record of Early Devonian-Early Carboniferous ductile extension and unroofing: Norwegian Journal of Geology/Norsk Geologisk Forening, v. 82, no. 4.

Evans, D., Geological Society of, L., Norsk, p., and Danmarks og Grønlands Geologiske, U., 2003, The Millennium atlas : petroleum geology of the central and northern North Sea, London, Geological Society of London.

Faleide, J. I., Kyrkjebo, R., Kjennerud, T., Gabrielsen, R. H., Jordt, H., Fanavoll, S., and Bjerke, M. D., 2002, Tectonic impact on sedimentary processes during Cenozoic evolution of the northern North Sea and surrounding areas: Exhumation of the North Atlantic Margin: Timing, Mechanisms and Implications for Petroleum Exploration, v. 196, no. 1, p. 235-269.

Fazlikhani, H., Fossen, H., Gawthorpe, R., Faleide, J. I., and Bell, R. E., 2017, Basement structure and its influence on the structural configuration of the northern North Sea rift.

Fossen, H., 1992, The role of extensional tectonics in the Caledonides of south Norway: Journal of structural geology, v. 14, no. 8, p. 1033-1046.

-, 2016, Structural geology, Cambridge, Cambridge University Press.

Fossen, H., and Hurich, C. A., 2005, The Hardangerfjord shear zone in SW Norway and the North Sea; a large-scale low-angle shear zone in the Caledonian crust: Journal of the Geological Society, v. 162, no. 4, p. 675-687.

Fossen, H., Odinsen, T., Faerseth, R. B., and Gabrielsen, R. H., 2000, Detachments and low-angle faults in the northern North Sea rift system: Dynamics of the Norwegian Margin, v. 167, no. 1, p. 105-131.

Fraser, A. J., and Gawthorpe, R. L., 1990, Tectono-stratigraphic development and hydrocarbon habitat of the Carboniferous in northern England: Geological Society special publication, v. 55, no. 1, p. 49-86.

Fraser, S., Robinson, A., Johnson, H., Underhill, J., and Kadolsky, D., 2003, The Millennium atlas Ch. 11. Upper Jurassic: petroleum geology of the central and northern North Sea. Evans, D, Graham, C, Armour, A, and Bathurst, P (editors and co-ordinators). London, Geological Society of London, 157-190.

Freeman, B., Klemperer, S. L., and Hobbs, R. W., 1988, The deep structure of northern England and the Iapetus suture zone from BIRPS deep seismic reflection profiles: Journal of the Geological Society, v. 145, no. 5, p. 727-740.

Færseth, R. B., 1996, Interaction of Permo-Triassic and Jurassic extensional fault-blocks during the development of the northern North Sea: Journal of the Geological Society, v. 153, no. 6, p. 931-944.

Færseth, R. B., Gabrielsen, R. H., and Hurich, C. A., 1995, Influence of basement in structuring of the North Sea Basin, offshore southwest Norway: Norsk Geologisk Tidsskrift, v. 75, no. 2-3, p. 105-119.

Gabrielsen, R., FOERSTH, R., Steel, R., Idil, S., and Klovjan, O., Architectural styles of basin fill in the northern Viking Graben, *in* Proceedings Tectonic evolution of the North Sea rifts1990, p. 158-179.

Gawthorpe, R. L., and Leeder, M. R., 2000, Tectono-sedimentary evolution of active extensional basins: Basin Research, v. 12, no. 3-4, p. 195-218.

Giltner, J. P., 1987, Application of extensional models to the northern Viking Graben: Norsk Geologisk Tidsskrift, v. 67, no. 4, p. 339-352.

Glennie, K., Higham, J., and Stemmerik, L., 2003, The Millennium atlas Ch. 8. Permian: petroleum geology of the central and northern North Sea. Evans, D, Graham, C, Armour, A, and Bathurst, P (editors and co-ordinators). London, Geological Society of London, 91-104.

Glennie, K. W., 1997, Recent advances in understanding the southern North Sea Basin: a summary: Geological Society special publication, v. 123, no. 1, p. 17-29.

Glennie, K. W., and Underhill, J. R., 1998, Origin, Development and Evolution of Structural Styles: Oxford, UK, Oxford, UK: Blackwell Science Ltd, p. 42-84.

Goldsmith, P. J., Hudson, G., and Veen, P. V., 2003, The Millennium atlas Ch. 9. Triassic: petroleum geology of the central and northern North Sea. Evans, D, Graham, C, Armour, A, and Bathurst, P (editors and co-ordinators). London, Geological Society of London, 105-128.

Goldsmith, P. J., Rich, B., and Standring, J., 1995, Triassic correlation and stratigraphy in the South Central Graben, UK North Sea: Geological Society special publication, v. 91, no. 1, p. 123-143.

Hamilton, E. L., 1976, Variations of density and porosity with depth in deep-sea sediments: Journal of Sedimentary Research, v. 46, no. 2, p. 280-300.

Hansen, J. A., Mondol, N. H., Jahren, J., and Tsikalas, F., 2020, Reservoir assessment of Middle Jurassic sandstone-dominated formations in the Egersund Basin and Ling Depression, eastern Central North Sea: Marine and petroleum geology, v. 111, p. 529-543.

Haq, B. U., Hardenbol, J., and Vail, P. R., 1987, Chronology of Fluctuating Sea Levels since the Triassic: Science, v. 235, no. 4793, p. 1156-1167.

Hawkesworth, C. J., Cawood, P. A., and Dhuime, B., 2020, The evolution of the continental crust and the onset of plate tectonics: Frontiers in earth science, v. 8, p. 326.

Heeremans, M., Faleide, J. I., and Larsen, B. T., 2004, Late Carboniferous-Permian of NW Europe: an introduction to a new regional map: Geological Society special publication, v. 223, no. 1, p. 75-88.

Holloway, S., Cordey, W. G., Knox, R. W. O. B., British Geological, S., and United Kingdom Offshore Operators, A., 1992, Lithostratigraphic nomenclature of the UK North Sea : 1 : Paleogene of the Central and Northern North Sea, Nottingham, British Geological Survey on behalf of the UK Offshore Operators Association.

Husmo, T., Hamar, G., Høiland, O., Johannessen, E. P., Rømuld, A., Spencer, A., and Titterton, R., 2003, The Millennium atlas Ch. 10. Lower and Middle Jurassic: petroleum geology of the central and northern North Sea. Evans, D, Graham, C, Armour, A, and Bathurst, P (editors and co-ordinators). London, Geological Society of London, 129-156.

Hutton, D. H. W., 1987, Strike-slip terranes and a model for the evolution of the British and Irish Caledonides: Geol. Mag, v. 124, no. 5, p. 405-425.

Høiland, O., Kristensen, J., and Monsen, T., 1993, Mesozoic evolution of the Jæren High area, Norwegian Central North Sea: Geological Society, London, Petroleum Geology Conference Series, v. 4, no. 1, p. 1189-1195.

Jackson, C. A. L., Chua, S. T., Bell, R. E., and Magee, C., 2013, Structural style and early stage growth of inversion structures: 3D seismic insights from the Egersund Basin, offshore Norway: Journal of structural geology, v. 46, p. 167-185.

Jackson, C. A. L., and Lewis, M. M., 2013, Physiography of the NE margin of the Permian Salt Basin; new insights from 3D seismic reflection data: Journal of the Geological Society, v. 170, no. 6, p. 857-860.

-, 2016, Structural style and evolution of a salt-influenced rift basin margin; the impact of variations in salt composition and the role of polyphase extension: Basin Res, v. 28, no. 1, p. 81-102.

Jackson, M. P. A., and Talbot, C. J., 1986, External shapes, strain rates, and dynamics of salt structures: GSA Bulletin, v. 97, no. 3, p. 305-323.

Jones, I. F., and Davison, I., 2014, Seismic imaging in and around salt bodies: Interpretation, v. 2, no. 4, p. SL1-SL20.

Kalani, M., Faleide, J. I., and Gabrielsen, R. H., 2020, Paleozoic-Mesozoic tectono-sedimentary evolution and magmatism of the Egersund Basin area, Norwegian central North Sea: Marine and petroleum geology, v. 122, p. 104642.

Keym, M., Dieckmann, V., Horsfield, B., Erdmann, M., Galimberti, R., Kua, L.-C., Leith, L., and Podlaha, O., 2006, Source rock heterogeneity of the Upper Jurassic Draupne Formation, North Viking Graben, and its relevance to petroleum generation studies: Organic geochemistry, v. 37, no. 2, p. 220-243.

Klemperer, S. L., 1988, Crustal thinning and nature of extension in the northern North Sea from deep seismic reflection profiling: Tectonics, v. 7, no. 4, p. 803-821.

Leggett, J. K., McKerrow, W. S., and Soper, N. J., 1983, A model for the crustal evolution of southern Scotland: Tectonics, v. 2, no. 2, p. 187-210.

Lervik, K., Spencer, A., and Warrington, G., 1989, Outline of Triassic stratigraphy and structure in the central and northern North Sea, Correlation in hydrocarbon exploration, Springer, p. 173-189.

Lewis, M. M., Jackson, C. A. L., and Gawthorpe, R. L., 2013, Salt-influenced normal fault growth and forced folding: The Stavanger Fault System, North Sea: Journal of structural geology, v. 54, p. 156-173.

Loewenthal, D., Lu, L., Roberson, R., and Sherwood, J., 1976, THE WAVE EQUATION APPLIED TO MIGRATION: Geophysical Prospecting, v. 24, no. 2, p. 380-399.

Marcussen, Ø., Maast, T. E., Mondol, N. H., Jahren, J., and Bjørlykke, K., 2010, Changes in physical properties of a reservoir sandstone as a function of burial depth – The Etive Formation, northern North Sea: Marine and petroleum geology, v. 27, no. 8, p. 1725-1735.

Marshall, J. E. A., and Hewett, A. J., 2003, The Millennium atlas Ch. 6. Devonian: petroleum geology of the central and northern North Sea. Evans, D, Graham, C, Armour, A, and Bathurst, P (editors and co-ordinators). London, Geological Society of London, 65-82.

McClay, Norton, M. G., Coney, P., and Davis, G. H., 1986, Collapse of the Caledonian orogen and the Old Red Sandstone: Nature (London), v. 323, no. 6084, p. 147-149.

McDonough, W. F., and Sun, S.-S., 1995, The composition of the Earth: Chemical geology, v. 120, no. 3-4, p. 223-253.

McKerrow, W. S., 1988, The development of the Iapetus Ocean from the Arenig to the Wenlock: Geological Society special publication, v. 38, no. 1, p. 405-412.

McKerrow, W. S., Mac Niocaill, C., and Dewey, J. F., 2000, The Caledonian Orogeny redefined: Journal of the Geological Society, v. 157, no. 6, p. 1149-1154.

Miller, R. G., 1990, A Paleoceanographic Approach to the Kimmeridge Clay Formation: Chapter 2.

Mondol, N. H., Bjørlykke, K., and Jahren, J., 2008, Experimental compaction of clays: relationship between permeability and petrophysical properties in mudstones: Petroleum Geoscience, v. 14, no. 4, p. 319-337.

Morley, C., 1986, The Caledonian thrust front and palinspastic restorations in the southern Norwegian Caledonides: Journal of Structural geology, v. 8, no. 7, p. 753-765.

Norton, M. G., 1986, Late Caledonide Extension in western Norway: A response to extreme crustal thickening: Tectonics, v. 5, no. 2, p. 195-204.

Norton, M. G., McClay, K. R., and Way, N. A., 1987, Tectonic evolution of Devonian basins in northern Scotland and southern Norway: Norsk Geologisk Tidsskrift, v. 67, no. 4, p. 323-338.

Osmundsen, P., and Andersen, T., 2001, The middle Devonian basins of western Norway: sedimentary response to large-scale transtensional tectonics?: Tectonophysics, v. 332, no. 1-2, p. 51-68.

Osmundsen, P., Svendby, A., Braathen, A., Bakke, B., and Andersen, T., 2023, Fault growth and orthogonal shortening in transtensional supradetachment basins: Insights from the 'Old Red'of western Norway: Basin Research.

Osmundsen, P. T., Eide, E. A., Haabesland, N. E., Roberts, D., Andersen, T. B., Kendrick, M., Bingen, B., Braathen, A., and Redfield, T. F., 2006, Kinematics of the Hoybakken

detachment zone and the More-Trondelag fault complex, central Norway: Journal of the Geological Society, v. 163, no. 2, p. 303-318.

Paton, D. A., and Underhill, J. R., 2004, Role of crustal anisotropy in modifying the structural and sedimentological evolution of extensional basins: the Gamtoos Basin, South Africa: Basin Research, v. 16, no. 3, p. 339-359.

Patruno, S., and Reid, W., 2017, New plays on the Greater East Shetland Platform (UKCS Quadrants 3, 8-9, 14-16)–part 2: Newly reported Permo-Triassic intra-platform basins and their influence on the Devonian-Paleogene prospectivity of the area: First Break, v. 35, no. 1.

Penge, J., Taylor, B., Huckerby, J. A., and Munns, J. W., 1993, Extension and salt tectonics in the East Central Graben: Geological Society, London, Petroleum Geology Conference Series, v. 4, no. 1, p. 1197-1209.

Pharaoh, T. C., 1999, Palaeozoic terranes and their lithospheric boundaries within the Trans-European Suture Zone (TESZ): a review: Tectonophysics, v. 314, no. 1-3, p. 17-41.

Phillips, T. B., Fazlikhani, H., Gawthorpe, R. L., Fossen, H., Jackson, C. A. L., Bell, R. E., Faleide, J. I., and Rotevatn, A., 2019, The Influence of Structural Inheritance and Multiphase Extension on Rift Development, the NorthernNorth Sea: Tectonics (Washington, D.C.), v. 38, no. 12, p. 4099-4126.

Phillips, T. B., Jackson, C. A. L., Bell, R. E., Duffy, O. B., and Fossen, H., 2016, Reactivation of intrabasement structures during rifting: A case study from offshore southern Norway: Journal of structural geology, v. 91, p. 54-73.

Prosser, S., 1993, Rift-related linked depositional systems and their seismic expression: Geological Society special publication, v. 71, no. 1, p. 35-66.

Pujol, M., Marty, B., Burgess, R., Turner, G., and Philippot, P., 2013, Argon isotopic composition of Archaean atmosphere probes early Earth geodynamics: Nature, v. 498, no. 7452, p. 87-90.

Quirie, A. K., Schofield, N., Hartley, A., Hole, M. J., Archer, S. G., Underhill, J. R., Watson, D., and Holford, S. P., 2019, The rattray volcanics: Mid-jurassic fissure volcanism in the UK Central North Sea: Journal of the Geological Society, v. 176, no. 3, p. 462-481.

Rawson, P. F., and Riley, L. A., 1982, Latest Jurassic-Early Cretaceous events and the "late Cimmerian unconformity" in North Sea area: AAPG bulletin, v. 66, no. 12, p. 2628-2648.

Richards, P. C., Cordey, W. G., Knox, R. W. O. B., and Riding, J. B., 1993, Jurassic of the Central and Northern North Sea. Lithostratigraphic Nomenclature of the U.K. North Sea, Vol. 3. KNOX, R W O'B, and CORDEY, W G (editors). (Nottingham: British Geological Survey.), Nottingham, British Geological Survey on behalf of the UK Offshore Operators Association.

Roberts, A. M., Yielding, G., Kusznir, N. J., Walker, I., and Dorn-Lopez, D., 1993, Mesozoic extension in the North Sea: Constraints from flexural backstripping, forward modelling and fault populations: Geological Society, London, Petroleum Geology Conference Series, v. 4, no. 1, p. 1123-1136.

Roberts, D. G., Thompson, M., Mitchener, B., Hossack, J., Carmichael, S., and Bjørnseth, H. M., 1999, Palaeozoic to tertiary rift and basin dynamics: Mid-Norway to the bay of biscay - A new context for hydrocarbon prospectivity in the deep water frontier: Geological Society, London, Petroleum Geology Conference series, v. 5, no. 1, p. 7-40.

Scheiber, T., Viola, G., Bingen, B., Peters, M., and Solli, A., 2015, Multiple reactivation and strain localization along a Proterozoic orogen-scale deformation zone: The

Kongsberg-Telemark boundary in southern Norway revisited: Precambrian research, v. 265, p. 78-103.
Scruton, P. C., 1953, Deposition of evaporites: AAPG bulletin, v. 37, no. 11, p. 2498-2512.
Séguret M, S. M., Séranne, M., Chauvet, A., and Brunel, M., 1989, Collapse basin; a new type of extensional sedimentary basin from the Devonian of Norway: Geology (Boulder), v. 17, no. 2, p. 127-130.
Seranne, M., 1992, Devonian extensional tectonics versus Carboniferous inversion in the northern Orcadian Basin: Journal of the Geological Society, v. 149, no. 1, p. 27-37.
Serck, C. S., Braathen, A., Hassaan, M., Faleide, J. I., Riber, L., Messager, G., and Midtkandal, I., 2022, From metamorphic core complex to crustal scale rollover: Post-Caledonian tectonic development of the Utsira High, North Sea: Tectonophysics, v. 836, p. 229416.
Sheriff, R. E., 1977, Limitations on resolution of seismic reflections and geologic detail derivable from them: Section 1. Fundamentals of stratigraphic interpretation of seismic data.
Sherlock, S. C., 2001, Two-stage erosion and deposition in a continental margin setting; an 40Ar/39Ar laserprobe study of offshore detrital white micas in the Norwegian Sea: Journal of the Geological Society, v. 158, no. 5, p. 793-799.
Shirey, S. B., and Richardson, S. H., 2011, Start of the Wilson cycle at 3 Ga shown by diamonds from subcontinental mantle: Science, v. 333, no. 6041, p. 434-436.
Smith, K., and Ritchie, J. D., 1993, Jurassic volcanic centres in the Central North Sea: Geological Society, London, Petroleum Geology Conference Series, v. 4, no. 1, p. 519-531.
Soper, N. J., and Hutton, D. H. W., 1984, Late Caledonian sinistral displacements in Britain: Implications for a three-plate collision model: Tectonics, v. 3, no. 7, p. 781-794.
Steel, R., and Ryseth, A., 1990, The Triassic—Early Jurassic succession in the northern North Sea: megasequence stratigraphy and intra-Triassic tectonics: Geological Society, London, Special Publications, v. 55, no. 1, p. 139-168.
Stewart, S. A., and Clark, J. A., 1999, Impact of salt on the structure of the Central North Sea hydrocarbon fairways: Geological Society, London, Petroleum Geology Conference Series, v. 5, no. 1, p. 179-200.
Stuart, F. M., Bluck, B. J., and Pringle, M. S., 2001, Detrital muscovite 40Ar/39Ar ages from Carboniferous sandstones of the British Isles: Provenance and implications for the uplift history of orogenic belts: Tectonics, v. 20, no. 2, p. 255-267.
Sørensen, S., Morizot, H., and Skottheim, S., 1992, A tectonostratigraphic analysis of the southeast Norwegian North Sea Basin: Norwegian Petroleum Society Special Publications, v. 1, p. 19-42.
Tarling, D. H., 1985, Palaeomagnetic studies of the Orcadian Basin: Scottish journal of geology, v. 21, no. 3, p. 261-273.
Tenzer, R., and Gladkikh, V., 2014, Assessment of density variations of marine sediments with ocean and sediment depths: The Scientific World Journal, v. 2014.
Tommasi, A., and Vauchez, A., 2001, Continental rifting parallel to ancient collisional belts: an effect of the mechanical anisotropy of the lithospheric mantle: Earth and Planetary Science Letters, v. 185, no. 1-2, p. 199-210.
Torsvik, T. H., and Cocks, R. L. M., 2016a, Ch. 8. Devonian. Earth History and Palaeogeography p. 138-158.
-, 2016b, Ch. 9. Carboniferous. Earth History and Palaeogeography, p. 159-177.

Torsvik, T. H., Smethurst, M. A., Meert, J. G., Van der Voo, R., McKerrow, W. S., Brasier, M. D., Sturt, B. A., and Walderhaug, H. J., 1996, Continental break-up and collision in the Neoproterozoic and Palaeozoic — A tale of Baltica and Laurentia: Earth-science reviews, v. 40, no. 3, p. 229-258.

Torsvik, T. H., Sturt, B. A., Ramsay, D. M., Bering, D., and Fluge, P. R., 1988, Palaeomagnetism, magnetic fabrics and the structural style of the Hornelen Old Red Sandstone, western Norway: Journal of the Geological Society, v. 145, no. 3, p. 413-430.

Torsvik, T. H., Van der Voo, R., Meert, J. G., Mosar, J., and Walderhaug, H. J., 2001, Reconstructions of the continents around the North Atlantic at about the 60th parallel: Earth and planetary science letters, v. 187, no. 1, p. 55-69.

Trench, A., and Torsvik, T. H., 1992, The closure of the Iapetus Ocean and Tornquist Sea; new palaeomagnetic constraints: Journal of the Geological Society, v. 149, no. 6, p. 867-870.

Tucker, M. E., 1991, Sequence stratigraphy of carbonate-evaporite basins; models and application to the Upper Permian (Zechstein) of Northeast England and adjoining North Sea: Journal of the Geological Society, v. 148, no. 6, p. 1019-1036.

Underhill, J. R., and Partington, M. A., 1993, Jurassic thermal doming and deflation in the North Sea: implications of the sequence stratigraphic evidence: Geological Society, London, Petroleum Geology Conference Series, v. 4, no. 1, p. 337-345.

Vauchez, A., Tommasi, A., and Barruol, G., 1998, Rheological heterogeneity, mechanical anisotropy and deformation of the continental lithosphere: Tectonophysics, v. 296, no. 1-2, p. 61-86.

Vollset, J., and Doré, A. G., 1984, A Revised Triassic and Jurassic lithostratigraphic nomenclature for the Norwegian North Sea, Volume no. 3: Stavanger, Oljedirektoratet.

Warren, J. K., 2016, Evaporites : A Geological Compendium: Cham, Springer International Publishing : Imprint: Springer.

Watson, J., 1985, Northern Scotland as an Atlantic–North Sea divide: Journal of the Geological Society, v. 142, no. 2, p. 221-243.

Whipp, P. S., Jackson, C. A. L., Gawthorpe, R. L., Dreyer, T., and Quinn, D., 2014, Normal fault array evolution above a reactivated rift fabric; a subsurface example from the northern Horda Platform, Norwegian North Sea: Basin Res, v. 26, no. 4, p. 523-549.

White, S. H., Bretan, P. G., and Rutter, E. H., 1986, Fault-Zone Reactivation: Kinematics and Mechanisms: Philosophical transactions of the Royal Society of London. Series A: Mathematical and physical sciences, v. 317, no. 1539, p. 81-97.

Williams, G., Powell, C., and Cooper, M., 1989, Geometry and kinematics of inversion tectonics: Geological Society, London, Special Publications, v. 44, no. 1, p. 3-15.

Wilson, J. T., 1966, Did the Atlantic Close and then Re-Open?: Nature (London), v. 211, no. 5050, p. 676-681.

Yielding, G., Badley, M., and Freeman, B., 1991, Seismic reflections from normal faults in the northern North Sea: Geological Society, London, Special Publications, v. 56, no. 1, p. 79-89.

Ziegler, P. A., 1975, Geologic evolution of North Sea and its tectonic framework: AAPG bulletin, v. 59, no. 7, p. 1073-1097.

Ziegler, P. A., 1982, Geological atlas of western and central Europe.

-, 1988, Evolution of the Arctic-North Atlantic and the Western Tethys: A visual presentation of a series of Paleogeographic-Paleotectonic maps: AAPG memoir, v. 43, p. 164-196.
-, Geological atlas of western and central Europe1990, Geological Society of London.
Ziegler, P. A., 1992, North Sea rift system: Tectonophysics, v. 208, no. 1, p. 55-75.